Immunoglobulin Gene Repertoire Analysis During Therapeutic B Cell Depletion

---

Dissertation

zur

Erlangung der naturwissenschaftlichen Doktorwürde

(Dr. sc. nat.)

vorgelegt der

Mathematisch-naturwissenschaftlichen Fakultät

der

Universität Zürich

von

Michael Andreas Maurer

aus

Vechigen BE

Promotionskomitee

Prof. Dr. med. Jan Lünemann

Prof. Dr. rer. nat. Christian Münz

Prof. Dr. med. Adriano Fontana

Prof. Dr. rer. nat. Burkhard Becher

Prof. Dr. med. Norbert Goebels

Zürich, 2013

Disclaimer

The thesis was based upon and partly adapted form the following manuscript.

Michael A Maurer, Goran Rakocevic, Carol S Leung, Isaak Quast, Martin Lukačišin, Norbert Goebels, Christian Münz, Hedda Wardemann, Marinos Dalakas, and Jan D Lünemann.
Rituximab induces sustained reduction of pathogenic B cells in patients with peripheral nervous system autoimmunity,
J. Clin. Invest. (2012), doi:10.1172/JCI58743.

Table of contents

Zusammenfassung

Autoimmunkrankheiten gehören zu den schwersten Formen chronischer Krankheiten in der westlichen Welt. Bei diesen Krankheiten wendet sich das körpereigene Immunsystem gegen verschiedene Organe im Körper. Bis heute sind die Ursachen für diese Krankheiten weitgehend unbekannt und die Therapieoptionen sehr beschränkt. Es werden meist immunmodulierende Substanzen verwendet, welche das gesamte Immunsystem supprimieren, aber die Krankheit nicht heilen können. Eine neue Klasse von Medikamenten, für welche klinische Studien laufen, sind monoklonale Antikörper, die nicht mehr das gesamte Immunsystem modulieren sondern nur eine gewisse Zellpopulation des Immunsystems dezimieren. Es besteht die Hoffnung, dass die nach der Therapie vom Körper neu produzierten Zellen den autoimmunen Charakter verlieren.

Einer dieser Antikörper (Rituximab) wendet sich gegen die B Zellen und führt zu einer Zerstörung dieser Zellen. Rituximab wurde für die Krebstherapie entwickelt und wird heute auch bei Autoimmunkrankheiten verwendet. Es zeigte sich, dass gewisse Patienten mit Autoimmunkrankheiten stark von dieser Therapie profitieren können. Der genaue Wirkungsmechanismus zwischen der Zerstörung der B Zellen durch Rituximab und der daraus folgenden Besserung des Krankheitsverlaufs ist bis heute unbekannt. In der vorliegenden Studie versuchten wir herauszufinden, welcher Mechanismus diesem Zusammenhang zugrunde liegt. Hierfür haben wir die Immunglobulinsequenzen von Patienten mit anti-Myelin-assoziiertes-Glykoprotein Neuropathie (anti-MAG Neuropathie) vor und nach Gabe von Rituximab untersucht. Anti-MAG Neuropathie ist eine Autoimmunkrankheit des peripheren Nervensystems (PNS), welche sich in Patienten mit anti-MAG IgM Antikörpern entwickelt und zum Verlust der Nervenimpulsübertragung im PNS führt. Zur Analyse der Immunglobulinsequenzen haben wir eine Einzelzellen PCR verwendet, welche uns erlaubt die Entwicklung und Veränderung des B Zell Repertoires unter dem Einfluss von Rituximab zu untersuchen. Wir sortierten jeweils drei verschiedene B Zellengruppen vor und 12 Monate nach der Therapie. Die B Zellengruppen zeigten unterschiedliche Entwicklungsstufen und waren aufgeteilt in naïve, IgM memory und IgG memory B Zellen. Wir verglichen die Resultate innerhalb der anti-MAG Neuropathie-Gruppe zwischen mit Placebo und mit Rituximab behandelten Patienten, wie auch zwischen Patienten, die auf die Therapie ansprachen und solchen, die nicht ansprachen. Als Kontrolle verwendeten wir eine dem Alter angepasste gesunde Patientengruppe.

Mit dieser Studie konnten wir zeigen, dass anti-MAG Neuropathie Patienten eine grosse Expansion von IgM memory B Zellen, welche MAG erkennen, im Blut haben. Patienten, welche auf die Therapie ansprachen zeigten kleinere Expansionen vor und nach der Behandlung verglichen mit therapieresistenten Patienten. Des Weiteren fanden wir eine klonale Persistenz, eine statische Situation in der Mutationsfrequenz der variablen Region der IgM Antikörper bevor und nach der Therapie und ein Nichtvorhandensein der B Zell Maturierungscheckpoints in den therapieresistenten Patienten.

Aus diesen Daten schliessen wir, dass der Therapieerfolg davon abhängt wie gut die zirkulierenden pathogenen IgM memory B Zellen ausgelöscht werden können. Die effiziente Auslöschung führt zu einer Neukonfigurierung des Immunsystems, welches sich in einer Reetablierung der Checkpoints äussert und der Reduktion der pathogenen IgM Antikörper.

Summary

Autoimmune diseases include some of the most severe chronic diseases in the western world. In autoimmune diseases the immune system of the host attacks itself. Yet the underlying cause of most autoimmune mediated conditions is not completely understood and the development of efficient treatments is still ongoing. Different drugs have been tested for treating these kinds of diseases. Most of them primarily function in an anti-inflammatory manner, are often accompanied by severe side effects and the chronicity of the conditions often doesn't improve. The lack of knowledge about the mechanism of action and the progression of the disease in most of these patients led to numerous clinical trials alongside the establishment of new classes of drugs. In this work a new class of drugs for the treatment of autoimmune diseases is analyzed. This new class comprises antibodies, which do not suppress the immune system in general as is often done by old established drugs. These therapies deplete certain populations of cells of the adaptive immune system. This study focuses on the depletion of the B cells.

The B cell-depleting IgG1 monoclonal antibody Rituximab can persistently suppress disease progression in some patients with autoimmune diseases, but the mechanism has remained unclear. In this study the Ig gene usage in a group of patients with anti-myelin-associated glycoprotein (MAG) neuropathy, an autoimmune disease of the peripheral nervous system, which develops in individuals with an IgM monoclonal gammopathy and is mediated by IgM autoantibodies binding to the MAG antigen was evaluated. Single cell sorted naïve, IgM memory and IgG memory B cells were analyzed before and 12 months after treatment initiation and compared to age-matched healthy controls.

Patients with anti-MAG neuropathy showed substantial clonal expansions of blood IgM memory B cells which recognized MAG antigen. The group of patients showing no clinical improvement following Rituximab therapy could be distinguished from clinical responders through a higher load of clonal IgM memory B cell expansions before and after therapy, the persistence of clonal expansions despite efficient peripheral B cell depletion, the lack of significant changes in somatic hypermutation frequencies of IgM memory B cells and the lack of newly reestablished checkpoints in IgM memory and IgG memory compartments. We infer from these data that the beneficial long-term immunomodulatory effect of Rituximab therapy depends on efficient depletion of both circulating and non-circulating B cells and is associated with qualitative immunological changes that indicate reconfiguration of B cell memory through sustained reduction of autoreactive clonal expansions and the reestablishing of checkpoints for the controlling of the B cell maturation.

Introduction

The human immune system displays a striking similarity to that of other vertebrates. It is comprised of a complex and elegant network of numerous humoral and cellular components, which originate from hematopoietic stem cells (HSC) located in the bone marrow. The HSC generate two different kinds of immune cells. The innate immune cells defend the host immediately against pathogens by recognition of pathogen-associated molecular patterns (PAMPS). The second group of cells, which are differentiated from HSC are adaptive immune cells namely B and T cells. These cells have the ability to perform a highly specific response and additionally develop immunological memory against a specific pathogen. The blood stream and the lymphatic system are the major distributors of the immune system and connect the lymphoid organs with each other as well as the periphery with the immune system. Lymphoid organs are the sites of immune cells differentiation, maturation and further development. Vertebrates have primary and secondary lymphoid organs with specific functions. The bone marrow and the thymus constitute the primary lymphoid organs in adult humans. These organs possess the capacity to differentiate progenitor cells into different hematopoietic cell lineages (Figure 1). Most blood cells are generated in the bone marrow with the prominent exception of T cells, which develop from bone marrow derived precursors and mature in the thymus.

To reach the circulation immune cells have to differentiate through several precursor stages. This holds true for innate and adaptive immune cells as well for platelets and red blood cells.

Figure 1: The development of different hematopoietic cells

Next page: The hierarchy of the blood cell development is illustrated from the top to the bottom. Different precursors are depicted with colored nuclei and two major pathways are shown. The myeloid cells are shown on the left and the lymphoid cells on the right side.
The figure is adapted from [1-2]

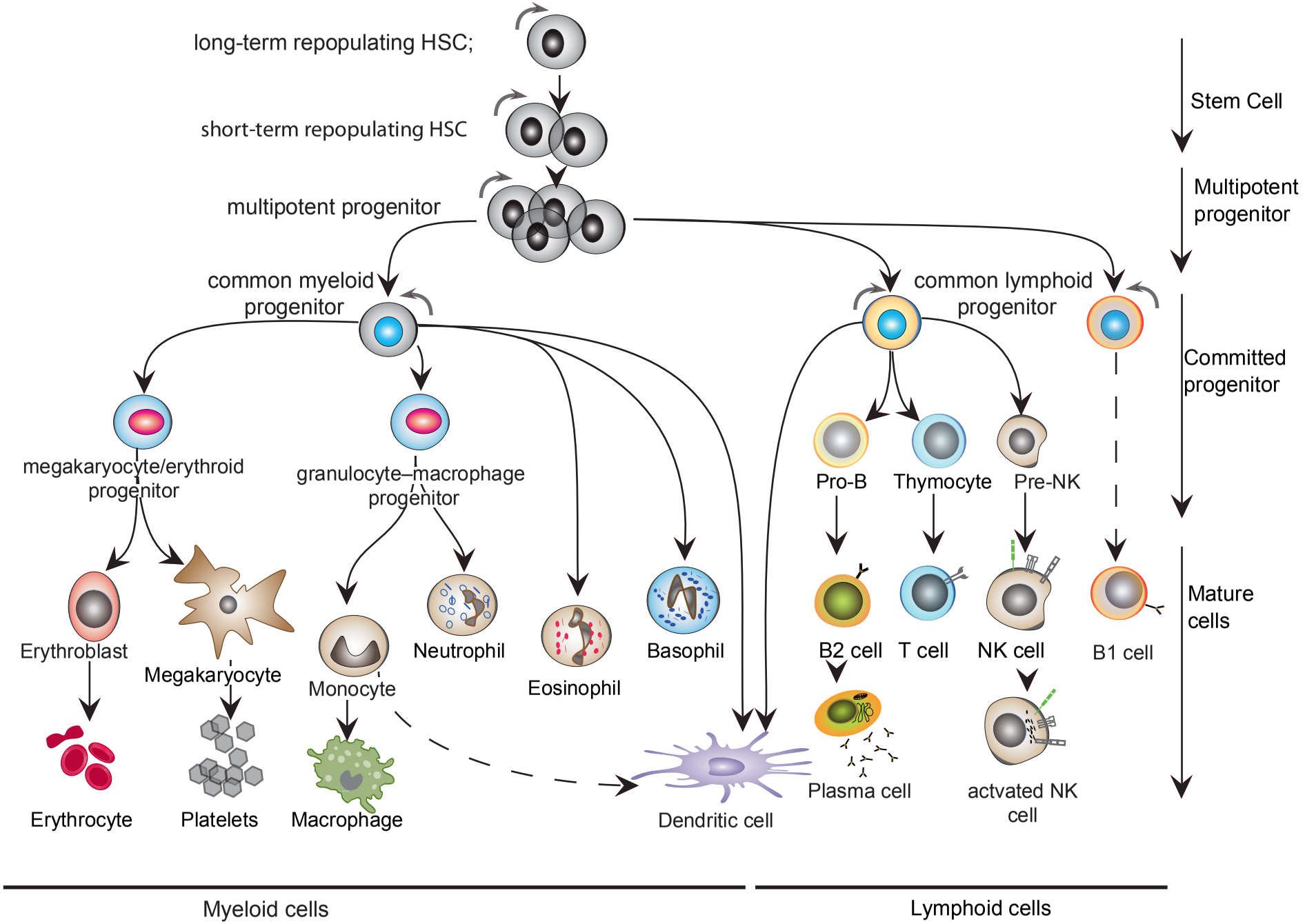
long-term repopulating HSC;
short-term repopulating HSC
multipotent progenitor
common myeloid progenitor
common lymphoid progenitor
megakaryocyte/erythroid progenitor
granulocyte–macrophage progenitor
Pro-B
Thymocyte
Pre-NK
Erythroblast
Megakaryocyte
Monocyte
Neutrophil
Eosinophil
Basophil
B2 cell
T cell
NK cell
B1 cell
Erythrocyte
Platelets
Macrophage
Dendritic cell
Plasma cell
actvated NK cell
Stem Cell
Multipotent progenitor
Committed progenitor
Mature cells
Myeloid cells
Lymphoid cells

The maturation steps have to be controlled and supported by surrounding cells such as stromal cells, which secret factors like chemokines, growth factors and interleukins to control the development of the precursor cells. The precursor cells do secret similar factors but with a different signature. This leads to a complex system of inhibition, activation as well as positive and negative feedback loops. In case one of these interactions is disturbed the system becomes deregulated and may start to attack the host instead of protecting it.

For a better overview of the different layers of self-tolerance see Table1. In recent years several discoveries have been made as of how this network interacts to protect the host from pathogens while retaining self-tolerance. One crucial step is the discrimination of self and non-self . This mechanism is based for T cells on the presentation of self-peptides on major histocompatibility complex (MHC) molecules, which are expressed on almost all nucleated cells (class I) and antigen presenting cells like B cells, macrophages and dendritic cells (class II) . Downregulation of MHC class I as occurring upon virus infection or tumor transformation leads to elimination of the cell *via* cytotoxic natural killer (NK) cells [3,4].

Layers of self-tolerance		
Type of tolerance	**Mechanism**	**Site of action**
Central tolerance	Deleting editing	Thymus T cells Bone marrow B cells
Antigen segregation	Physical barrier to self-antigen access to lymphoid system	Peripheral organs (e.g. thyroid, pancreas)
Peripheral anergy	Cellular inactivation by weak signaling without co-stimulus	Secondary lymphoid tissue
Regulatory cells	Suppression by cytokines intracellular signals	Secondary lymphoid tissue and site of inflammation
Cytokine deviation	Apoptosis post-activation	Secondary lymphoid tissue and site of inflammation
Clonal deletion	Apoptosis post-activation	Secondary lymphoid tissue and site of inflammation

Table 1: The different checkpoints in the development of lymphocytes

Summary of the different checkpoints in the development of the adaptive immune system. Table addapted from[2]

On the other hand the adaptive immune system, which generates a broad diversity of antigen receptors in a random way, has to learn to distinguish self and non-self to reach self-tolerance. Adaptive T/B cells have to pass tight selection checkpoints for testing the newly generated antigen receptors for self-reactivity and functionality to further develop. These are important steps in the maturation of these cells and can protect the host from autoimmune diseases (see p18).

One crucial element in the adaptive immune system is the occurrence of two random site-specific DNA recombination events, which are called V(D)J recombination, during which the antigen receptor is created [5,6].

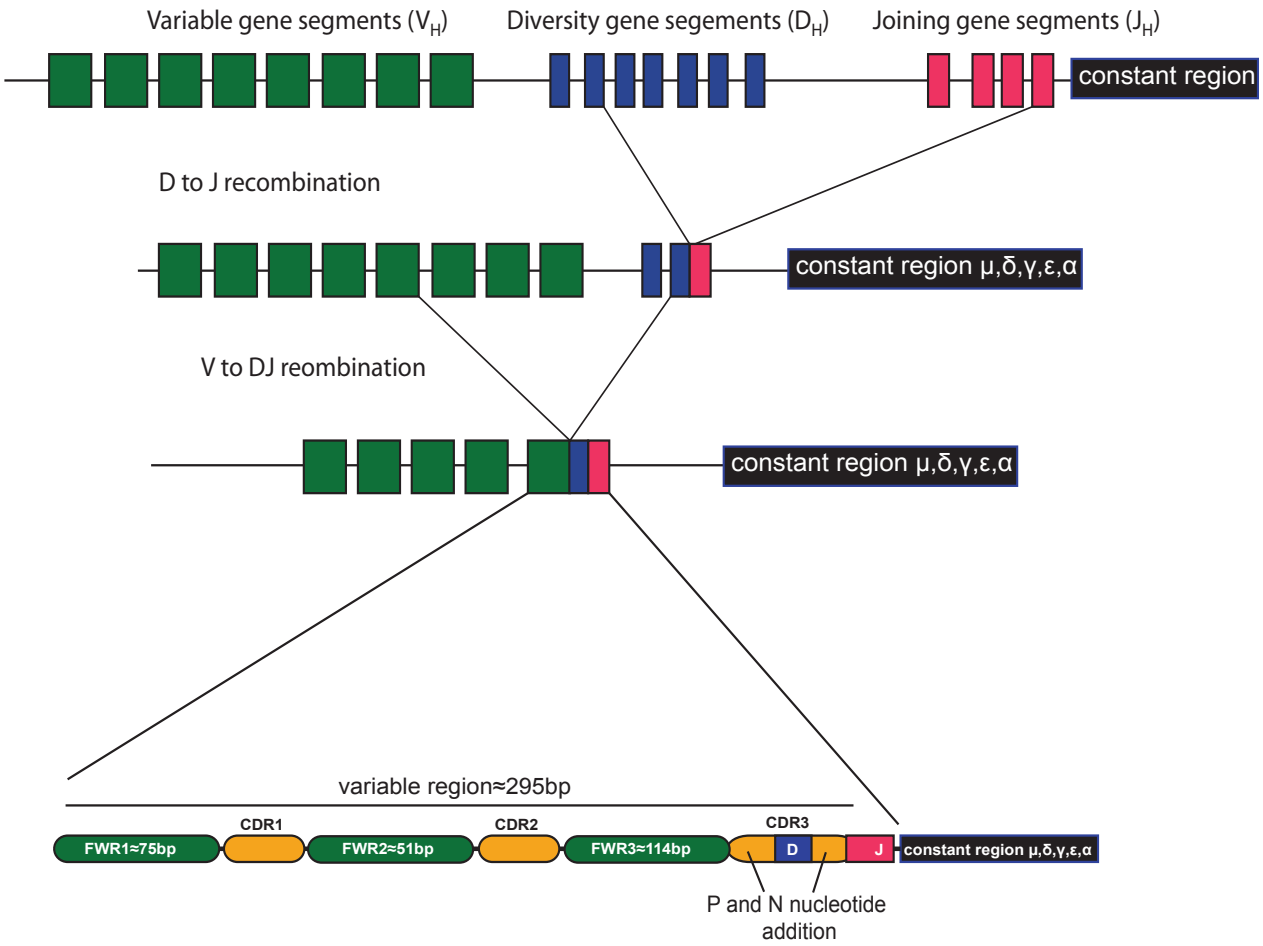

Figure 2: The distribution of the three different gene elements V_H, D_H, and J_H of the heavy chain

The V_H gene element is depicted in green, D_H in blue and J_H in pink. The different segments are the repetitive boxes of the same color. First, the D_H and J_H recombine and excise the surplus gene segments. Next, the V_H element recombines with the DJ_H element. After these two recombinations the variable region is generated, which encode for two secondary structure elements. The β sheet (FWR) and in orange loops (CDR) are depicted in green and orange, respectively. The figure is adapted from [2]

The receptor is generated through a random combination of one variable V, a diversity D and a joining J segment (Figure 2). The first recombination is the VDJ recombination of the heavy chain for B cells or α/γ-chain for T cells followed be the VJ recombination of the light chain (B cell) or β/δ -chain (T cell) (see p15). Together the heavy and light chains form the B cell receptor (BCR) and the α/β or γ /δ the T cell receptor (TCR). In the case of B cells these events generate a theoretical variation of $1.9*10^6$ different variable region on the (BCR). The variable region of the BCR is the part of the receptor, which binds the antigen and therefore defines part of the binding properties of the BCR and its secreted form, the antibody (Figure 3). The BCR is the sensor that guides the B cells through the different maturation steps, which start in the bone marrow, proceed in the secondary lymphoid organs and finally may end as an antibody secreting plasma cells back in the bone marrow (Figure 4).

B lineage cells generate antibodies against epitopes of antigens and neutralize these *via* a high binding affinity. This is achieved by the combined structure of both variable regions from the heavy and light chain. The structure of the variable region has a β-sheet framework with three loops called the complementary determining regions (CDR1, CDR2, CDR3). These CDRs are highly variable and are mainly involved in binding their respective antigen[7] through van der Waals force, hydrogen- and ionic bonds. Especially the CDR3, which is the loop with the highest variable amino acid composition and length, is primarily involved in the binding [8]. But it is not exclusively the V(D)J recombination that generates the high variability and ultimately the avidity of the antibodies. In the vertebrate immune system an interaction of both adaptive immune cells (B/T cells) and innate immune cells diversifies the variable region of the BCR. This mechanism is called somatic hypermutation (SHM) and introduces mutations in the variable region of the antibody especially so in the CDRs. These mutations are changing the avidity of the antibody. Due to positive selection, the avidity increases and the antibody reaches a stronger binding avidity towards the antigen. The process of the SHM takes place in the germinal center (GC) of the secondary lymphoid organs (see p25).

Antibodies have a very important function in the immune system and link the adaptive part with the innate immune system due to the variable part and its specific avidity towards a particular antigen and the different modification in the constant region, which is called fragment crystallizable region or Fc that can be introduced by the class switch recombination (see p23). The constant part is called the isotype. The isotype regulates the signals that are sent to the rest of the immune system, modulates stability (half-life), neutralization, opsonization, complement activation as well the trans tissue transport. Antibodies have different ways to signal to the immune system, which differ between the

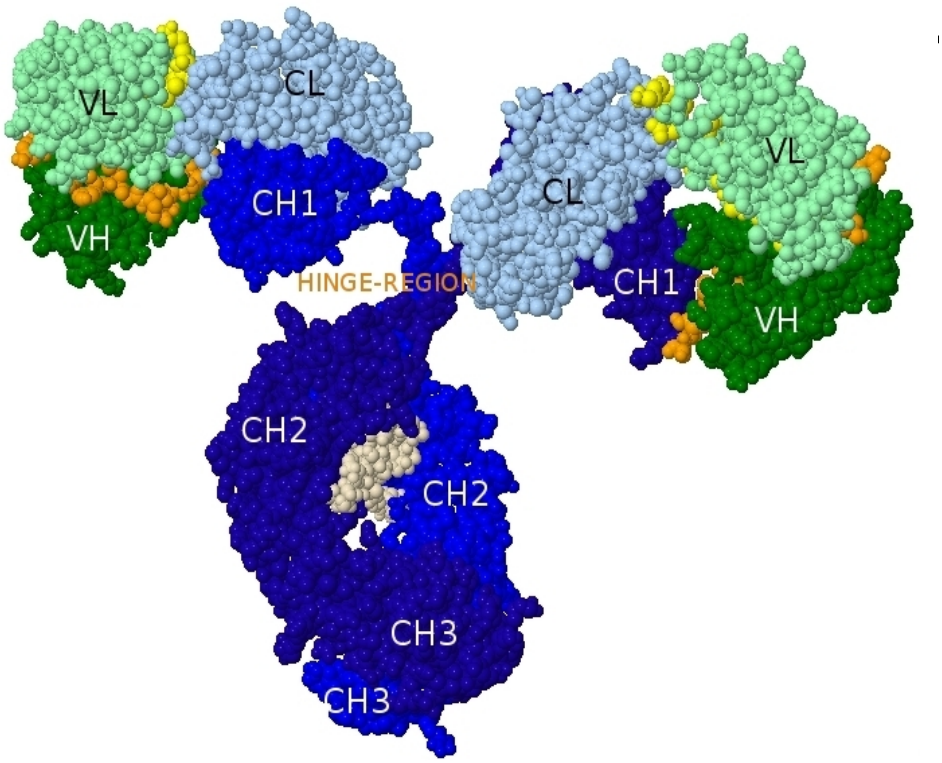

Figure 3: The structure of an IgG antibody:

An antibody contains two major parts, a constant part (depicted in blue CL, CH1, CH2 and CH3) and a variable part (labeled in green VL and V_H), which recognizes the target antigen. The variable part consists of two protein chains one from the light and one from the heavy chain, which together form the binding site. The diversity and the recognition of an antigen are due to the V(D)J recombination of heavy and light chain and the different combinations that can be achieved. The complementary determined regions (CDR) are formed *via* this re-combination (depicted in orange, and yellow). These highly variable parts are mainly involved in the binding of antigen. Figure is adapted from THE INTERNATIONALIMMUNOGENET-ICSINFORMATION SYSTEM www.IMGT.org

isotype classes. In humans five different isotype classes are to be found (IgM, IgD, IgE, IgG, IgA) [9].

The different interactions with the rest of the immune system is listed in the Table 2 .

Since B cells undergo the VDJ recombination and SHM in the different maturation steps it is likely that a mal-function in one of the checkpoints for self-tolerance can lead to an autoimmune diseases [12].

There are actually several autoimmune diseases linked to autoantibodies including Rheumatoid arthritis, Neuromyelitis optica, Myasthenia gravis, Systemic lupus erythematosus (SLE), Primary Sjögren's syndrome, Ideopathic thrombocytopenic purpura, Autoimmune hemolytic anemia, Cold agglutinin disease, Cryoglobulinemia, ANCA-associated vasculitis, Pemphigus vulgaris, Graves' disease, Anti-MAG neuropathy.

Isotypes	Structure	g/l	Specialty
IgM	Pentamer	1.5	Initial antibody class, does not require class switch. Binds viral particles and complement
IgD	Monomer	0.04	Only expressed on cell surface, e.g. transmembrane Ig molecule
IgG	Monomer	10	Most abundant class with four isotype subclasses- IgG1, IgG2, IgG3, IgG4. Binds to the Fc receptors on monocytes, B cells, NK
IgG1	Monomer	9	Second most effective complement activator after IgG3, mediates opsonization
IgG2	Monomer	3	Weak complement activator
IgG3	Monomer	1	Most effective complement activator, mediates opsonization
IgG4	Monomer	0.5	Cannot activate complement, mediates opsonization with intermediate affinity for Fc (Fragment crystallizable) receptors
IgA	Monomer/ Dimer	2.1	Mainly secreted in mucosa, gastrointestinal tract and tears. Inhibits attachment of pathogens to mucosal cells.
IgA1	Dimer		Present in blood as monomer and as dimer or oligomer in the mucosa
IgA2	Monomer		Present in blood as monomer and as dimer or oligomer in the mucosa
IgE	Monomer	$3*10^{-5}$	Binds to Fc receptors on basophiles and mast cells inducing degranulation. Accounts for hypersensitivity reactions (allergies). Found mainly in tissues

Table 2: Properties and biological activities of human Ig isotype classes

Modified from [2,10,11]

B cell development

Since the anti-MAG neuropathy is a clearly an antibody mediated disease the following parts will focus on the different B cell linages B1 and B2 B cells and the distinctive developmental features of B2 B cells starting from the bone marrow too different effector linages. The pathway and checkpoints for B cell development are summarized in Figure 4. The next chapter starts with the first step in the life of B cells, which is the VDJ recombination of the BCR.

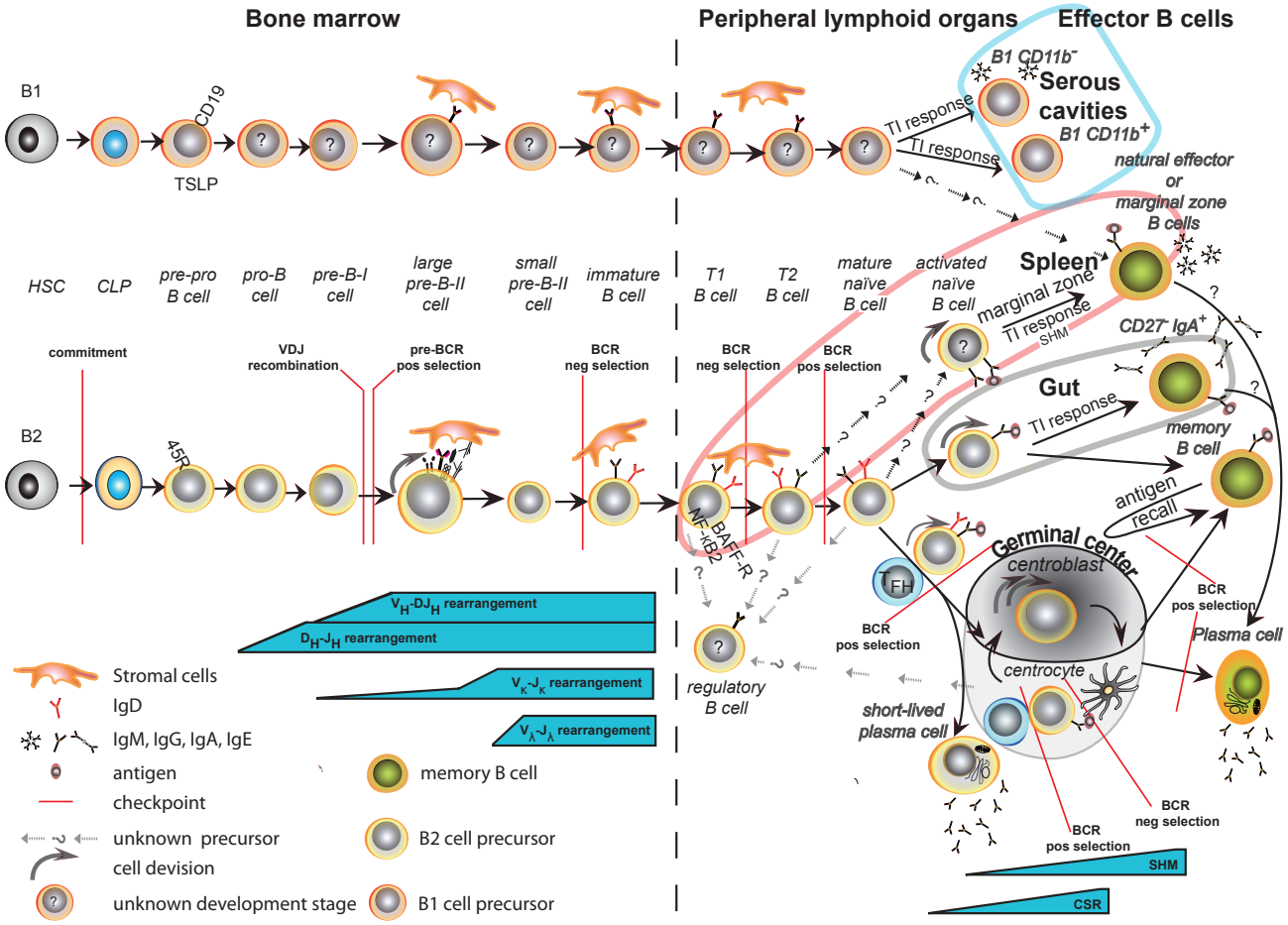

Figure 4: B cell development

The maturations of the B cells is illustrated from left to the right. There are two different kinds of B cells the B1 and the B2 B cells, which have different lymphoid progenitor cells. The development starts in the bone marrow and ends as memory B cell and plasma cell for the B2 B cells. The B2 B cells have different ways to enter the memory compartment. One is T cell- dependent and takes place in the germinal center and the other route is T cell-independent (TI). The TI pathway takes place in the marginal zone of the spleen and the gut. Regarding the B1 B cells not much is known as of how they develop. Unknown developmental steps are indicated with a question mark (?). B cell checkpoints are indicated with a red line. Dotted arrows reflect origin of estimated precursor. Figure is adapted from[13-15]

V(D)J recombination

For the adaptive immune system recombination of a unique receptor for pathogen recognition is a key step in the development. For B cells this receptor (BCR) is used for the specific recognition of an epitope of an antigen. The construction of the BCR involves double strand breaks (DSB) of the DNA and re-ligation with a different part of the DNA. This event is named V(D)J recombination or site-specific DNA recombination (SSR) [16-18]. The genetic information for the BCR is located on different chromosomes, namely 14 for the heavy chain (IgH) [19], 2 for the kappa light chain (IgK) [20,21] and 22 for the lambda light chain (IgL) [21,22]. This has the advantage that the recombination site for each chain is located spatially independent from each other and do not interfere with the sequential intra-chromosomal recombination events.

The first V(D)J recombination in B cells starts with the heavy chain at the early pro-B cell stage and recombines in a random selection one diversity IGHD with one joining IGHJ element [23] followed by an additional V(D)J recombination, where one variable IGHV segment is ligated with the already combined DJ segments and build together the exon of the variable region of the BCR heavy chain. A successful in-frame heavy chain recombination suppresses further recombination of the second chromosome 14. This control mechanism is called allelic exclusion. In the pre-B cell stage the V(D)J recombination for the light chain starts, which only recombines variable and joining segments to form the variable region of the light chain . Light chain recombination starts with the kappa light chain. If this V(D)J recombination for the kappa light chain is successful the lambda light chain recombination is suppressed. This mechanism is called isotype exclusion [24]. In the case of a non-functional/autoreactive kappa light chain the lambda light chain is recombined and the kappa light chain locus is silenced *via* the kappa deletion element (KDE) [25]. The KDE is located 3' downstream of the constant region of the kappa light chain. The locus is then silenced through the recombination of the KDE with either Jκ or Vκ, which leads to an excised constant region and silencing of the kappa light chain . The allelic exclusion for the light chain is not yet understood. The high diversity of the variable region is generated by the numerous variable, diversity and joining segments, which are placed next to each other on the chromosome. Due to close sequence homologies of some IGHV, IGHD and IGHJ segments these segments can be summarized as families [26].

For the heavy chain of an antibody 123-129 different immunoglobulin heavy chain variable gene segments (IGHV) are known, deriving from 7 different families. Of these IGHV segments 79 are classified as pseudogenes and 43 as functional.

While the IGHV-3 family is the largest one followed by IGHV-1 and IGHV-4 (Table 3)

Of the diversity elements IGHD 27 segments exist and can be grouped into 7 different families and for IGHJ element 9 segments were found, which can be summarized into 6 families [26]. Since there are three different elements and at least 43 IGHV, 27 IGHD and 9 IGHJ segments the cells have to discriminate between the variable, diversity and joining elements to avoid the combination of joining and variable segments in the case of the heavy chain. To prevent this mistake the ligation of the different gene elements is directed by a specific recombination signal sequence (RSS). These sequences are flanking the coding sequence of the IGHV, IGHD and IGHJ segments. RSS do have a special architecture of a conserved palindromic heptamer sequence spaced by 12 or 23 bases from a second conserved nonamer sequence, which lead to the name 12- or 23-RSS.

Each gene segment has a 12- or 23 RSS. The SSR follows the 12/23 rule where only segments with 12 bp spaces can be fused to 23 bp spaced segments [27]. During the recombination several proteins assemble on the DNA and loop out the DNA to form a synaptic complex (Figure 5B). The first proteins are the DNA-binding high-mobility group box (HMGB) proteins 1 and 2 [28]. These proteins bind in the minor grove of the 23 RSS and prepare the binding of the most important proteins RAG1 and RAG2 to the 12-and 23 RSS (Figure 5 A and B) [29,30]. The binding of RAG1 and RAG2 proteins to the DNA synergistically increases the binding affinity and initiates a DNA double strand break [6,31].

	V_H family							
Classification	V_H 1	V_H 2	V_H 3	V_H 4	V_H 5	V_H 6	V_H 7	Total
Functional	9	3	19	6	1	1	0	39
Transcribed	0	0	0	1	0	0	0	1
Open reading frame	0	0	3	0	0	0	1	4
Pseudogene								
Point mutation								
Truncation	3	1	21	2	0	0	2	29
Total	2	0	22	23	1	0	2	50
	14	4	65	32	2	1	5	123

Table 3: Human V_H segments found on the chromosome 14

The table sorts the 123 V_H segments that are located on the chromosome 14 into the different families and by functionality. The table is adapted from [26]

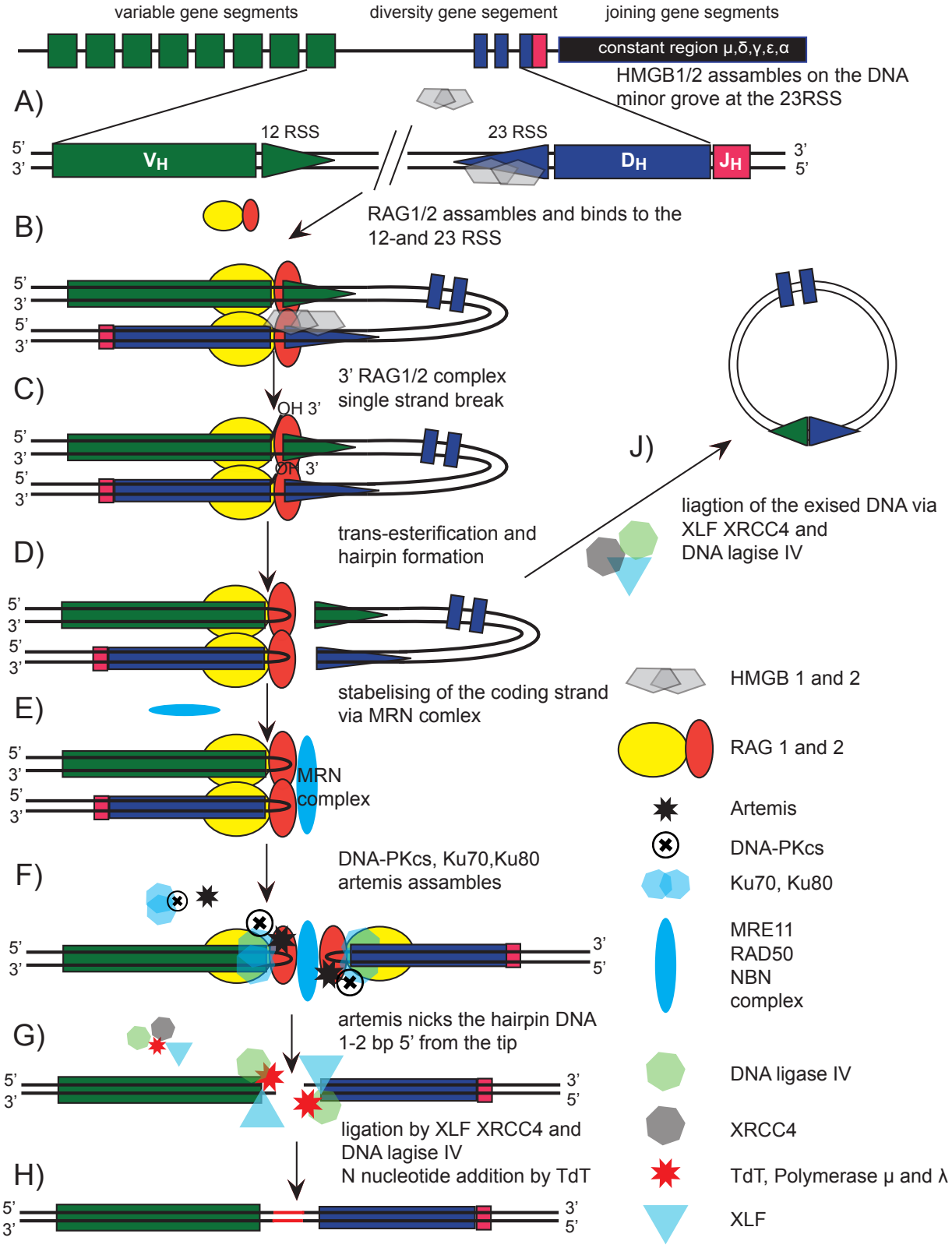

Figure 5: The DNA recombination machinery

Form the top to the bottom the sequential events of the DNA recombination are depicted. **A)** The first step is the binding of HMGB1/2 to the 23SSR. **B)** The binding of the HMGB facilitates the binding of RAG1/2, which loops the remaining DNA out. **C)** RAG1/2 introduce a 3' single strand break. **D)** The 3' hydroxyl group binds to the antisense DNA and generates a loop. **E)** The two coding segments are stabilized *via* the MRN complex. **F)** Ku70, Ku80, DNA PKcs and Artemis assemble on the hairpin loop. **G)** Artemis cleaves the hairpin and generates a 5' overhang at the coding DNA strand. **H)** TdT and polymerases *μ* and λ fill up the gaps and DNA ligase IV, XRCC4 and XLF ligate the DNA together. **J)** The ligation of the excised DNA *via* DNA ligase IV, XRCC4 and XLF is illustrated. The figure is adapted from [13,32]

In the process of the DNA double strand break (DSB) two sequential events occur [33]. The RAG1/2 complex introduces a single strand break (SSB) at the 3' end of the DNA, which leads to a free 3' OH group at the gene segment (Figure 7B and C). The 3' hydroxyl group is further processed into a hairpin loop *via* a direct *trans*-esterification [34,35], which leads to blunt ends of the excised DNA (Figure 5D). The hairpin of the coding segments are stabilized *via* a complex consisting of MRE11, RAD50 and NBN named MRN complex) (Figure 5E) [36-39]. Additional factors are assembled to the RAG1/2 DNA complex namely Ku70, Ku80, XRCC4, DNA-Ligase4, XLF, DNA-dependent protein kinase (DNA-PKcs) and Artemis [40-45]. The excised blunt end DNA is then ligated by the common mechanism non-homologous DNA end-joining NHEJ *via* the XLF XRCC4 DNA-Ligase4 complex, which connects the excised DNA to a circle [45] (Figure 5 F and J).

The DNA-PKcs Artemis complex opens the hairpin of the DNA 1-2 bp 5' away from the tip of the hairpin and generates a palindromic overhang up to 4 bp (P-element) at the 5' end of the coding DNA (Figure 5 F to G) [40,46]. Polymerase μ and λ, as well as the terminal deoxynucleotidyl transferase (TdT) are recruited and fill the cap with non-template-encoding-nucleotides (N-elements). While Polymerase λ can only fill in caps in a template dependent manner, TdT and with less activity Polymerase μ are able to add nucleotides in a template-independent way [47-49]. Finally the DNA ends are ligated with the XLF XRCC4 DNA-Ligase4 complex (Figure 5 G and H).

If the V(D)J recombination of the heavy chain is functional, the pro-B cells are positively selected by testing for the BCR expression enter a small proliferation round[13]. Then, after one to two cell divisions, the B cells slightly induces the V(D)J recombination for the light chain. Finally the fully functional BCR has to undergo numerous rounds of positive and negative selections, until the B cells are allowed to produce antibodies with the specificity of the BCR. These selection points are named checkpoints and the next chapter is focusing on these events during the B cell development.

B cell selection

To ensure that developing B cells are functional and self-tolerant the cells have to pass positive and negative selection checkpoints. Positive selection always includes steps where the BCR binds an antigen, clusters and sends signals to the cells. These selections lead to survival of the cells. In the case of negative selection the cells only survive if the BCRs are not cross-linked and do not signal to the nucleus. The high diversity of antibody recombination needs a discrimination of self and non-self to protect the host from autoantibody mediated diseases. This idea dates back to Paul Ehrlich in 1902, when he first formulated the hypothesis of *horror autotoxicus*. He postulated that an immune system, which is not able to distinguish between self and non-self is connected to certain human diseases. Today the sites of the checkpoints to protect the host from autoimmune diseases are known and some of the selection mechanisms as well. This chapter will mainly focus on the different checkpoints, which are in involved in the B cell development.

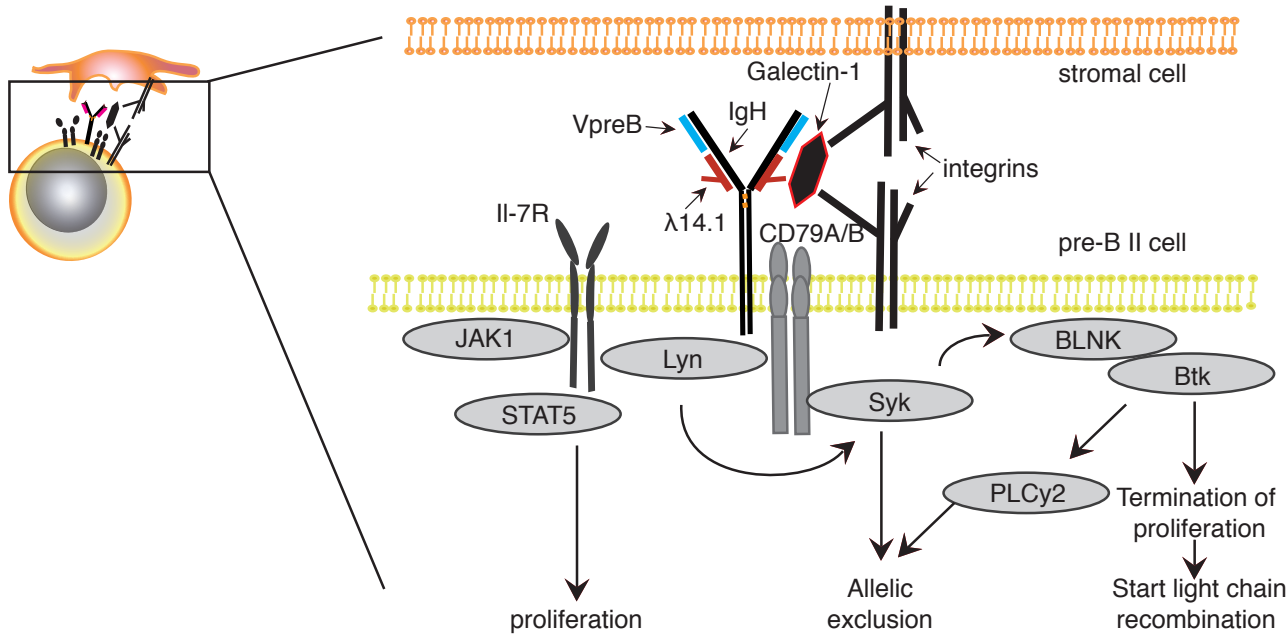

Figure 6: The positive selection of the pre B 2 cell after the heavy chain VDJ recombination

Galectin-1 crosslinks the pre-BCR of the pre-B-II cell *via* binding to λ14.1 on the pre-BCR and integrins on the stromal and B cell, this provides four main signals to the pre B II. (i) the cell receives a signal for proliferation, which lead to 1-2 cell divisions. (ii) At the same time the signal for the allelic exclusion is provided (iii) and the proliferation stops and (iv) the light chain VJ recombination starts. Figure adapted from [13]

The first selection in the life of B cells is a positive selection after the successful VDJ recombination and expression of a functional heavy chain. The expression of the heavy chain has to be tested in the bone marrow to provide the cells with further survival and proliferation signals. The stromal cells in the bone marrow have the capability to check the pre-B-II cells for the heavy chain expression. Pre-B-II cells express a pre-BCR bound on the cell membrane composed of the newly recombined heavy chain and instead of a κ or λ light chain two special proteins called VpreB and λ14.1 (also called λ5). Taking the roles of signaling proteins CD79A (Igα) and CD79B (Igβ) are clustered to the receptor [50,51]. To test the expression of the heavy chain, stromal cells are secreting Galectin-1, which is able to bind to the λ14.1 on pre-B-II cells and at the same time to α4β1 α5β1 α4β7 integrins on the pre-B-II and stromal cells [52-54]. The binding of Galectin-1 to the stromal cell and the pre-B-II cells leads to clustering of the pre-BCR that finally induces a signal for survival [54,55] (Figure 6). It is very important for precursor-B cells to check the signal capacity of the BCRs for the further maturation and selection steps of the B cells [13].

After this positive selection the recombination of the light chain starts. As already mentioned above there are two different light-chains present namely κ and λ. Interestingly, the light chains are not expressed in equal amounts, but there is a clear bias towards the κ light chain [56]. In humans the κ/λ ratio is 3/2 whereas it is 20/1 in mice. In the case of a λ light chain-positive B cells both kappa light chain loci are either not in frame or the produced light chain is autoreactive and deleted [25]. This indicates that the rearrangement of the λ light chain occurs later in the B cell development than the κ light chain rearrangement [25,57,58], which gave a first hint for a negative selection at this stage of the B cell development (Figure7). Wardemann *et. al* could show that the replacement of a light chain in the case of an autoreactive antibody can reduced the reactivity to a model antigens [59].

During early B cell development the process of rearranging the light chains to create new variants of the BCR is called receptor editing. This step is necessary if the newly formed BCR has a high avidity for self-antigens [59,61-65]. Receptor editing is a frequent event in the development of pre-B-II cells in the bone marrow. Between 20-50% of all developing B cells undergo receptor editing [61].

If the BCR crosslinks with the self antigen on the stromal cells a new round of light chain rearrangement starts [66]. Until today it is not known how the stromal cell present the autoantigen to the BCR of the immature B cells [66]. First the second kappa allele is rearranged and if the BCR is still autoreactive

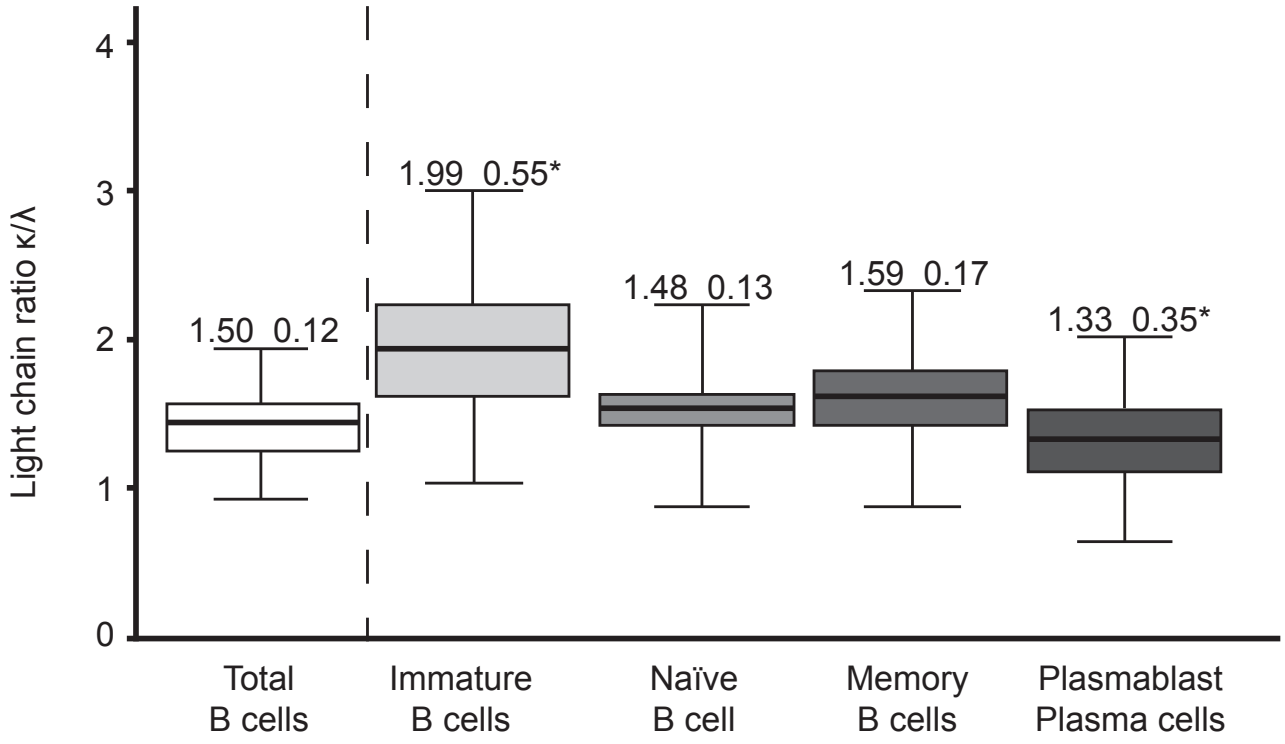

Figure 7: κ/λ ratio in different B cell lineages in humans

The checkpoints during the maturation of B cells lead to changes in the distribution of κ/λ light chains. Numbers express mean values +/- one standard deviation. The figure is adapted from [60]

the lambda chain locus starts to rearrange [25,67]. Wardemann showed in 2003 that more then 70% of the antibodies expressed by early immature B cells show self-reactive binding to different model antigens like ssDNA, dsDNA, LPS, Insulin and HEp-2 cells [62]. About 45% of these self-reactive antibodies can be silenced *via* light chain exchange [59].

These self-reactive antibodies are further distinguished into two subgroups. The first subgroup is named polyreactive with binding to ssDNA, dsDNA and LPS and the second subgroup is referred to as autoantibodies, which binds to protein-derived self-antigens like Insulin and stains the human cell line HEp-2 and binds to lysate of these cells. The strength of the checkpoint can be seen as an impressive drop of polyreactivity from 55% of immature B cells to 7% in the T1, T2 and mature naïve B cell stages in the blood (Figure 8) [62].

If the B cells still do not pass the autoreactivity test from the stromal cells due to BCR crosslinking with self-antigens on stromal cells, the cells will undergo apoptosis, turn into an anergic B cells or the cells have to undergo a new IgH VDJ recombination [68-71]. However a new VDJ recombination is not that trivial because all the 12bp RSS were deleted on one or both alleles during the first recombination event [72-74].

Due to selection, the amount of immature B cells that are able to leave the bone marrow is very small. Only 10-20% are finally ending up in the periphery to undergo further maturation. This strong selection reduces the autoreactivity of the immature B cells by half [75,76] (Figure 8). However some autoreactive B cells do escape *via* the expression of two different light chains or two BCRs and in certain cases the B cells still express the V-pre-B light chain, which has an isoelectric point of 5.67 and might neutralize the positive charge of the heavy chain [77,78] thereby neutralizing positive charges of variable regions, which are thought to be responsible for the binding to negatively charged DNA [62].

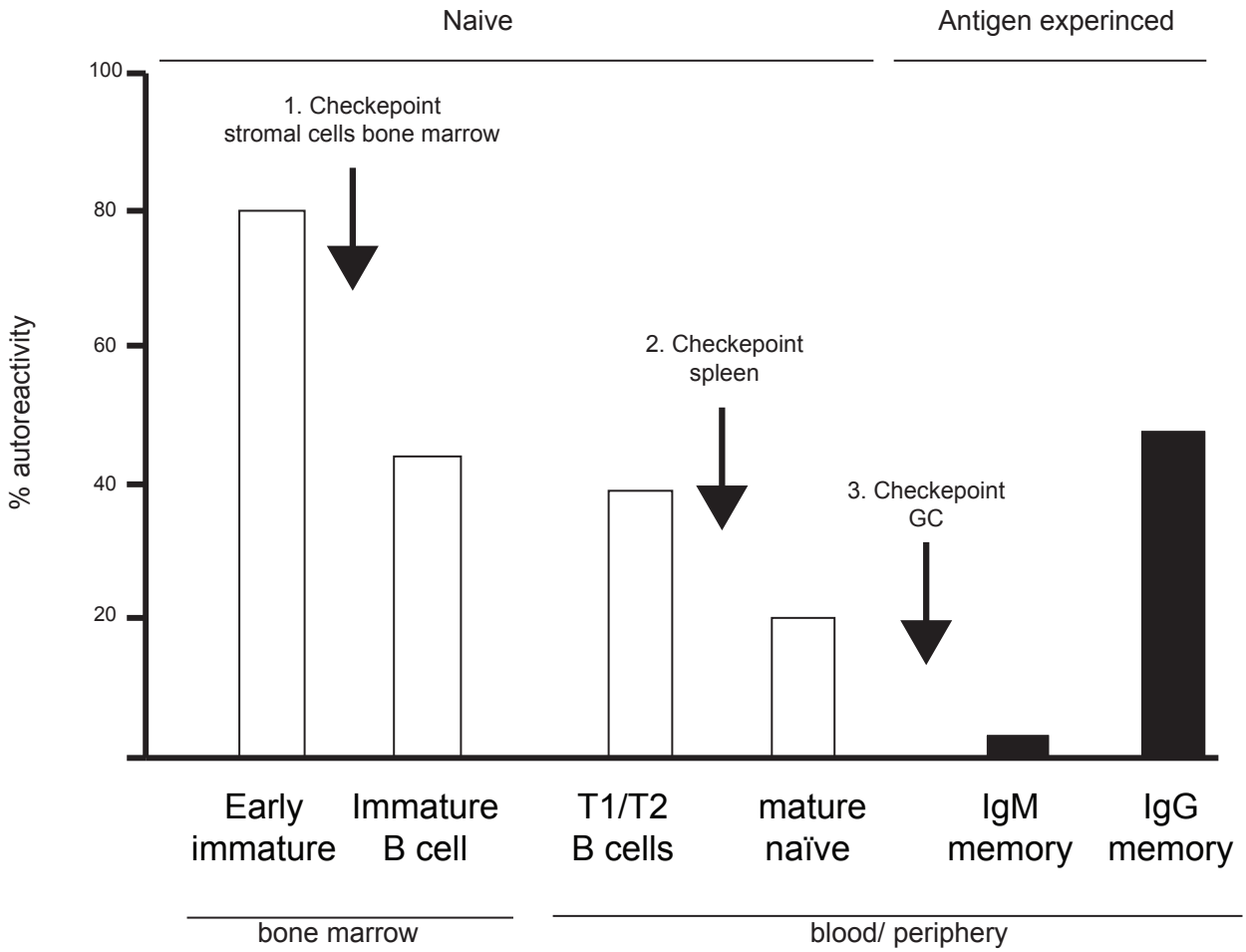

Figure 8: BCR autoreactivity of B cell

BCR autoreactivity is reduced after passing the different checkpoints during the development of B cells: Different maturation stages of B cells were single-cell sorted and the individual antibodies recombinantly expressed and tested for autoreactivity in an ELISA based on HEp-2 lysate. There are decreases of the autoreactivity after each checkpoint and an increase after the GC reaction. This increase is due to SHM, which are randomly introduced in to the variable region of the BCR. The graph was adapted from [75]

After immature B cells pass the checkpoints in the bone marrow they will migrate *via* the central sinus into the blood stream [79,80]. In the blood the new emigrants mature *via* the transitional stage T1-T2 towards the mature naïve stage [81-83]. In mice and humans the immature T1 stage is present in the bone marrow, blood and spleen; while in mice the T2 stage is restricted to the spleen [84], in humans the T2 stage is less stringently located to the spleen. T2 cells are able to develop outside of the spleen in splenectomized humans [85]. Since the self-reactivity of the new emigrants is not removed sufficiently yet, the B cells in the transitional stage have to pass an additional negative selection point in the spleen. Between the T1/T2 and the mature naïve stage self-reactivity is reduced again by half, down to 20% [62,86] (Figure 8). Further evidence for a checkpoint comes from the differences in sensitivity of BCR crosslinking in the two different transition stages. T1 is highly sensitive for BCR crosslinking and undergoes apoptosis. T2 in contrast gets activated and turns in a mature naïve B cell phenotype [87,88].

After the checkpoint in the spleen the T2 B cells further develops into a mature naïve B cells. What the checkpoint is composed of is still under debate. Data from mice suggested that the signal strength of the BCR either induces survival or cell death in T1 B cells [89-92] and an involvement of FcγRIIB [93] and the TNF-families members BAFF and APRIL [94] was also reported. BAFF signaling induces survival of B cells and an excess of BAFF/BAFFR signaling can promote the survival of autoreactive B cells [95-97].

Mature naïve B cells can develop in two different directions [13]. Either the cells mature T cell-independently in the gut and the marginal zone of the spleen or the cells pass through the GC where they undergo follicular helper T cell (T_{FH}) dependent maturation [13].

In the GC the B cells undergo the last checkpoints before entering the memory and plasma cell compartment [75]. Before the mature naïve B cells enters any of the three pathways they have to be activated by an antigen. *Via* Toll-like receptor engagement or BCR crosslinking with a multi-epitope antigen the mature naïve B cells can mature in a TI way [98-102]. Overexpression or activation of Toll-like receptors have the capability to rescue anti-DNA and -RNA autoreactive B cells from negative selection [103].

For a better representation of the two pathways I will split them in subchapters. One part sheds light on the T cell-dependent affinity maturation in the germinal centers and the other part on the TI maturation of the two linages $CD27^{+}IgA^{+}$ and marginal zone B cells (MZ). But before we start with the GC reaction, we have to understand the class switch recombination, which is a very important step in the final maturation of the B cell.

Class switch recombination:

In GC and in the gut the $CD27^{+}$IgA2 B cells undergo class switch recombination to exchange the constant part of the antibodies. The different constant parts are called isotypes. These isotypes have distinct functions within the immune system due to their binding affinity to cell surface receptors recognizing the constant part of the heavy chain (Fc-receptors), different activation of the complement system and due to varying accessibility to different compartments (Table 1). Poltooralsky *et. al* established the basic principles of class switch recombination model in 2000 [105-107]. During the B cell development the DNA recombination is a complex and fragile event that has to be carefully controlled by the cells to avoid translocation mistakes, which can lead to malignant transformations. One of the most common translocation mistakes is the translocation of the oncogene c-myc under the Igh promoter. This translocation is often responsible for B cell lymphomas . The main enzyme involved for the malignant transformation in B cells is activation-induced cytidine deaminase (AID)[108-110].

The CSR mechanism is based on an intrachromosomal deletion recombination between switch (S) regions that are located 5` of the heavy chain constant region sequence (Figure 9). These regions have a special nucleotide motive containing 20-80 bp Guanine (G)-rich tandem repeats on the nontranslated DNA strand. The recombination site between the two S regions is very flexible and occurs near or within the S region[111-113]. CSR is induced *via* activation of B cells by cytokines such as interferon-(IFN)-γ, interleukine (Il)-4 or transforming growth factor-(TGF)-β and in the case of T cell independent class switch (TI) *via* Toll-like receptors (TLR) [101,102]. These activation signals lead to the expression of AID by regulatory factors like paired box protein 5 (PAX5), E-box proteins [114], homeobox C4 (HOXC4) [115], interferon regulatory factor (IRF)-4 [116] and fork head box O1 (FOXO1) [117]. AID deaminates deoxy Cytidine to deoxyuracil (dU) together with the protein 14-3-3 [118-124]. The protein 14-3-3 is important for the recruitment of AID to the donor and acceptor S region. The recruitment is achieved *via* the specific binding of the protein 14-3-3 to the repetitive S region motive 5'-AGCT-3 [124]. The deamination of the deoxycytidine activates the base excision repair enzyme uracil DNA glycosylase (UNG), which removes the dU residues and introduces a SSB [125,126].

Sequentially after the action of UNG the apurinic/apyrimidinic endonuclease APE1/2 nicks the DNA a second time and introduces double strand breaks (DSBs) [127]. These DSBs are then ligated *via* the ubiquitous non-homologous end-joining (NHEJ) DNA repair machinery composed of Ku70, Ku80 and XRCC4-ligaseIV to the acceptor S region [45,128-130].

Finally the B cell changed the isotype of the BCR but not the avidity of the variable region. The way how a B cell decides, which isotype switch it has to perform is still not known. There is evidences that during the GC reaction the cells receive certain stimuli to switch to the right isotype [131]. This will be explained in more detail in the next chapter.

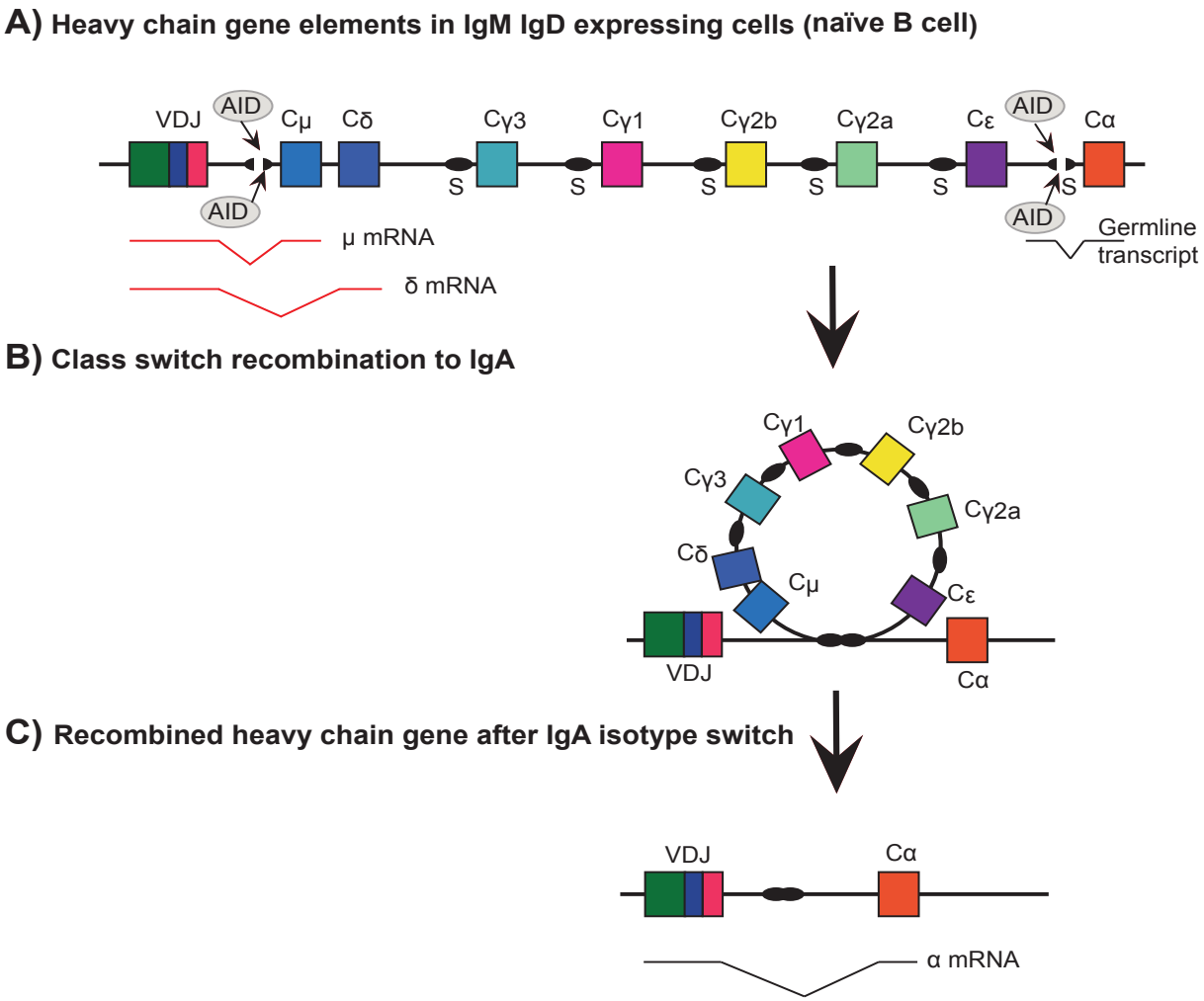

Figure 9: The distribution of the different constant region isotype classes for the human IgH on the chromosome 14

A) Represents the already recombined variable region (pink box) followed by a nicked switch S region and the sequence for the Ig isotype constant regions C*μ* (coding for IgM) and Cδ (coding for IgD), which are expressed simultaneously in the cell until the first CSR. These are indicated by the two mRNAs *μ* and δ (red line). The other isotype constant parts are located 3' from Cδ with the corresponding S regions 5' from the corresponding constant region. **B)** shows the recombination of the two nicked S regions after the variable region (VDJ) and before the Cα. Now a DDS break is introduced and the DNA is religated. **C)** the new immune globulin isotype is expressed. Adapted from[104]

The Germinal center reaction:

Walther Flemming first described the GC in 1884 as a very dense and hyperproliferative area. He speculated that the lymphopoiesis occurs in these regions. In fact the GC is a microanatomical structure in secondary lymphoid organs where the adaptive B lymphocytes are selected for recognition of a specific antigen, while retaining self-tolerance. The maturation of the adaptive immune system is highly dependent on the reactions taking place in the secondary lymphoid organs. A complex interaction with stromal cells, dendritic cells (DC), macrophages and antigens support the development of antigen specific B and T cells (Figure 10). Naïve T cells develop to memory T cells, effector T cells and T_{FH}. Antigen-specific activated mature naïve B cells acquire a memory B cell phenotype, affinity mature the BCR *via* somatic hyper mutation and eventually switch to different isotypes and further develop into antibody secreting plasmablasts and/or plasma cells. The major part of B cell development in the secondary lymphoid organs happens in the GC reaction. A GC follicle is a structure that is stable for more than 3 weeks where B cells undergo several rounds of selection, affinity maturation and proliferation (Figure 12). Antigen-specific memory B cells are able to enter the GC reaction more than once. Especially after an antigen recall second GC reaction can be formed [132,133] (Figure 12D). It is very characteristic for class switched B cells that they can only reach the memory compartment after interacting with T_{FH} cells (Figure 12). T_{FH} cells have the only sole purpose of checking indirectly the BCR for its antigen specificity. The whole anatomical structure of secondary lymphoid organs is made for capturing, concentrating and presenting antigens to support proliferation and selection of the adaptive immune system (Figure 11). This is why the GCs are located in the secondary lymphoid organs namely spleen, Peyer's patches, tonsils and lymph nodes, where the chances to encounter antigens and pathogen is the highest. In this section the focus will be on the GC in lymph nodes.

The lymph node is a secondary lymphoid organ with a fibrous capsule, which connects the lymphatic system and the blood stream. The capsule has afferent lymph vessels where the interstitial fluid enters the lymph node and efferent vessels to drain the lymph node (Figure 10A). The inner part of the capsule where the afferent lymph vessels enter the lymph node is called the subcapsular sinus. The area where the blood enters and leaves together with the efferent lymph vessels is called medulla. These two regions contain two types of macrophages.

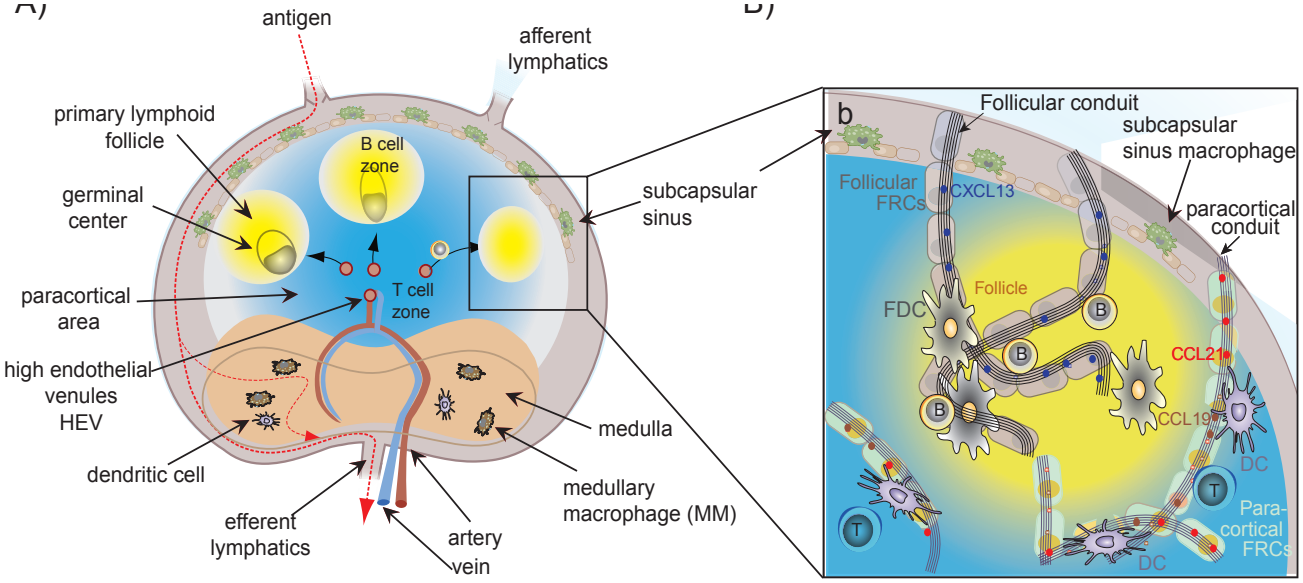

Figure 10 The anatomy of a Lymph node

A) Illustrates the different microanatomical structures of a lymph node in blue the T cell zone, in yellow the B cell zone, in grey the subcapsular sinus together with the afferent and efferent lymphatic vessels, in green the subcapsular macrophages and in brown the medulla. **B)** shows the follicular conduit where fibroblastic reticular cells (FRCs) and the follicular dendritic cells (FDCs) are attached to the collagen fibers of the conduit. Close to the paracortical conduit the dendritic cells are located. The B cells and T cells move along the conduits, which have the corresponding chemokines bound. Blue dots stand for the B cell chemokine CXCL13 and in red and brown the T cell chemokines CCL21 and CCL19, respectively.
Figure adapted from [141,187]

The first type is located at the afferent part of the lymphatic vessel and called the subcapsular sinus macrophages ($CD169^+$ $CD11c^{lo}$ $CD11b^+$) (SSMs) or (SCSs). In the medulla the medullary macrophages (SIGN-$R1^+$ $F4/80^+$) (MMs) are located [135-137] (Figure 10). The SSM protect the lymph node from direct contact to pathogens and support the antigen sampling in the afferent lymph [134]. The two different macrophages vary in their endocytic activity and the lysosomal degradation of pathogens [134]. SSMs retain the pathogens much longer on the surface than MMs and have a less mature phenotype [135,136,138]. This properties of SSMs might be important for retaining the antigens longer in the lymph node therefore allowing its presentation to B cells much longer, which will be important for the distribution of the antigen through the B cells in the antigen transport part (Figure 11) [134]. In general the two macrophages are important to protect the host from systemic

distribution of pathogens [139,140].

Below the subcapsular sinus the lymph node is filled with fibroblastic reticular cells (FRCs) of two different types: the follicular conduits (B cell zone), the paracortical conduits (T cell zone) and marginal reticular cells (MRCs) (Figure 10B) [134]. These cells are important to provide the

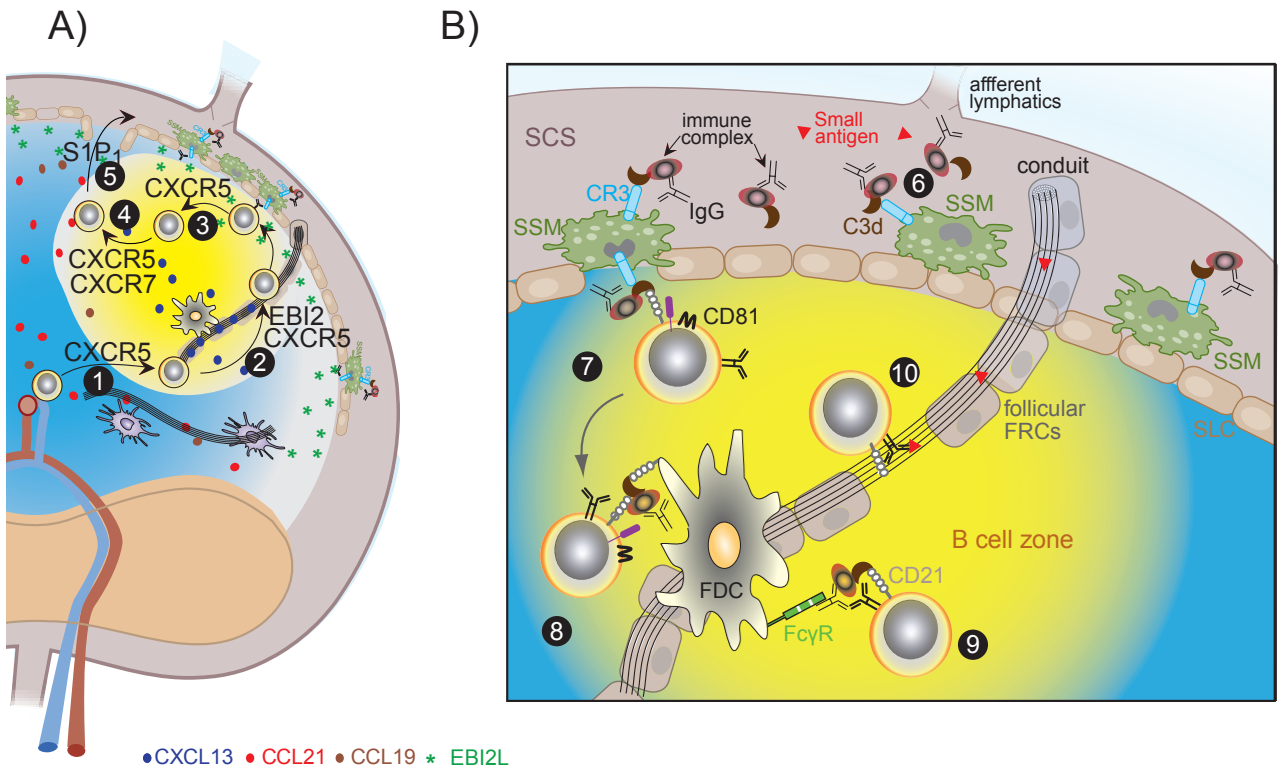

Figure 11: The movement and antigen interaction of the B cell in the lymph node

A) 1. After a B cell enters the lymph node through a high epithelial venule the chemokine receptor CXCR5 attracts the B cell along the CXCL13 gradient to the B cell follicle. **2.** In the B cell zone the cell moves along the conduit and expresses the EBI2 receptor. The EBI2 receptor attracts the B cell to the supcapsular sinus where the EBI2L ligand is present at highest concentration. **3.** The cell down-regulates the EBI2 receptor and moves away from the subcapsular sinus, loaded with immune complexes either on the CD21 or the BCR receptor. **4.** The cell strolls back to the center. On the way to the center of the B cell zone the cell looses the previously CD21-bound antigen to FDCs and upregulates the chemokine receptor CXCR7. **5.** Finally, the B cell leaves the lymph node *via* the Sphingosine 1 phosphate (S1P) signal. The figure is adapted from [143]: **B)** 6. The binding of complemen-bound immune complex (IC) to the complement receptor 3 CR3 on the SSMs. The IC is then shuttled to the inner site of the subcabsular sinus. **7.** The B cell interacts with the complement receptor CD21 and the bound IC in the SSM. **8.** The IC detaches from the SSM. The IC-loaded B cell moves through the follicle and deposits the IC on FDCs. **9.** An alternative to the CD21 binding of the IC is the binding *via* the FcR. **10.** An antigen specific B cell captures a small soluble antigen from the conduit. The figure is adapted from [134]

infrastructure and to guide the B and T cells between the different microanatomical structures. The FRCs produce type 1 collagen fibers which are called conduits. The collagen fibers, form a robe-like structure of 1-2 μm in diameter, where B and T cells can crawl along [141,142].

Near the conduits the follicular dendritic cells (FDCs) and FRCs produce chemokine gradients, which guide B and T cells along the conduits to different locations in the lymph node. The FRCs of the follicular conduits produce a chemokine gradient of CXCL13 together with MRCs to attract the B cells towards the subcapsular sinus region (Figure 10B and 11) [134].

Interestingly, the chemokine CXCL13 has a high affinity to collagen fibers and concentrates along the collagen fibers, which facilitates the movement of the B cells[144]. Furthermore the CXCL13 production is highly dependent on the lymphotoxin-α1β2 production of B cells, which leads to a positive feedback loop and increasing the production of both chemokines [145]. FRCs and FDCs in the paracortical conduits transport CCL19 and CCL21 to guide T cells and dendritic cells along the collagen fibers to the paracortical region [146-149]. This is where the naïve CD4 T cells develop to effector, memory and T_{FH} by encountering the processed antigen as a peptide on the MHC II of dendritic cells [150]. The T cells with the highest TCR-binding affinity to the bound peptide on MHC class II receive a signal to up-regulate CXCR5 and subsequently enter the T_{FH} maturation pathway [151]. The pre-GC T_{FH} cell waits at the T/B zone interphase until an activated naïve B cell with the affinity for the corresponding antigen arrives (Figure 12A). Together the cells start to form the immune synapse [155]. The scanning of activated B cells in the T/B interphase by the T_{FH} cells is important to reduce auto-reactivity of memory B cells. Several studies could show that autoreactive B cells are enriched in the T/B interphase zone [152-154].

The immune synapse has a bilateral effect, B and T cells receive co-stimulatory signals together with cytokine signals, which lead to further maturation of the T_{FH} and B cells [156]. The B cells either mature into short-lived plasma cells or follicular B cells, which then end up as GC B cells (Figure 12B) [157].

During the immune synapse formation the T_{FH} screens the peptide-loaded MHC-class-II molecules on the B cells for the right peptide. Peptide recognition induces a positive feedback signaling, which induces the upregulation of co-stimulatory molecules such as CD40L/CD40[106,158,159], (CD80/CD86)/CTLA-4[160], OX40/OX40L[161], ICOS/ICOSL[162]. T_{FH}-derived IL-21 and ICOS/ICOSL interaction induce expression of the factor B cell lymphoma 6 (Bcl-6) in both cells, which is important for T_{FH} and B cells maturation to form the GC reaction [163-166] (Figure 12B).

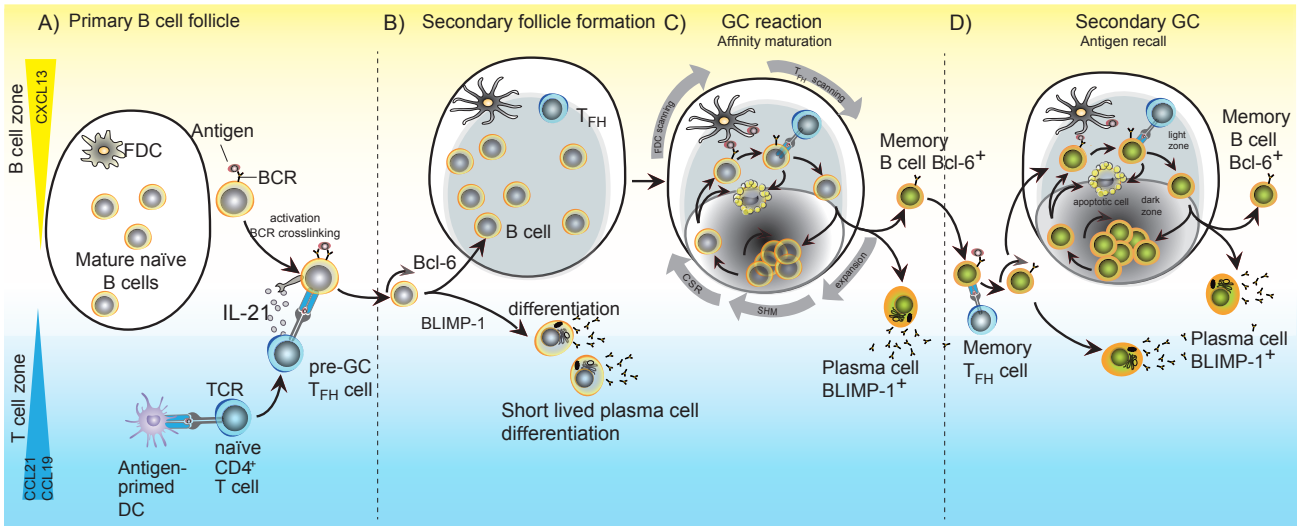

Figure 12: Induction of a GC reaction

A) Antigen activated B cell leave the B cell zone and processes the antigen for further presentation to the antigen specific T_{FH} cell at the border of T and B cell zone. During the B/T cell interaction of the pre-GC T_{FH} cell releases Il-21 and mature to a GC-T_{FH} cell by Bcl-6 expression. **B)** The Bcl-6 B cell starts to proliferate and form the secondary follicle while BLIMP-1 B cell develops to short lived plasma cells in the extra follicular space. **C)** The Bcl-6 B cells polarize and divide the follicle into a hyper-proliferative dark zone that contains centroblasts and a light zone with activated follicular dendritic cells (FDC), a few B cells which are here called centrocytes and GC T_{FH}. This polarization induces the GC reaction **D)** After antigen re-challenge the already mature memory B cell pool can start to form a secondary GC reaction and further mature and produce new variants of memory and plasma cells. The figure was adapted from [157]

Alternatively, B cells start to express B lymphocyte-induced maturation protein 1 (BLIMP-1 or PRDM1), which leads to short-lived plasma cell differentiation without GC formation and no SHM but eventually with CSR in the extrafollicular space [167]. Furthermore IL-21 induces the proliferation of B cells [168] (Figure 12A and B), which is very important to fuel the GC with enough B cells before the SHM starts [169]. Before the initiation of GC reaction, proliferating B cells start to form the secondary follicle composed of Bcl-6-positive B cells, FDCs and T_{FH} cells (Figure 12B) [157]. After the secondary follicle is formed, it starts to polarize into a light zone containing antigen-loaded FDCs together with antigen-scific GC-T_{FH} and a dark zone with proliferating B cells [170]. Now the GC reaction starts and high affinity class switch memory B cells and plasma cells are generated (Figure 12C and D).

Plasma cells - the effector B cells

The last step in the development of B cells is the stage when all the checkpoints are passed and the cells turn into a highly productive antibody-secreting phenotype. This state of maturity is called plasma cells. B cells have two developmental routes to enter the plasma cell compartment. The first one is the extra-follicular route (MZ in the spleen and T/B cell border in lymph nodes), which is less controlled than the intra-follicular pathway. In the extra-follicular space B cells mature to plasma cells due to relatively high affinity of the BCR for an antigen and generate short-lived plasma cells [171]. This fast response is important to generate the early response against pathogens. Since the short-lived plasma cells are less controlled by checkpoints the secreted antibodies might be cross-reactive (Figure 12 and 8) [75]. To protect the organism from autoreactive antibodies the cells will only survive for 3 days. In contrast to the extra-follicular pathway the intra-follicular differentiation produces long-lived plasma cells, which secrete high-affinity CSR antibodies [157]. The BLIMP-1 expressing plasma cells up-regulate the chemokine receptor CXCR4 and migrate to the bone marrow where the cells searche for a niche between the stromal cells.

The principle mechanism for the maturation of short-or long-lived plasma cells is similar. Due to IL-21 stimulation B cells start to up-regulate the expression of interferon regulatory factor 4 (IRF4). The amount of IRF4 expression influences the expression level of different proteins like AID [116] and at high levels IRF4 induces the expression of BLIMP-1 [172]. Blimp-1 is the master switch regulator for plasma cell differentiation, which sequentially downregulates the Bcl-6, AID and the PAX5 expression [173-175]. A negative feedback loop of BLIMP-1 changes the fate of the cells towards the plasmablast/plasma cell lineage and upregulates the X-box-binding protein-1 (Xbp-1) [176]. Xbp-1 is necessary to handle the high amount of antibody that plasma cells produce, which leads to an increase of the unfolded protein response.

Anti-MAG neuropathy

Anti-MAG neuropathy is an autoimmune disease, which is characterized by IgM antibodies recognizing myelin-associated glycoprotein (MAG), which is a component of the nervous system [177,178]. In anti-MAG neuropathy patients the production of anti-MAG IgM antibodies is associated with an IgM-monoclonal gammopathy of unknown significance (MGUS) [179]. IgM-MGUS is defined by a serum concentration of a monoclonal IgM <30g/l, the amount of clonal plasma cells in the bone marrow is less than 10% and the absence of end-organ damage due to plasma cell proliferation [180]. An important criterion is the absence of any evidence of multiple myeloma, macroglobulinemia, amyloidosis or similar plasma cell proliferative disorders [181]. In general, MGUS does not necessary involve a malignancy. The incidence of monoclonal gammopathy is increasing in aging humans with 3% in patients >70 years [182] and 10% in individuals >80 years [183].

The risk for a MGUS carrier to develop a malignant stage is 1% per year [180]. Predominantly males between the ages of 40-70 years are affected by anti-MAG neuropathy [181,184].

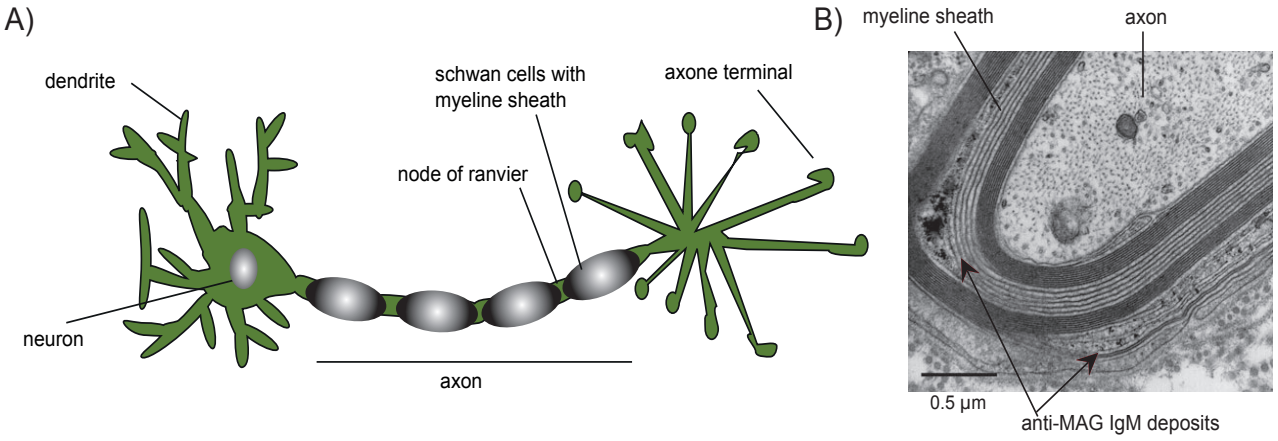

Figure 13: IgM deposits between the myelin sheath

A) Illustrates an axon wrapped with myelin sheaths from Schwann cells. **B)** Electron microscopy picture of anti-MAG neuropathy biopsy with IgM kappa paraprotein deposits in the myelin sheath. The figure is adapted from [180]

MAG is expressed on myelin-producing cells like Schwann cells in the peripheral nervous system (PNS) and on oligodendrocytes in the central nervous system (CNS) (Figure 13A). Due to the binding of the IgM antibody to MAG, the antibody forms aggregates and induces a widening of the myelin sheath (Figure 13B)[185] or leads to inflammation, demyelination and axonal degeneration *via* activation of the complement system (Figure 14B). The damage to the myelin sheaths around the axon reduces the nerve conductivity and slows down the transmission of nerve impulses [180] (Figure 13). This leads to reduced sensory and motor function in the PNS and beginning first in the distal extremities and later extending to proximal extremities. Usually the symptoms start in the toes and spread to the feet and legs. The symptoms resulting from the loss of nerve conductivity usually progress symmetrically and include primarily sensory loss, paraesthesia, loss of vibration sense and proprioception, subsequently leading to sensory ataxia, muscle weakness, tremor of the hand and areflexia. The disease course is slowly progressive over some months to several years [180,181,184].

The diagnosis of the disease is accomplished by electroephysiology of the PNS, histology of nerve fibers, serum IgM anti-MAG antibody titer, free light chains in the urine and serum protein electrophoresis for the monoclonal IgM paraprotein [180,186].

Tested therapies for the anti-MAG neuropathy are plasma exchange, intravenous immunoglobulin application (IVIG), chlorambucil, cyclophosphamide, fludarabine, cladribine, interferone-alpha and autologous bone marrow transplantation. Unfortunately, all of these therapies do not lead to a scinificant benefit for the patients [180,187]. The lack of therapeutic agents led to the idea of using Rituximab, which is a chimeric monoclonal antibody against CD20. CD20 is a pan B cell marker and Rituximab depletes B cells in the periphery (Figure 14A). The clinical efficacy and safety of this antibody is now in clinical trial phase 3 (RIMAG study http://clinicaltrials.gov/ct2/show/NCT00259974) for Anti-MAG neuropathy.

Rituximab

Rituximab is the first therapeutic monoclonal antibody (mAb), which was approved by the food and drug administration (FDA) in the USA for the treatment of B cell lymphomas [188] and later on for the autoimmune disease RA. More recently, Rituximab received FDA approval for the treatment of patients with granulomatosis with polyangiitis (Wegener's granulomatosis) and microscopic polyangiitis. Today it is often used in off-label studies, for other autoimmune diseases like, SLE, idiopathic thrombocytopenic purpura, myasthenia gravis, inflammatory neuropathies, multiple sclerosis and in this case anti-MAG neuropathy [189].

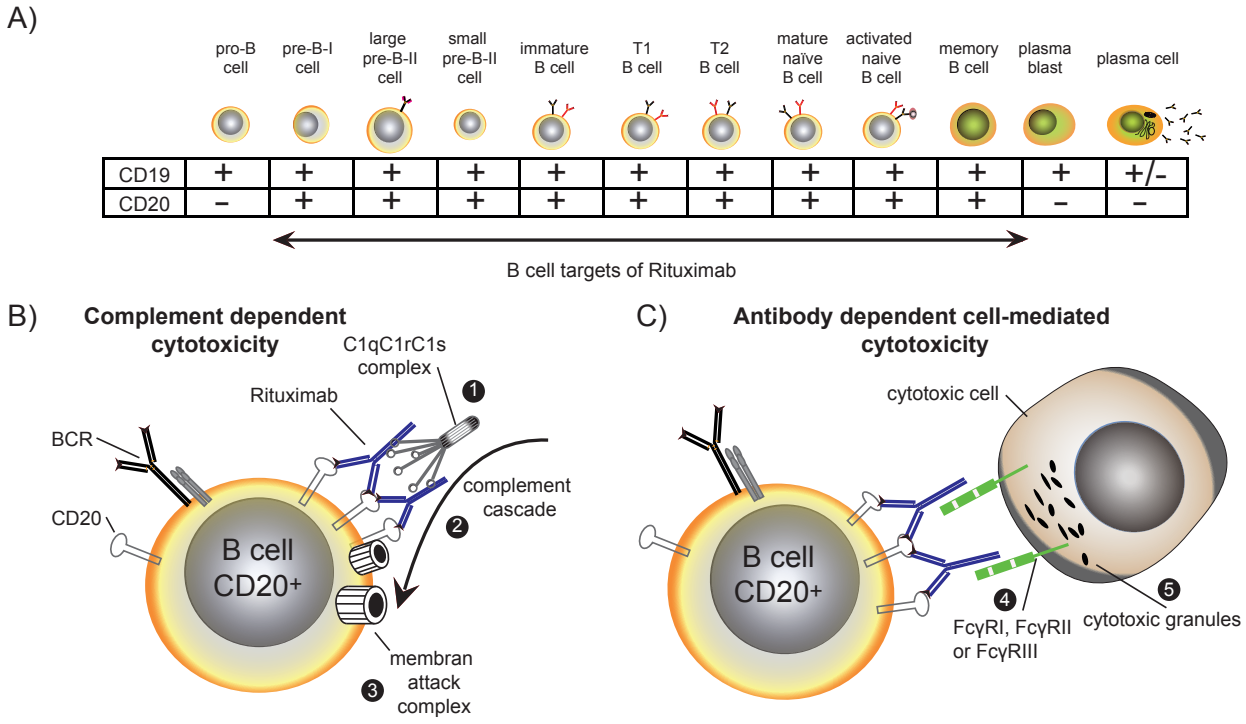

Figure 14: Pan B cell markers and the action of Rituximab

A) All the B cells with CD20 on the surface can theoretically be depleted by Rituximab starting from the pre-B-I cell and ending at the memory B cell stage. The figure is adapted from[189]. **B)** Illustration of complement-dependent cytotoxicity. **1.**Rituximab binds to CD20 the complement complex C1qC1rC1s assembles on the Fc part of Rituximab. **2.** The C1qC1rC1 catalyze the processing of C4, C2 and C3, which lead to the deposition of C3b convertase. **3.** The C3b convertase processes additional complement factors (C5b, C6, C7, C8, C9) that lead to the membrane attack complex and lyse the cell. **C) 4.** The FcR of the cytotoxic cell recognizes the bound Rituximab. **5.** The cell polarizes and releases cytotoxic granules, which induce apoptosis of the cell. Figure is adapted from [191]

The suffix stem -xi indicates that Rituximab is a chimeric antibody derived from an anti-human CD20 mouse mAb and genetically engineered on the basis of the sequence of a human constant region [190]. CD20 is a pan B cell marker, which is expressed on immature and mature B lymphocytes and lost upon plasma cell differentiation [189] (Figure 14).

The human constant part used in this particular mAb is IgG1, which is able to eliminate antibody target cells in the blood (Table 2). A single course of Rituximab leads to depletion of B cells from peripheral blood for 6–12 months [189]. IgG1 has two major pathways to deplete cells (see table 1). The first pathway is the complement-dependent-cytotoxicity (CDC) [192]. Rituximab binds and redistributes CD20 to lipid rafts allowing antibody clustering [193]. Subsequently, C1q binds to the constant part of the clustered antibodies and initiates the complement cascade that finally lyses the target cells (Figure 14 B) [194,195].

The second mechanism is the antibody-depended cell-mediated cytotoxicity (ADCC). During ADCC the antigen-bound antibodies on the target cells binds to activating FcγR on myeloid cells in particular monocytes/macrophages and lymphoid NK cells. The binding of the antigen-bound antibodies to the FcγR activates the NK cells and induces cell death of the target cells (Figure 14 C) [2]. It is still under debate, which of the two pathways is the more important for Rituximab efficacy. In certain studies Rituximab showed less efficacy due to a FcγR polymorphism, which reduces the binding affinity of the Fc-part of the mAb to the receptor [196-199]. These studies underline the strong ADCC component for the B cell depletion of Rituximab.

Since the first generation of anti-CD20 antibody showed a high efficacy in depleting B cells, while still some patients are not responding to it the search for better mAb is ongoing. Nowadays the third generation of anti-CD20 antibodies is in the last step of the clinical phase III study. The novelties of these antibodies are that their variable region is fully human and the Fc domain is mutated to enhance the binding affinity to the FcγR. These improvements should reduce the side effects of Rituximab treatment as an immune reaction towards the murine parts of the antibody can develop and enhanced FcγR binding should enhance ADCC dependent depletion [200].

The aim of the study

The rationale for B cell-depleting therapies in autoimmune diseases has been the concept that immune depletion could eliminate autoreactive B lymphocytes and that a de novo regeneration of B cell memory from pro-B cell precursors - which do not express CD20 - could reestablish tolerance. However, no study has demonstrated that B cell-depleting therapies can actually reconfigure B cell memory through detection of phenotypic or functional renewal of the B cell repertoire. Thus, despite its clinical efficacy and widespread use, the mechanisms whereby Rituximab treatment confers its long-term clinical efficacy in patients with autoimmune diseases are unclear [201].

Anti-MAG neuropathy is a well-defined antibody-mediated disease of the peripheral nervous system, which develops in individuals with an IgM monoclonal gammopathy of unknown significance (MGUS) and is characterized by autoreactivity towards MAG, a protein expressed in the peripheral myelin sheaths. IgM anti-MAG antibodies, which are consistently detectable in these patients are very likely pathogenic since their adoptive transfer to susceptible host animals induces peripheral demyelination and symptoms resembling these observed in patients with anti-MAG neuropathy[202-205]. Thus, anti-MAG neuropathy stands out among other human autoimmune diseases due to the known identity of the target antigen and a clear disease-association with IgM autoantibodies. Most available immunomodulatory treatments offer only transient benefits to some patients with anti-MAG neuropathy, whereas most remain treatment-resistant [185]. A recent randomized controlled clinical trial demonstrated that Rituximab is, so far, the most effective therapeutic agent providing long-term benefits to a subset of these patients[206]. To understand whether these beneficial effects are mediated by lymphodepletion alone or are sustained by a newly developed peripheral B cell compartment we examined the Ig gene repertoire in patients with anti-MAG neuropathy during Rituximab therapy. To get more insight into the B cell compartment we used single-cell PCR, which has a very high resolution for the different BCR recombinations in different B cell compartments. In this study we analyzed three different B cell compartment before and one year after Rituximab therapy, namely mature naïve B cells ($CD19^+$ $CD27^-$ IgM^+), IgM memory B cells ($CD19^+$ $CD27^+$ IgM^+) and IgG memory B cells ($CD19^+$ $CD27^-$ IgG^+). These three compartments are the main populations in the blood and IgM memory B cells are suspected to be involved in this disease.

Results

Ig gene repertoire analysis during therapeutic B cell depletion

To determine whether Rituximab-mediated B cell depletion leads to significant changes in the peripheral Ig gene repertoire, we amplified and sequenced Ig heavy chain genes (IgH) of single-sorted naïve, IgM memory and IgG memory B cells before and 12 months after therapy. Samples were obtained during a placebo-controlled clinical trial of Rituximab in patients with anti-MAG neuropathy, during which patients were randomized to four weekly infusions of 375mg/m^3 Rituximab or placebo, i.e. normal saline solution [206]. The first point we addressed was the recombination of the antibody heavy chain in different B cell compartments. For this we blasted the single cell PCR-derived IgH sequences against germline sequences and compared the different V_H, D_H and J_H gene segments in amount and percent of usage. As controls we used age-matched healthy controls (Figure 15). To avoid a bias of the analytical bias due to PCR amplification efficiency we calculated the percentage of total derived sequences form all the patients. Single patients are depicted in Figure 16, 17 and 18.

Figure 15: Ig gene repertoire analysis in patients with anti-MAG neuropathy before and 12 months after Rituximab-mediated B cell depletion

Next page: IgH chain gene variable (V) region (Figure 1A), diversity (D) region (Figure 1B), and joining (J) regions (Figure 1C) repertoires in single-cell sorted $CD19^+CD27^-IgM^+$, $CD19^+CD27^+IgM^+$ and $CD19^+CD27^+IgG^+$ B cells, respectively. Samples were analyzed before and 12 months after Rituximab, placebo (normal saline solution) therapy and age-matched healthy controls. Clonally expanded sequences were counted as one sequence. The numbers in circles indicate the number of individual sequences per patient cohort and per time point that were analyzed. Data for each individual donor are provided in Figure 17-19. The two-tailed Fisher's exact test was used to evaluate V_H, D_H, and J_H repertoires.

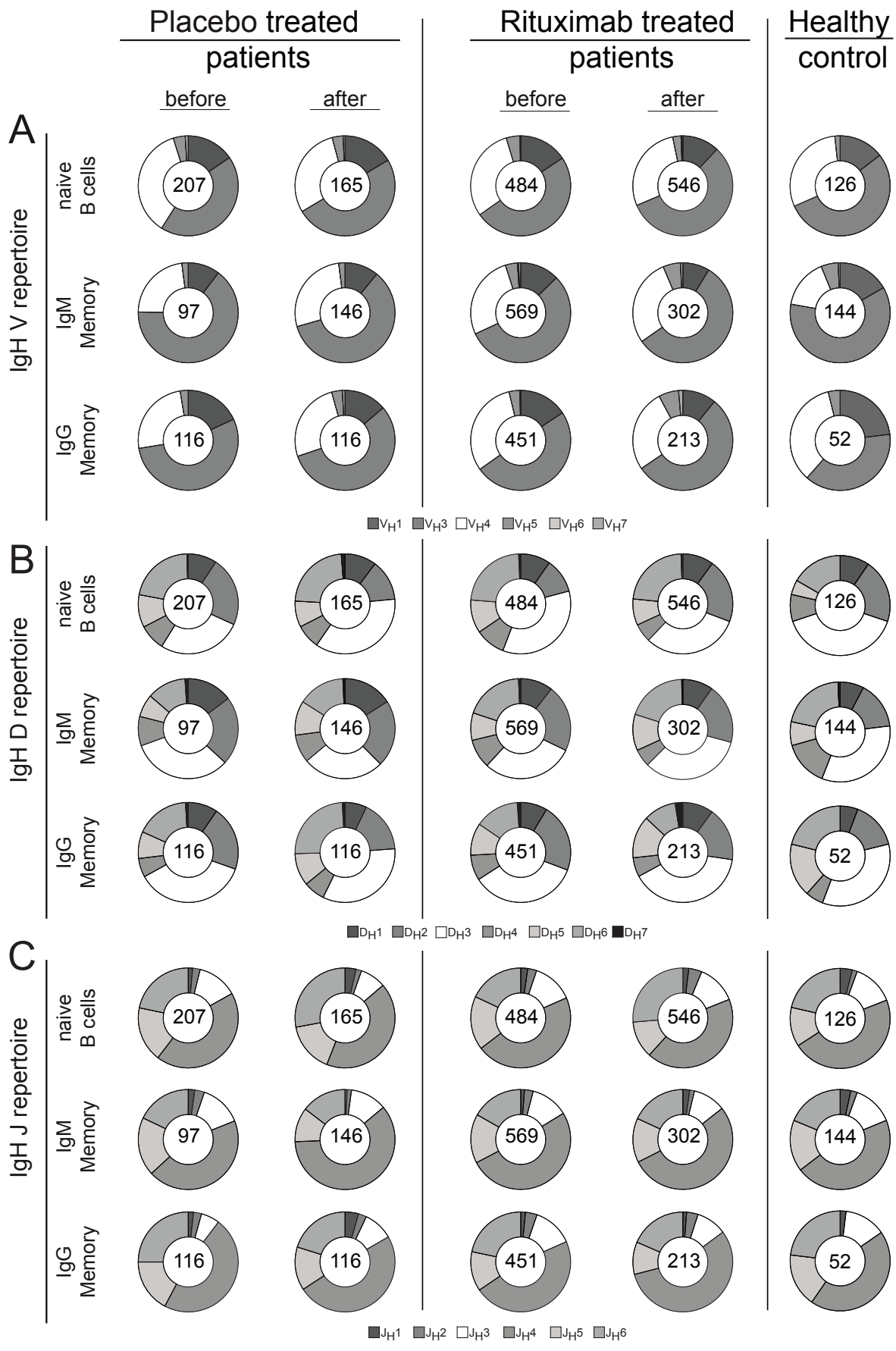
Placebo treated patients
Rituximab treated patients
Healthy control
before
after
before
after
A
IgH V repertoire
naive B cells
IgM Memory
IgG Memory
207
165
484
546
126
97
146
569
302
144
116
116
451
213
52
VH1 VH3 VH4 VH5 VH6 VH7
B
IgH D repertoire
DH1 DH2 DH3 DH4 DH5 DH6 DH7
C
IgH J repertoire
JH1 JH2 JH3 JH4 JH5 JH6

Figure 16: Single patient V_H elements analysis of anti-MAG neuropathy patients before and 12 month after Rituximab treatment

Page 39: IgH chain gene variable (V_H) repertoires in single-cell sorted $CD19^+CD27^-IgM^+$, $CD19^+CD27^-IgM^+$ and $CD19^+CD27^+IgG^+$ B cells, respectively. Samples were analyzed before and 12 months after Rituximab and placebo (normal saline solution) therapy. Clonally expanded sequences were counted as one sequence. The numbers in circles indicate the number of individual sequences per patient.

Figure 17: Single patient D_H elements analysis of anti-MAG neuropathy patients before and 12 month after Rituximab treatment

Page 40: IgH diversity (D_H) region repertoires in single-cell sorted $CD19^+CD27^-IgM^+$, $CD19^+CD27^-IgM^+$ and $CD19^+CD27^+IgG^+$ B cells, respectively. Samples were analyzed before and 12 months after Rituximab and placebo (normal saline solution) therapy. Clonally expanded sequences were counted as one sequence. The numbers in circles indicate the number of individual sequences per patient.

Figure 18: Single patient J_H elements analysis of anti-MAG neuropathy patients before and 12 month after Rituximab treatment

Page 41: IgH chain joining (J_H) regions repertoires in single-cell sorted $CD19^+CD27^-IgM^+$, $CD19^+CD27^-IgM^+$ and $CD19^+CD27^+IgG^+$ B cells, respectively. Samples were analyzed before and 12 months after Rituximab and placebo (normal saline solution) therapy. Clonally expanded sequences were counted as one sequence. The numbers in circles indicate the number of individual sequences per patient.

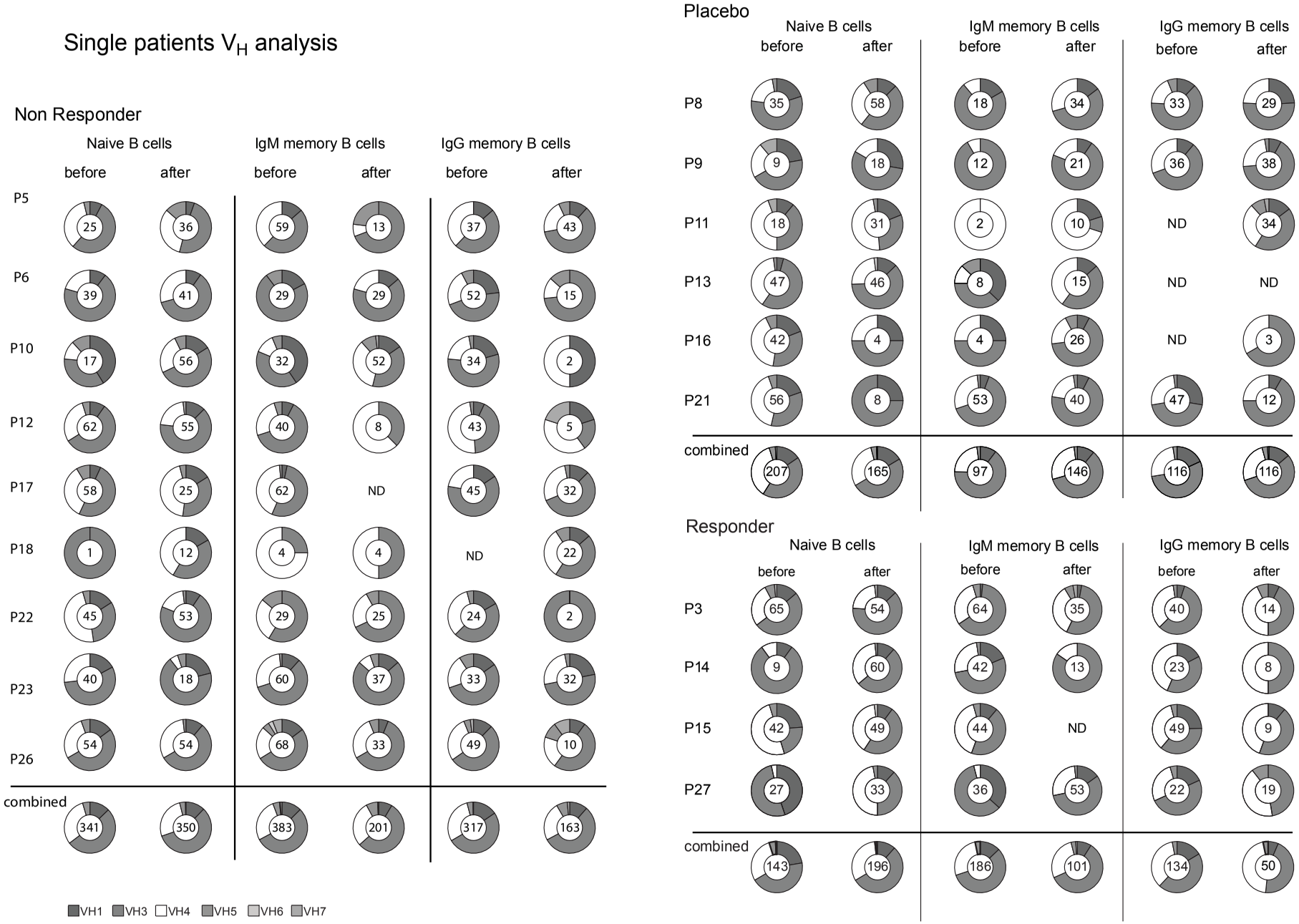
Single patients V_H analysis
Non Responder
Naive B cells
IgM memory B cells
IgG memory B cells
before
after
P5
25
36
59
13
37
43
P6
39
41
29
29
52
15
P10
17
56
32
52
34
2
P12
62
55
40
8
43
5
P17
58
25
62
ND
45
32
P18
1
12
4
4
ND
22
P22
45
53
29
25
24
2
P23
40
18
60
37
33
32
P26
54
54
68
33
49
10
combined
341
350
383
201
317
163
VH1 VH3 VH4 VH5 VH6 VH7
Placebo
Naive B cells
IgM memory B cells
IgG memory B cells
before
after
P8
35
58
18
34
33
29
P9
9
18
12
21
36
38
P11
18
31
2
10
ND
34
P13
47
46
8
15
ND
ND
P16
42
4
4
26
ND
3
P21
56
8
53
40
47
12
combined
207
165
97
146
116
116
Responder
Naive B cells
IgM memory B cells
IgG memory B cells
before
after
P3
65
54
64
35
40
14
P14
9
60
42
13
23
8
P15
42
49
44
ND
49
9
P27
27
33
36
53
22
19
combined
143
196
186
101
134
50

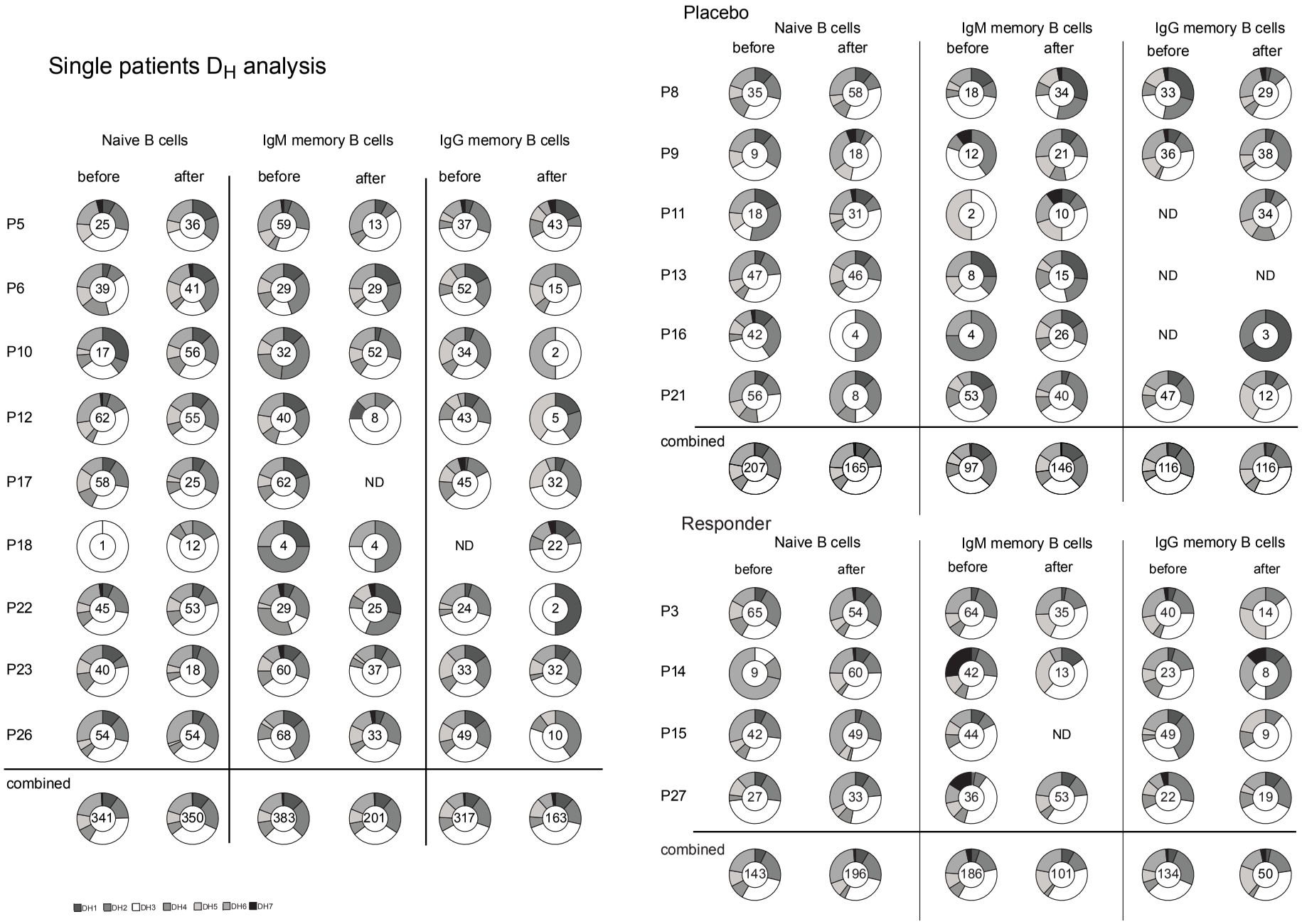
Single patients D_H analysis
Naive B cells
IgM memory B cells
IgG memory B cells
before
after
P5 25 36 59 13 37 43
P6 39 41 29 29 52 15
P10 17 56 32 52 34 2
P12 62 55 40 8 43 5
P17 58 25 62 ND 45 32
P18 1 12 4 4 ND 22
P22 45 53 29 25 24 2
P23 40 18 60 37 33 32
P26 54 54 68 33 49 10
combined 341 350 383 201 317 163
DH1 DH2 DH3 DH4 DH5 DH6 DH7
Placebo
Naive B cells
IgM memory B cells
IgG memory B cells
before
after
P8 35 58 18 34 33 29
P9 9 18 12 21 36 38
P11 18 31 2 10 ND 34
P13 47 46 8 15 ND ND
P16 42 4 4 26 ND 3
P21 56 8 53 40 47 12
combined 207 165 97 146 116 116
Responder
Naive B cells
IgM memory B cells
IgG memory B cells
before
after
P3 65 54 64 35 40 14
P14 9 60 42 13 23 8
P15 42 49 44 ND 49 9
P27 27 33 36 53 22 19
combined 143 196 186 101 134 50

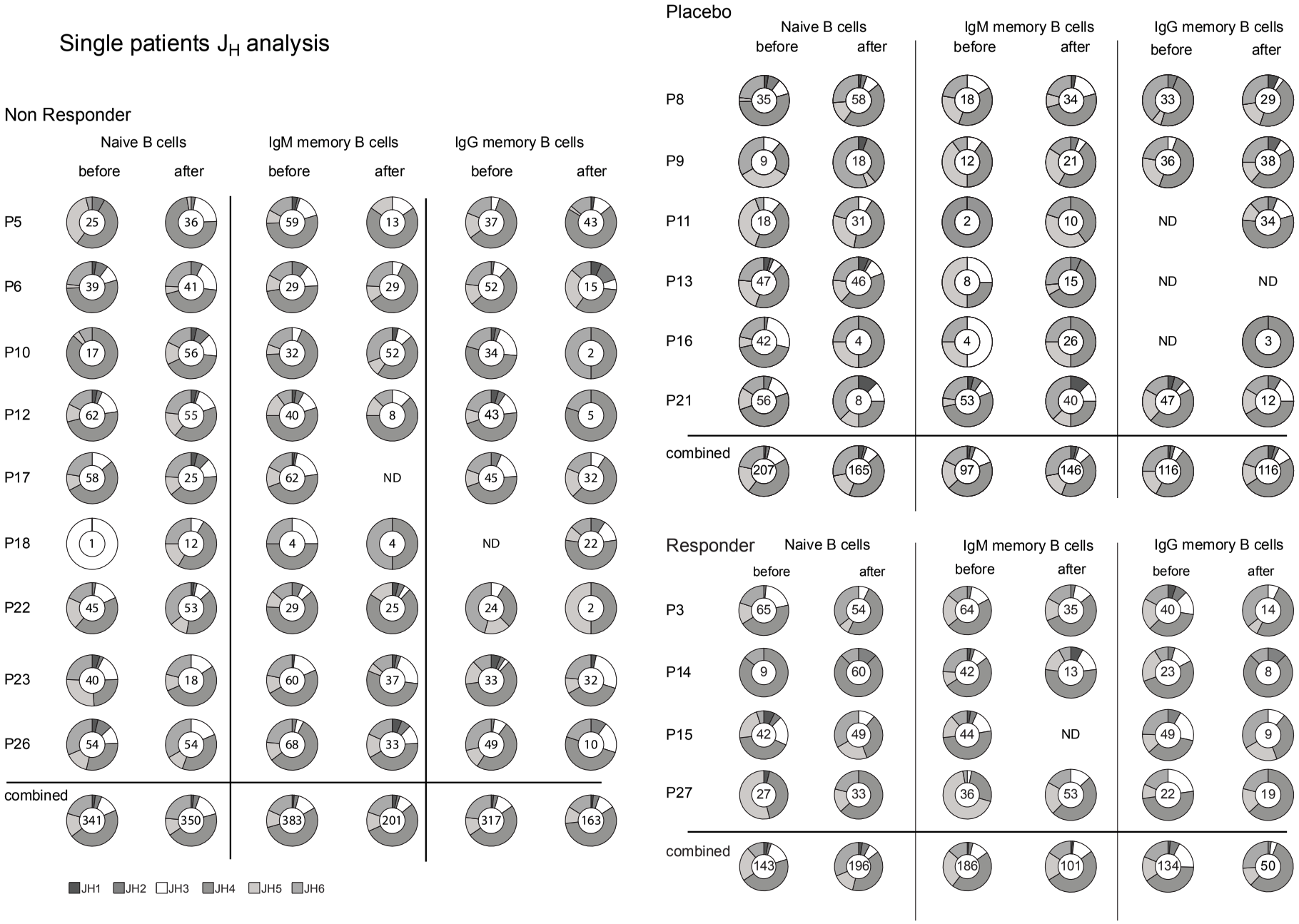
Single patients J_H analysis
Non Responder
Naive B cells
IgM memory B cells
IgG memory B cells
before
after
P5 25 36 59 13 37 43
P6 39 41 29 29 52 15
P10 17 56 32 52 34 2
P12 62 55 40 8 43 5
P17 58 25 62 ND 45 32
P18 1 12 4 4 ND 22
P22 45 53 29 25 24 2
P23 40 18 60 37 33 32
P26 54 54 68 33 49 10
combined 341 350 383 201 317 163
JH1 JH2 JH3 JH4 JH5 JH6
Placebo
Naive B cells
IgM memory B cells
IgG memory B cells
before
after
P8 35 58 18 34 33 29
P9 9 18 12 21 36 38
P11 18 31 2 10 ND 34
P13 47 46 8 15 ND ND
P16 42 4 4 26 ND 3
P21 56 8 53 40 47 12
combined 207 165 97 146 116 116
Responder
Naive B cells
IgM memory B cells
IgG memory B cells
before
after
P3 65 54 64 35 40 14
P14 9 60 42 13 23 8
P15 42 49 44 ND 49 9
P27 27 33 36 53 22 19
combined 143 196 186 101 134 50

The V_H, D_H and J_H gene family usage before treatment initiation did not differ between these two subgroups and was similar to demographically age-matched healthy blood donors (Figure 15). V_H3, the largest variable region family was found most frequently in any of the B cell subsets, followed by V_H4 and V_H1. B cell reconstitution 12 months after Rituximab treatment did not significantly alter the V_H, D_H and J_H gene repertoire in circulating naïve-, IgM memory- and IgG memory B cells. Additionally, we could not observe an increase of V_H3 usage comparing the mature naïve B cell with the IgM memory B cells, which was reported by Tsuiji et al. [86]

Next, we examined IgH chain characteristics such as the length, isoelectric point of the IgH complementarity-determining region 3 (CDR3), which have previously been associated with antibody-mediated autoreactivity [12,62]. The analysis of a large number of sequences enabled us to detect small differences such as a modest increase in IgH CDR3 lengths in naïve and IgM-expressing memory B cells from Rituximab-treated patients, whereas isoelectric points remained unchanged following peripheral B cell reconstitution comparing the individual B cell linages before and after the therapy (Figure 19). We conclude that there are no consistent abnormalities in the IgH chain repertoires in patients with anti-MAG neuropathy and that Rituximab-mediated peripheral B cell depletion does not significantly change the V_H, D_H and J_H gene family usage of naïve and memory B cells.

Size and antigen-specificities of IgM memory B cell expansions in anti-MAG neuropathy

Patients with anti-MAG neuropathy showed substantial clonal and oligoclonal expansions within the IgM memory B cell compartment before treatment initiation: 21.5% of 809 analyzed single-sorted cells had identical IgH CDR3 gene sequences compared to 2.3% of 574 sequences derived from IgG memory B cells ($p < 0.0001$) (Figure 20A). The size of clonal IgM memory B cell expansions was markedly reduced following Rituximab therapy but not in placebo-treated patients (Figure 20B).

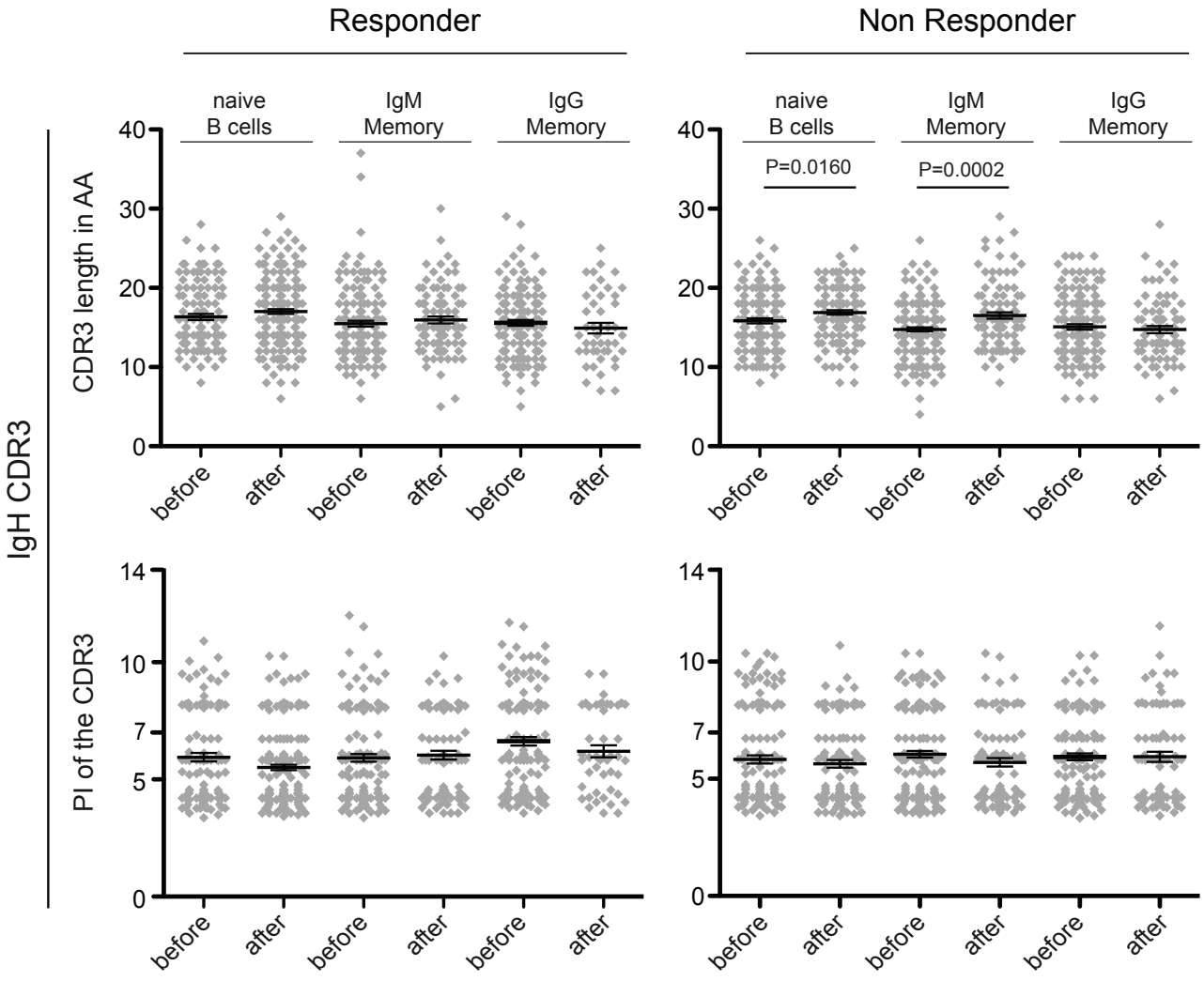

Figure 19: CDR3 length and CDR3 isoelectric points before and after Rituximab therapy

The same number of individual Igh chain gene sequences as in Figure 1 were analyzed and the results are displayed as data derived from individual sequences. The first row shows the length of the CDR3 for the placebo treated (left panel) and Rituximab treated patients (right panel). The lower graphs show the isoelectric points of the CDR3 for placebo and treated patients. Data points represent individual sequences. Horizontal bars and error bars indicate mean ± standard error mean (SEM). The unpaired student t-test was used to evaluate CDR3 lengths and isoelectric points.

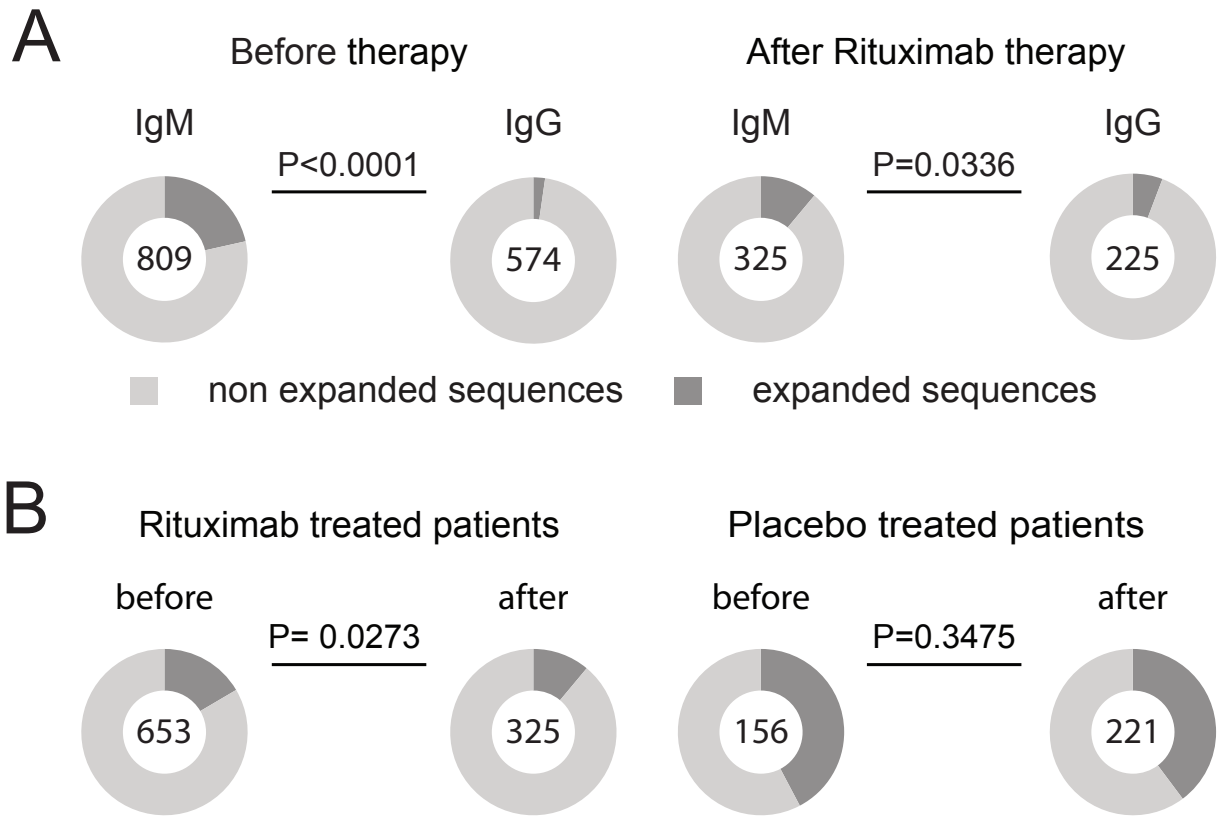

Figure 20: Comparing the size of IgM memory and IgG memory expansions before and after Rituximab treatment:

Frequency of clonally expanded IgM memory B cells in patients with anti-MAG neuropathy before and after Rituximab therapy as compared to the IgG memory compartment. Before therapy, data from all study subjects were included. Post-treatment data are referring to those patients that received Rituximab therapy. The numbers in circles indicate the number of individual sequences per patient cohort and per time point that were analyzed. B IgM memory B cell clonal expansions before and after therapy in placebo-treated patients compared to Rituximab treated patients. Results are based on the analysis of individual sequences in both clinical subgroups. The two-tailed Fisher's exact test was used to compare proportions of clonal expansions.

We detected a few expanded clones in the $CD19^{+}CD27^{-}IgM^{+}$ compartment: in placebo-treated patients 0% of a total of 207 sequences before and 3% of 170 sequences after therapy, in Rituximab-treated patients 0.3% of 539 sequences before and 1.4% of 353 sequences after therapy. These expansions but not non-expanded sequences were somatically hypermutated suggesting that these clones represent post-GC B cells. In our opinion, the most likely explanation for the presence of these few expanded and somatically hypermutated sequences are $CD27^{-}$ memory B cells that occur at low frequencies in the blood of healthy individuals and patients with autoimmune diseases [207].

The overall size of these expansions was minimal in comparison to the size of expanded sequences within the $CD19^{+}CD27^{+}IgM^{+}$ compartment (Figure 20). We observed that the frequency of expanded IgG memory B cells increased over time in placebo-treated patients. However, Rituximab therapy had only a small effect on the size of clonally related IgG memory B cells (Figure 21). Compared to the placebo treated patients the expansion is minor.

Figure 21: The size of the IgG memory B cell expansions in placebo and Rituximab treated patients:

Comparison of the frequency of clonally expanded IgG memory B cell before and after therapy in placebo-treated patients and Rituximab treated patients. The numbers in circles indicate the number of individual sequences per patient cohort and per time point that were analyzed. The two-tailed Fisher's exact test was used to compare proportions of clonal expansions.

Since anti-MAG neuropathy is an IgM mediated disease we determine whether expanded IgM memory B cell clones recognize MAG. For this we re-sorted IgM memory B cells isolated before treatment initiation and amplified full-length IgH and IgL chain variable region gene transcripts derived from highly expanded sequences by RT-PCR. Amplified products were cloned into eukaryotic expression vectors to produce monoclonal IgG antibodies with antigen specificities identical to the initial B cell antigen receptors [208]. The antigenic determinant of MAG resides in the carbohydrate component of the molecule, as demonstrated by the loss of reactivity following deglycosylation of purified human MAG [209]. A similar carbohydrate structure is found in the ganglioside fraction of the human peripheral nerve and has been identified as sulfoglucuronyl glycosphingolipid (SGPG), an acidic glycolipid exclusively expressed in the peripheral nervous system [210]. Pathogenic IgM antibodies in patients with MAG neu-

ropathy may recognize both MAG and SGPG, although the avidity for SGPG is reported to be 10-100 fold lower compared to MAG [211]. Therefore, we tested both specificities in comparison to an irrelevant control protein, a prominent B cell antigen of the ubiquitous gamma herpesvirus Epstein-Barr virus (EBV), i.e. the EBV nuclear antigen 1 (Figure 22)

All of the 5 clones optained from blood IgM memory B cell expansions before therapy recognized MAG purified from human myelin in a concentration-dependent manner. One out of these 5 clones showed a strong cross-reactivity towards SGPG (Figure 22). Non-expanded IgM memory clones neither recognized MAG nor SGPG (Figure 22). Moreover, we did not observe any binding to EBNA1 (Figure 22) indicating that IgM memory B cell expansions in patients with MAG-neuropathy recognize the target antigen of the disease. The sequences of the 5 expanded antibody clones are derived from different germline V_H elements and show some similarity in the amino acid content (Figure 23). The sequences homologies are manly located in the framework regions. The CDRs do only show minor conservations. In CDR1 the phenylalanine (F) in all the clones and in CDR2 isoleucine is conserved in 3 out of 5 expanded antibody clones namely P5 and P11. The CDR3 do not show any homology between the different heavy chains. P27 shows the highest amino acid exchange 85.25% compared to other at around 91%.

Figure 22: Anti-MAG ELISA of 5 expanded and 2 non-expanded IgM memory B cells.

Page 48: Specificity of IgM memory B cell expansions as assessed by ELISA**.** Recombinant antibodies expressed from highly expanded sequences, which are highlighted as circles in Figure 23, were tested for binding to purified MAG protein, to SGPG, an acidic glycolipid exclusively expressed in the peripheral nervous system towards which cross-reactivity of anti-MAG antibodies is described, and to EBNA1, an immunodominant protein expressed by the ubiquitous γ-herpesvirus EBV. OD-values from the positive control provided by the manufacturer, a secondary antibody control, an antibody (hu-8-18C5) that recognizes myelin oligodendrocyte glycoprotein (MOG) to control for antigen specificity and recombinantly expressed antibodies from patients with anti-MAG neuropathy are shown.

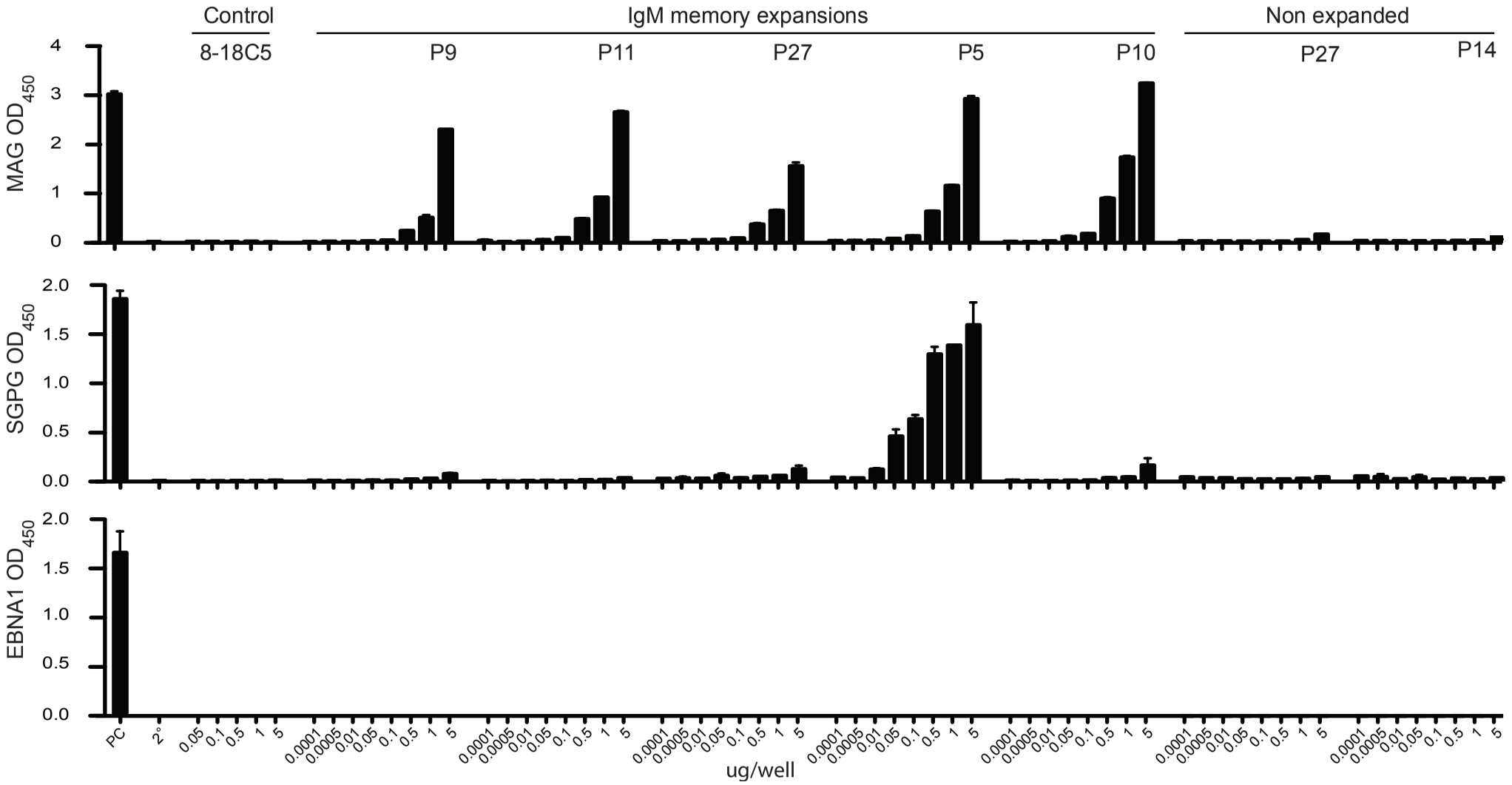
Control
IgM memory expansions
Non expanded
8-18C5
P9
P11
P27
P5
P10
P27
P14
MAG OD450
SGPG OD450
EBNA1 OD450
PC
2°
ug/well

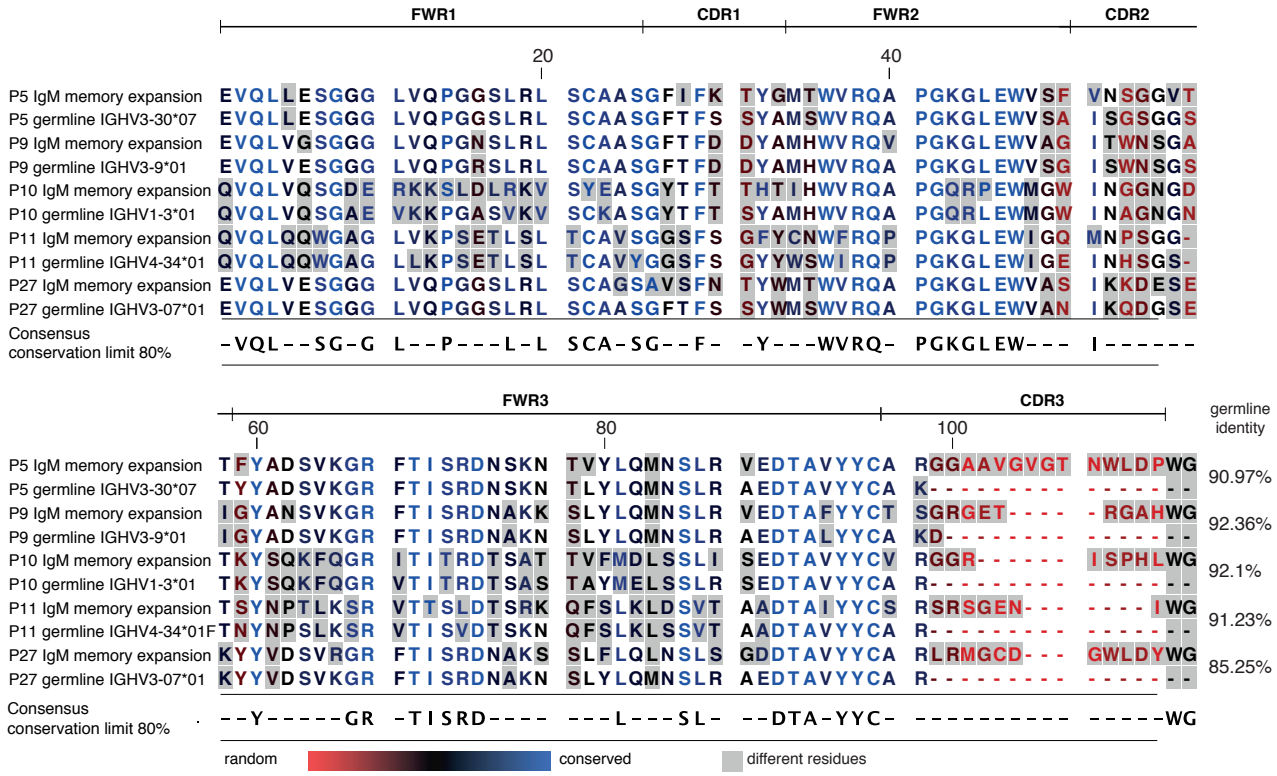

Figure 23: Alignment of the 5 expressed IgM memory expansions

The germline V_H elements and the expanded mutated heavy chain amino acid sequences were aligned with each other. The corresponding germline amino acid sequence of the expanded IgM memory B cell is depicted below each sequence. The alignment was performed with the T-coffee alignment algorithm. The letter color indicates the homology of the amino acids red reflects 0% black 50% and blue 100% identity. The grey box shows different residues. For the consensus sequence a conservation of 80% was defined. On the left side the germline identity for each clone is shown. The identity was calculated with the IMGT web tool.

Responder vs non-responder

Next, we determined whether patients showing a clinical improvement following Rituximab treatment, hereafter referred to as clinical responders (n = 4), can be distinguished from patients with stable or worsened disease, i.e. clinical non-responders (n = 9), through IgH chain gene repertoire changes, CDR3 characteristics, and the kinetics of clonal expansions during Rituximab treatment. The clinical response was quantified using a standardized clinical disability scale and details are reported in the publication of the clinical trial [206]. Data obtained in clinical responders and non-responders were compared to placebo-treated patients (n = 6) and age-matched healthy control (n=3).

V_H and D_H gene family usage in circulating naïve, IgM memory and IgG memory B cells before treatment initiation did not differ between these clinical subgroups and peripheral B cell reconstitution did not significantly alter the V_H and D_H gene repertoire one year after treatment (Figure 16 , 17 and 18). Before therapy, J_H5 usage was more frequently found in clinical responders compared to non-responders, but these differences lost statistical significance 12 months after Rituximab therapy (Figure 18). These data indicate that the clinical response to Rituximab therapy is not associated with significant changes in the V_H, D_H and J_H gene family usage of naïve and memory B cells. The modest increase in CDR3 lengths in the naïve B cell compartment following peripheral B cell reconstitution, could be attributed to clinical non-responders [212].

A much more important finding in the CDR3 analysis of responder and non-responder was the insufficient selection of the CDR3 usage in respect to length and isoelectric point compared to age-matched healthy controls. Healthy controls show a significant selection of shorter CDR3 in the IgM memory and IgG memory compartment compared to naïve B cells [86]. A similar trend was observed for the isoelectric point, where the CDR3 is selected towards higher pH starting from the mature naïve to the IgG memory B cell compartment in healthy controls. These changes in the CDR3 might reflect different checkpoints in the development from naïve to IgM and IgG memory B cells [12,86]. The length of the CDR3 in the case of responder patients shows no selection before the therapy and after the Rituximab treatment there is a clear stepwise shortening of the CDR3 length similar to the healthy control (Figure 24).

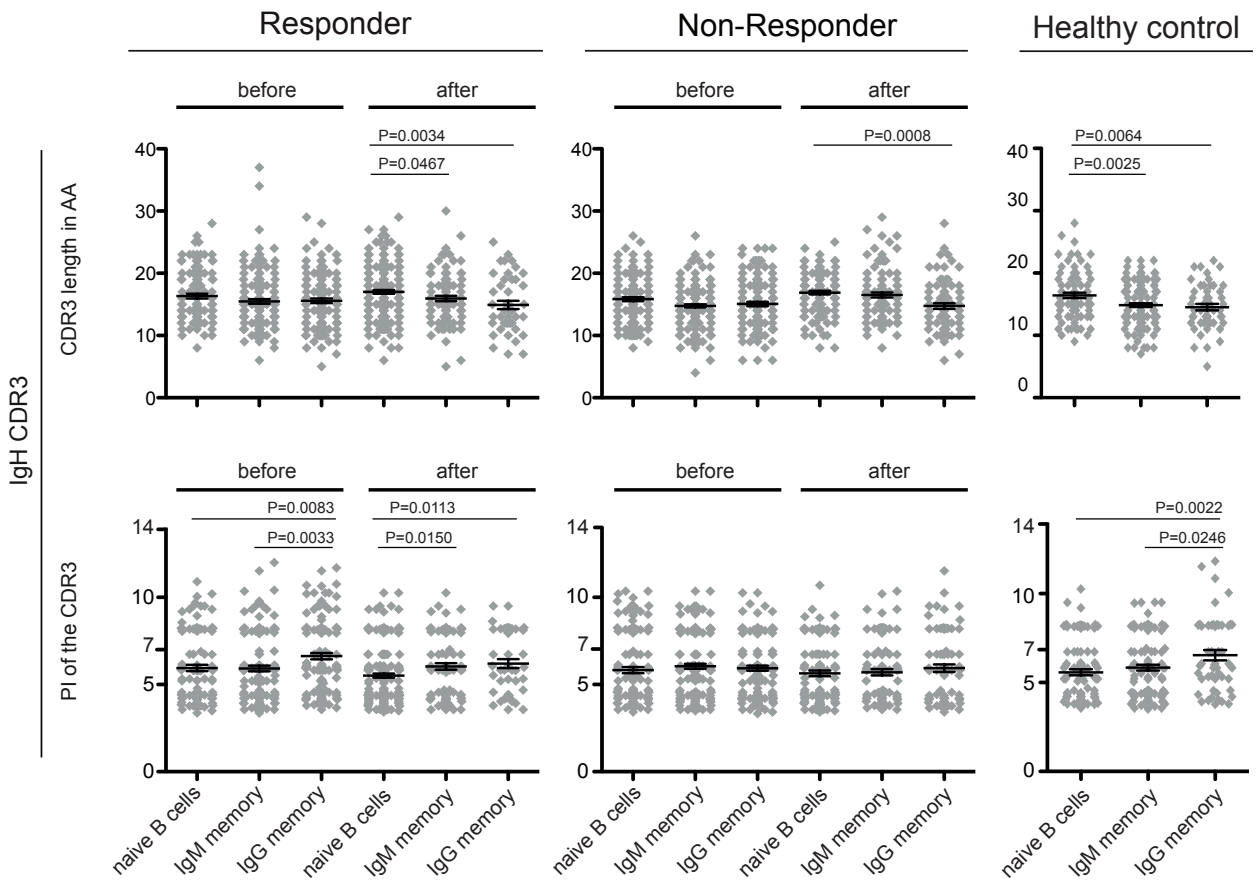

Figure 24: Comparison of the CDR3 of responder, non-responder healthy control in the context of length and PI

Patients showing a clinical improvement following therapy were classified as Rituximab responders, patients with stable or worsened disease severity were classified as Rituximab non-responders. The same number of individual IgH chain gene sequences derived from Rituximab-treated patients as displayed in Figure 16 were analyzed and the results are displayed as data derived from individual sequences. Data points represent individual sequences. Horizontal bars and error bars indicate mean ± SEM. The unpaired student t-test was used to evaluate IgH chain characteristics

Non-responders display a reduced length after the therapy only for the IgG memory B cells. In the placebo group the CDR3 length drop significantly (P=0.001) from an average of 15.7 AA in the naïve B cells down to 14.12AA in the IgM memory B cell compartment, which is more pronounced in all the pooled anti-MAG neuropathy patients before therapy (P<0.0001). But there was no change comparing naïve B cells with IgG memory B cells. For the isoelectric point we see a significant selection in the responder before the therapy but only from the IgM memory to the IgG memory compartment, which is similar to the healthy control. The difference to healthy controls is that the healthy controls have a stepwise increase of the isoelectric point during the maturation. Since only 3 healthy controls were used the increase from the naïve to the IgM memory B cell compartment might not be significant. Responders show a lake of selection from the naïve to the IgM memory compartment before therapy (Figure 24). After Rituximab the CDR3s have a shift to higher pH in the IgM- and IgG memory compartment. The significance between the IgM- and IgG memory B cell CDR3 pH is lost (Figure 24). The Placebo group has no change in the pH of the isoelectric point between all the compartments similar as the non-responders. Since the analysis in Figure 23 was performed with pooled sequence data we additionally analyzed the groups with mean values of the single patients with the paired Wilcoxon signed rank test. The result that we received reflects a similar situation as for the pooled sequence data for the non-responders (CDR3 length naïve after vs IgG memory after P=0.0078). The significance in the responder group was lost due to the small sample size.

We observed that clinical non-responders started with a higher load of IgM memory B cell expansions compared to patients who had a clinical benefit from Rituximab (p=0.0043) (Figure 25). Moreover, the reduction of IgM memory B cell expansions following B cell depletion as determined by IgH gene sequence analysis was less strong in non-responders (expansions were reduced by a factor of 1.3) compared to clinical responders (expansions were reduced by a factor of 2.7). Consequently, the amount of IgM memory B cell expansions remained increased in treatment non-responders compared to responders following peripheral B cell reconstitution (p = 0.0041). Notably, clinical responders that were included in our study showed a higher than 2-fold decrease in MAG-specific IgM antibody titers[206] indicating that inhibition of MAG-specific B cell expansions is associated with inhibition of pathogenic MAG-specific antibody secretion. However, we did not detect a significant correlation between MAG-titers and the size of clonal IgM memory expansions in individual patients.

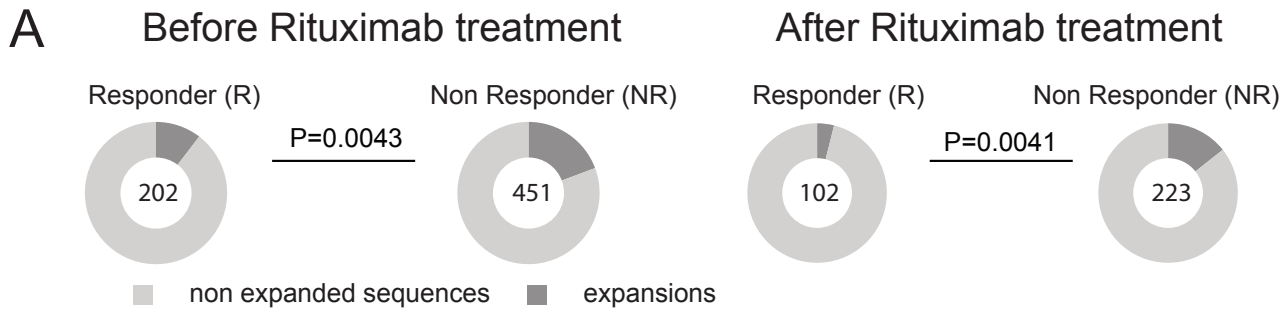

Figure 25: The IgM memory B cell expansions in responder and non-responder before and after therapy

IgM memory expansions before and after therapy in pooled samples from Rituximab responder and Rituximab non-responder. Results are based on the analysis of individual sequences in both clinical subgroups. The numbers in circles indicate the number of individual sequences per patient cohort that were analyzed. The two-tailed Fisher`s exact test was used to compare proportions of clonal expansions

Since the Ig gene repertoire analysis is based on pooled individual sequences, we additionally analyzed the proportions of clonal expansions per individual patient and compared the mean proportions between both Rituximab-treated subgroups, i.e. 4 responder and 9 non-responder. In line with the analysis based on sequences, clinical non-responders tended to start with a higher load of IgM memory B cell expansions compared to patients who had a clinical benefit from Rituximab and the amount of IgM memory B cell expansions tended be higher in treatment non-responders compared to responders following peripheral B cell reconstitution (Figure 26). The statistical significance was, however, lost, possibly due to the small sample size. Both the analysis of pooled sequences and of sequences per individual patient did not detect any changes in the Ig gene family usage during Rituximab therapy. Continuous as well as categorical outcomes per individual patient are shown in Table 5.

We identified several identical, expanded IgM memory B cell clones, which persisted for 12 months in individual placebo-treated patients as well as in clinical non-responders P5 and P23 (Figure 26).

Persisting clonal expansions were not observed in clinical responders suggesting that these persisting expansions may have contributed to the progression of the disease (Figure 26), although we cannot exclude the possibility that persisting, low-abundant clonal expansions would have been detected if a larger number of samples had been analyzed. Frequencies of expanded sequences per individual patients are listed in the Table 4.

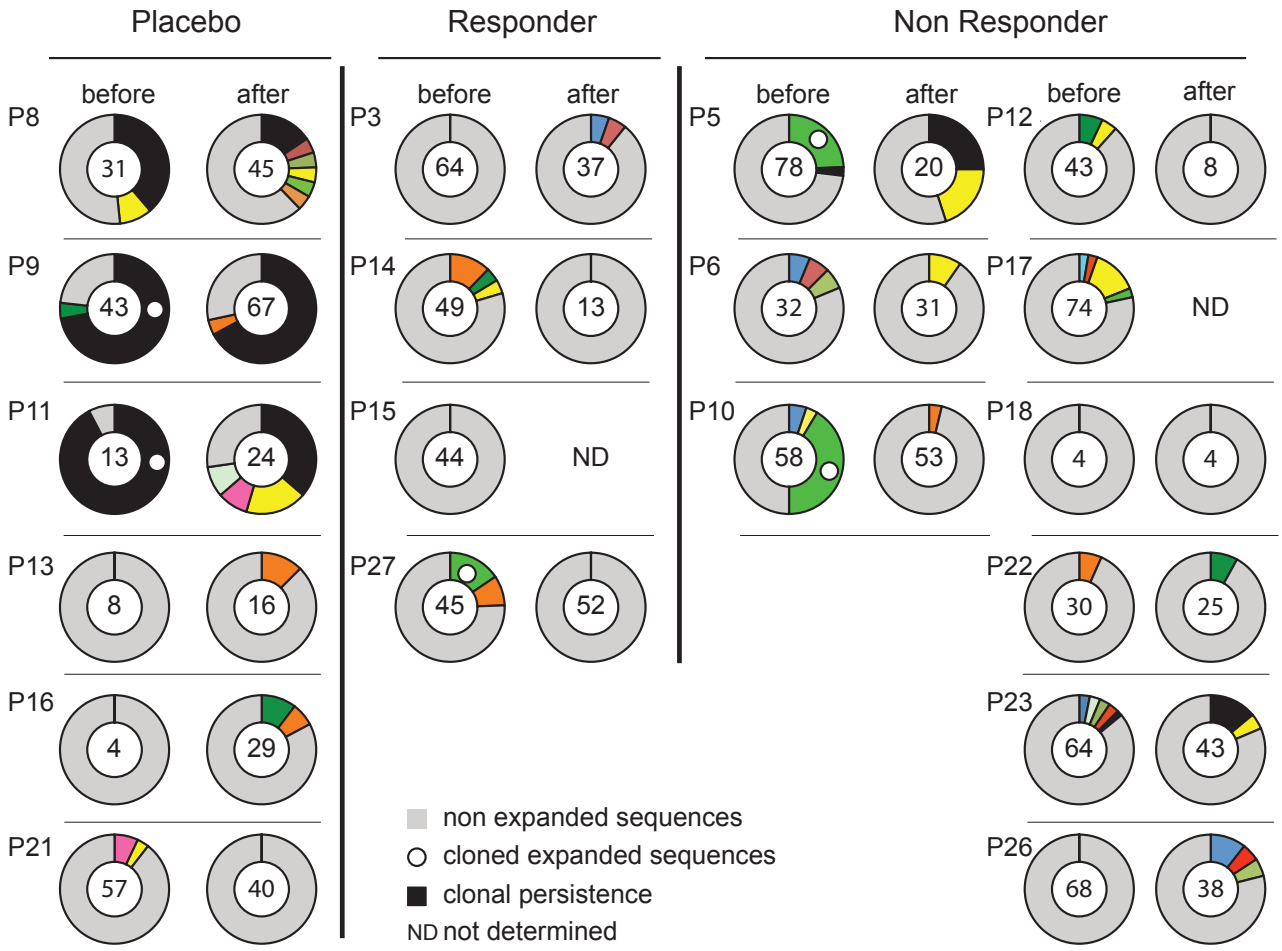

Figure 26: The clonal expansions in the IgM memory compartment of individual patients

IgM memory B cell expansions in individual patients classified as Rituximab responder or non-responder compared to placebo-treated patients. Non-expanded sequences are highlighted in grey, clonally expanded CDR3 sequences are highlighted in different colors. Sequences that were detected before and after therapy in individual patients are highlighted in black. Expanded sequences that were resurrected as IgG monoclonal antibodies, whose specificities are shown in Figure 3B, are marked with circles. ND denotes not determined: due to the low frequency of memory B cells in these 2 post-Rituximab samples, we were not able to amplify PCR products.

Patient Subgroup Before versus. After therapy	Patient	Memory compartment	Before	Frequency of exp. seq. (%)
Placebo	P8	IgM	after	7/45 (15.6%)
Placebo	P8	IgM	after	2/45 (4.4%)
Placebo	P8	IgM	after	2/45 (4.4%)
Placebo	P8	IgM	after	2/45 (4.4%)
Placebo	P8	IgM	after	2/45 (4.4%)
Placebo	P8	IgM	after	2/45 (4.4%)
Placebo	P8	IgM	before	12/31 (38.7%)
Placebo	P8	IgM	before	3/31 (9.7%)
Placebo	P8	IgG	before	2/37 (5.4%)
Placebo	P8	IgG	before	3/37 (8.1%)
Placebo	P8	IgG	before	2/37 (5.4%)
Placebo	P8	IgG	after	3/31 (9.7%)
Placebo	P9	IgM	before	31/43 (72.1%)
Placebo	P9	IgM	before	2/43 (4.7%)
Placebo	P9	IgM	after	45/67 (67.2%)
Placebo	P9	IgM	after	3/67 (4.5%)
Placebo	P9	IgG	after	20/60 (33.3%)
Placebo	P9	IgG	after	2/60 (3.3%)
Placebo	P9	IgG	after	2/60 (3.3%)
Placebo	P9	IgG	after	2/60 (3.3%)
Placebo	P11	IgM	before	12/13 (92.3%)
Placebo	P11	IgM	after	8/24 (33.3%)
Placebo	P11	IgM	after	4/24 (16.7%)
Placebo	P11	IgM	after	2/24 (8.3%)
Placebo	P11	IgM	after	2/24 (8.3%)
Placebo	P13	IgM	after	2/16 (12.5%)
Placebo	P16	IgM	after	3/29 (10.3%)
Placebo	P16	IgM	after	2/29 (6.9%)
Placebo	P21	IgM	before	4/57 (7.0%)
Placebo	P21	IgM	before	2/57 (3.5%)
Responder	P3	IgM	after	2/37 (5.4%)
Responder	P3	IgM	after	2/37 (5.4%)
Responder	P3	IgG	after	3/16 (18.8%)
Responder	P14	IgM	before	6/49 (12.2%)
Responder	P14	IgM	before	2/49 (4.1%)
Responder	P14	IgM	before	2/49 (4.1%)
Responder	P14	IgG	after	2/9 (22.2%)
Responder	P27	IgM	before	7/44 (15.9%)
Responder	P27	IgM	before	4/44 (9.1%)

Patient Subgroup Before versus. After therapy	Patient	Memory compartment	Before	Frequency of exp. seq. (%)
Non-responder	P5	IgG	after	2/44 (4.5%)
Non-responder	P5	IgG	before	2/38 (5.3%)
Non-responder	P5	IgM	after	5/20 (25%)
Non-responder	P5	IgM	after	4/20 (20%)
Non-responder	P5	IgM	after	4/20 (20%)
Non-responder	P5	IgM	before	19/78 (24.4%)
Non-responder	P5	IgM	before	2/78 (2.6%)
Non-responder	P6	IgM	before	2/32 (6.3%)
Non-responder	P6	IgM	before	2/32 (6.3%)
Non-responder	P6	IgM	before	2/32 (6.3%)
Non-responder	P6	IgM	after	3/31 (9.7%)
Non-responder	P10	IgG	before	2/35 (5.7%)
Non-responder	P10	IgM	after	2/53 (3.8%)
Non-responder	P10	IgM	before	3/58 (5.2%)
Non-responder	P10	IgM	before	2/58 (3.4%)
Non-responder	P10	IgM	before	24/58 (41.4%)
Non-responder	P12	IgM	before	3/43 (7.0%)
Non-responder	P12	IgM	before	2/43 (4.7%)
Non-responder	P17	IgM	before	2/74 (2.7%)
Non-responder	P17	IgM	before	2/74 (2.7%)
Non-responder	P17	IgM	before	10/74 (13.5%)
Non-responder	P17	IgM	before	2/74 (2.7%)
Non-responder	P17	IgG	after	2/33 (6.1%)
Non-responder	P18	IgG	after	2/23 (8.7%)
Non-responder	P22	IgG	after	2/3 (66.7%)
Non-responder	P22	IgM	before	2/30 (6.7%)
Non-responder	P22	IgM	after	2/25 (8.0%)
Non-responder	P23	IgM	after	6/43 (14.0%)
Non-responder	P23	IgM	after	2/43 (4.7%)
Non-responder	P23	IgM	before	2/64 (3.1%)
Non-responder	P23	IgM	before	2/64 (3.1%)
Non-responder	P23	IgM	before	2/64 (3.1%)
Non-responder	P23	IgM	before	2/64 (3.1%)
Non-responder	P23	IgM	before	1
Non-responder	P26	IgM	after	4/38 (10.5%)
Non-responder	P26	IgM	after	2/38 (5.3%)
Non-responder	P26	IgM	after	2/38 (5.3%)

Table 4: Frequency of expanded sequences in the memory compartment

Frequency of expanded sequences in the memory compartment of all patients before and after therapy are depicted as frequency of expanded sequences divided by the total sequence count for each patient.

To further address whether IgM memory B cells in Rituximab-treated patients developed newly or persisted over time, we compared the frequency of SHM in IgM memory B cells before and after therapy. Comparing the SHM level of all the anti-MAG neuropathy patients before treatment with age-matched healthy controls did not show any difference. The only exception is P27, which was excluded in this analysis due to its exceptional high level of SHM (Figure 27). The degree of SHM was stable in placebo-treated patients (Figure 28A). Likewise and despite efficient depletion of circulating B cells, the overall SHM frequency in circulating IgM memory B cells remained unchanged in clinical non-responders (Figure 28A).

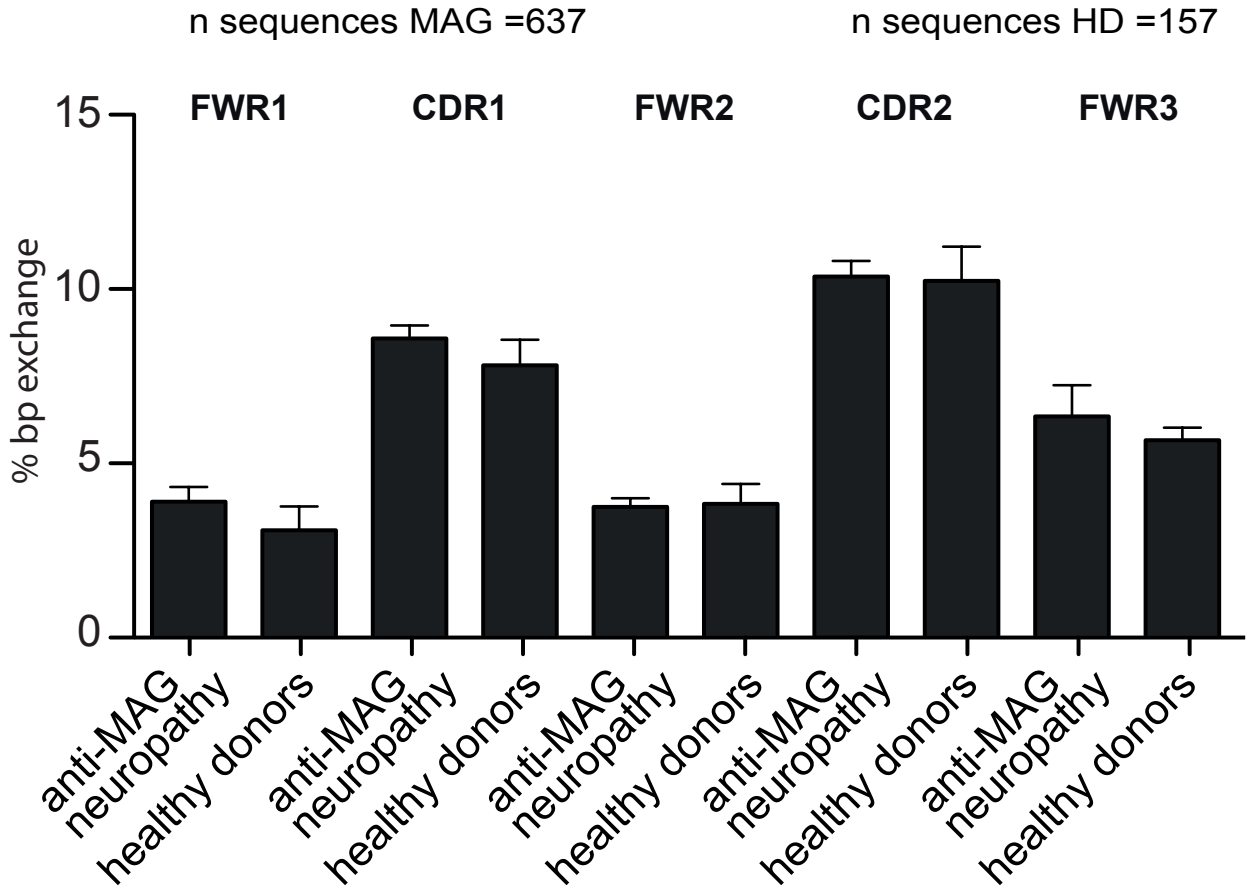

Figure 27: The SHM level in the IgM memory compartment of anti-MAG neuropathy patients is normal compare to age-matched healthy donors

Mean SHM frequencies of $CD19^{+}CD27^{+}IgM^{+}$ memory B cells in framework- and CDR-regions (FWR1, CDR1, FWR2, CDR2 and FWR3). P27 was excluded from the data, due to its elevated SHM levels. Expanded sequences were taken into account only once in order to analyze SHM frequencies in IgM memory B cells independent from clonal expansions. Results are based on the analysis of individual sequences in clinical subgroups. The unpaired student t-test was used to compare SHM frequencies.

In contrast, clinically effective Rituximab treatment was associated with a significant reduction in the SHM frequency in variable region of IgM memory BCR (p = 0.0001) (Figure 28A). Notably, the frequency of somatic mutations in clinical responders, was higher before but lower 12 months after Rituximab therapy compared to non-responders (Figure 28B).

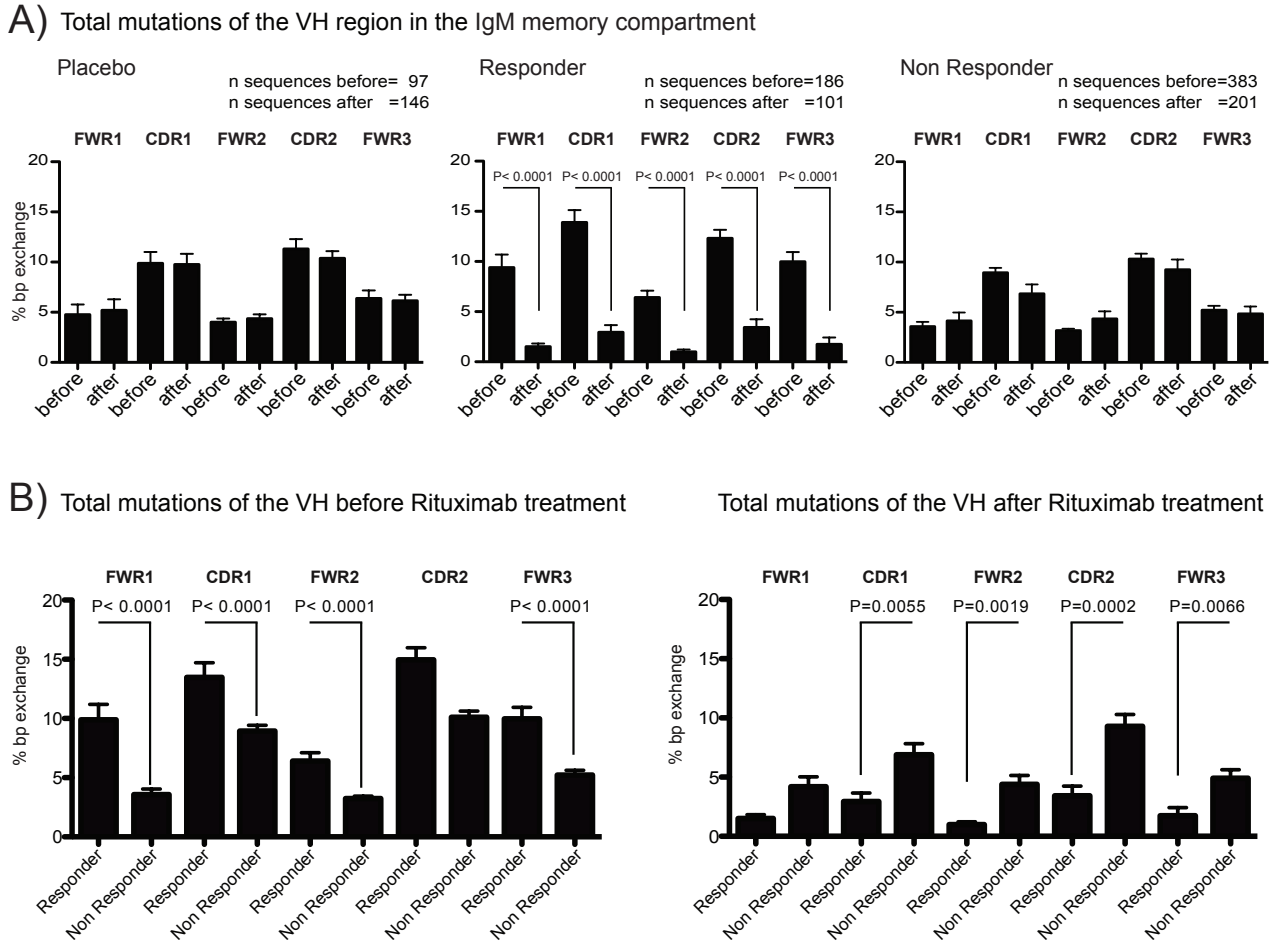

Figure 28: Lack of changes in somatic hypermutation (SHM) frequencies in IgM memory B cells are associated with a poor clinical response to Rituximab

A) Mean SHM frequencies of $CD19^{+}CD27^{+}IgM^{+}$ memory B cells in framework- and CDR-regions (FWR1, CDR1, FWR2, CDR2 and FWR3) in placebo-treated patients (left diagram), Rituximab-treated responders (middle diagram), and Rituximab-treated non-responders (right diagram) before and after Rituximab therapy. **B)** Mean SHM frequencies before (left diagram) and after Rituximab therapy (right diagram) in patients who showed a clinical benefit from Rituximab therapy as compared to patients with stable or worsened disease 12 months after treatment, i.e. clinical non-responder. Expanded sequences were taken into account only once in order to analyze SHM frequencies in IgM memory B cells independent from clonal expansions. Results are based on the analysis of individual sequences in clinical subgroups. The unpaired student t-test was used to compare SHM frequencies.

The reduction after therapy was strongest in patient P27 who showed the strongest clinical improvement in response to Rituximab as compared to all clinical responders. But all of the clinical responders showed the same trend of SHM reduction after therapy (Figure 29). The overall SHM level in the IgM memory compartment is normal compared to healthy control for responders and non-responders. The only exception is again P27, which has a significant elevated level of SHM for the total variable region of the IgM memory compartment. The reduction of mutations reflects the renewal of the IgM memory compartment in responder patients.

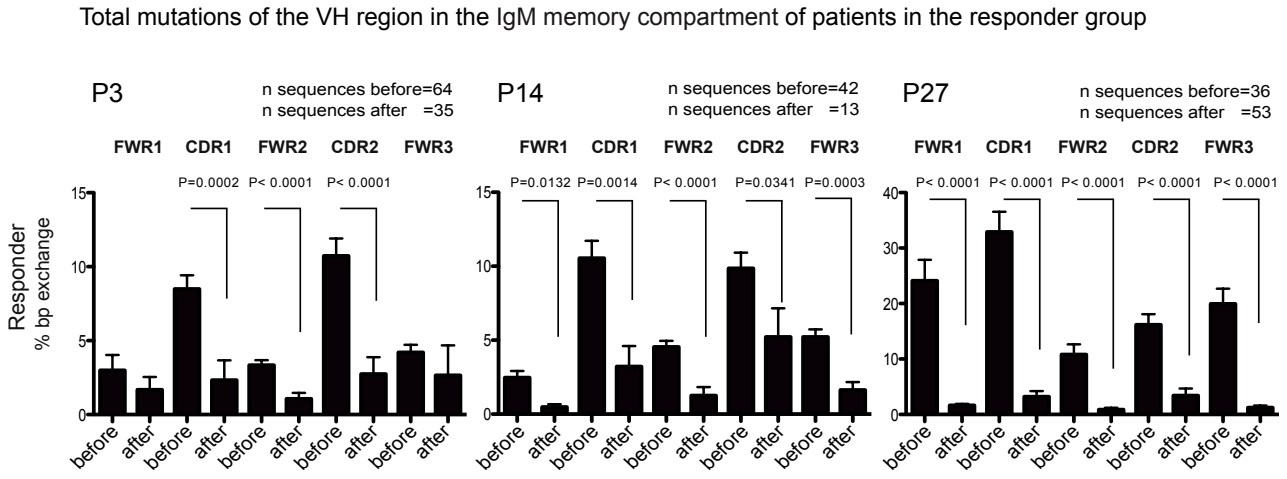

Figure 29: The individual SHM reduction in the IgM memory compartment for three individual responder patients before and after Rituximab treatment

Mean SHM frequencies of $CD19^{+}CD27^{+}IgM^{+}$ memory B cells in framework- and CDR-regions (FWR1, CDR1, FWR2, CDR2 and FWR3). The 3 responding patients show a reduced SHM frequency after Rituximab therapy.

To further validate our interesting finding of SHM in the IgM memory compartment we sorted and sequenced the naïve B cells as negative control and the IgG memory B cell compartment as clearly GC derived SHM positive control (Figure 30A and B).

As expected, the non-expanded (CD19+ CD27- IgM+) naïve B cells show a very low percentage of base pair exchange before and after the therapy, which reflects the unchanged germline sequence of the naïve B cells after VDJ recombination. This finding is true for placebo treated, Rituximab treated patients (Figure 30B) and age-matched healthy controls. In contrast to the IgM memory compartment we found no significant reduction in SHM frequency in the IgG memory B cell compartment comparing responder and non-responder (Figure 30A).

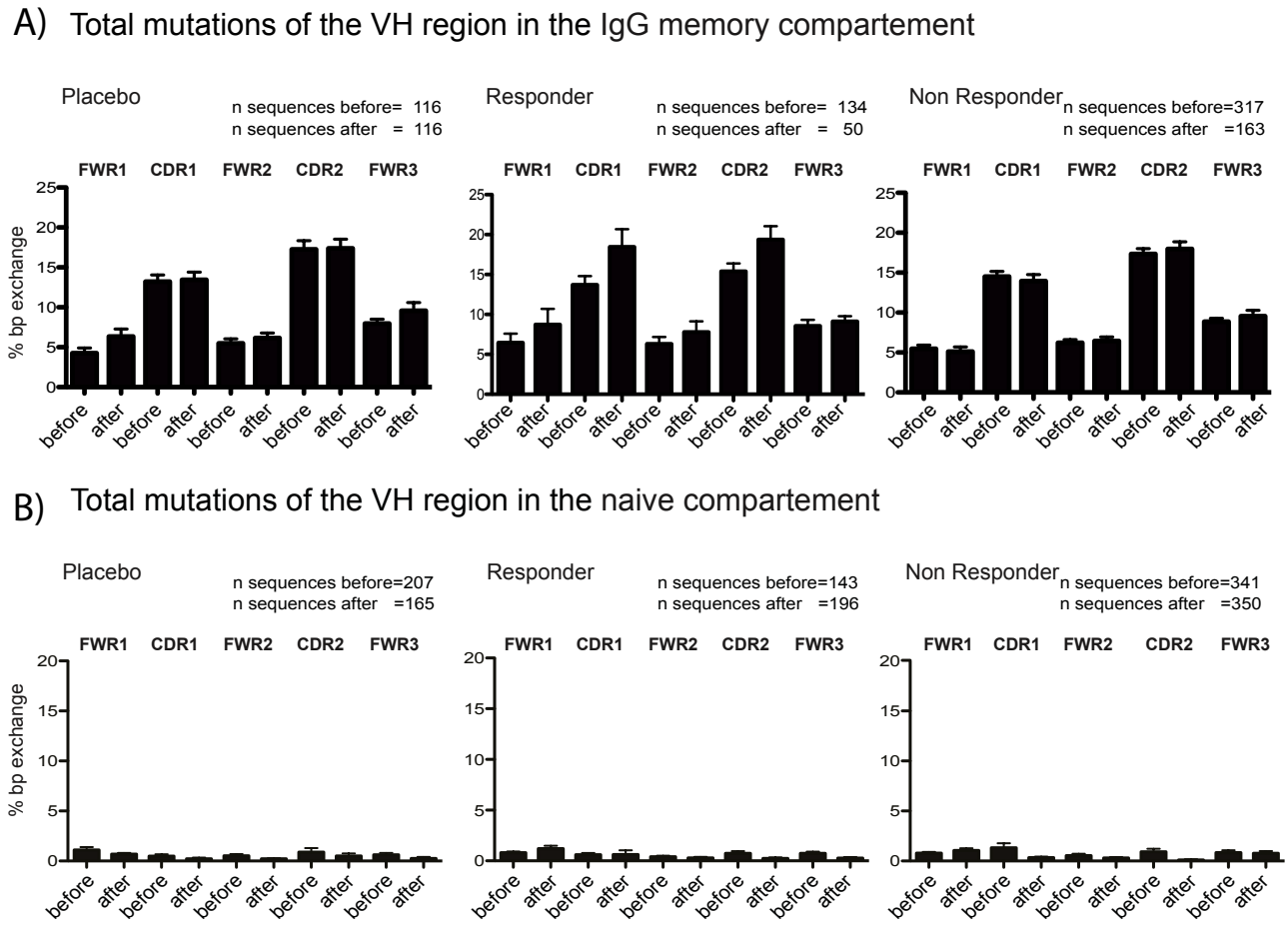

Figure 30: SHM frequency in the IgG memory - and naïve B cell compartments

Mean SHM frequencies of $CD19^{+}CD27^{+}IgG^{+}$ memory B cells and $CD19^{+}CD27^{-}IgM^{+}$ naïve B cells in framework- and CDR-regions (FWR1, CDR1, FWR2, CDR2 and FWR3)
A) illustrates the SHM level before and after Rituximab therapy for the three different patients groups placebo responder and non-responder. **B)** shows a similar analysis for the naïve B cell compartment.

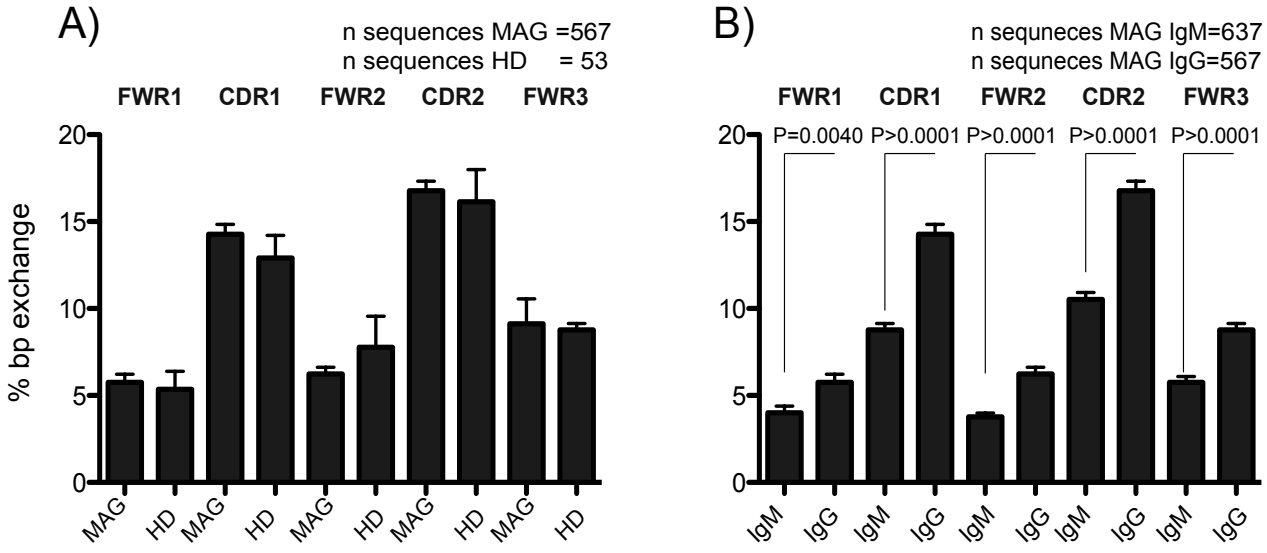

Figure 31: The SHM level in the IgG memory compartment of anti- MAG neuropathy patients is normal compares to age-matched healthy donors

A) Mean SHM frequencies of $CD19^{+}CD27^{+}IgG^{+}$ memory B cells in framework- and CDR-regions (FWR1, CDR1, FWR2, CDR2 and FWR3). Healthy donors and anti-MAG neuropathy patients have a similar level of SHM in the IgG memory compartment. MAG stands for anti-MAG neuropathy and HD for healthy donors **B)** The level of SHM in the IgG memory compartment is elevated compared to the IgM memory compartment. For **A)** and **B)** expanded sequences were taken into account only once in order to analyze SHM frequencies in IgM and IgG memory B cells independent from clonal expansions. Results are based on the analysis of individual sequences in clinical subgroups. The unpaired student t-test was used to compare SHM frequencies.

The overall SHM level is the same before and after the Rituximab therapy and is comparable between placebo, Rituximab treated responder and non-responder patients and healthy control Figure 31A. The SHM in the IgM memory compartment is significantly lower than in the IgG memory compartment, which reflects the high proliferation and the high AID expression in the GC IgG memory B cells (Figure 31B).

Discussion

Our study demonstrates that the long-term immunomodulatory effects of Rituximab in anti-MAG neuropathy are mediated through the sustained reduction of expanded autoreactive IgM memory B cells. In patients with peripheral nervous system autoimmunity associated with IgM MGUS, which is believed to arise from somatically hypermutated but non-class-switched B cells that acquire IgM secretory capacity [213,214], we show that IgM memory B cells contain an important reservoir of autoreactive species and that the sustained elimination of these cells is associated with clinical disease remission. Conversely, high load and clonal persistence of expanded autoreactive IgM memory B cell clones despite efficient depletion of circulating B cells were associated with a poor clinical response to Rituximab.

Previous studies demonstrated expansion and persistence of foreign antigen-specific memory B cells following infection and vaccination [215-217] and of candidate pathogenic T cell clones in human autoimmune diseases such as multiple sclerosis and type 1 diabetes [218-220]. The known identity of the target antigen allowed us to address the dynamic behavior of expanded autoreactive B cells in patients with anti-MAG neuropathy. The presence of oligoclonal expansions within the IgM memory B cell compartment before treatment initiation, their ability to recognize MAG protein and their persistence in the group of patients with stable or worsened disease suggest that these persisting expansions may have contributed to disease progression and argue for an important role of MAG-specific IgM memory B cells in the pathogenesis of this inflammatory neuropathy.

Clinical responders showed qualitative immunological changes that indicate reconfiguration of B cell memory through sustained reduction of autoreactive expansions and changes in somatic mutation frequencies in the IgM memory compartment. While these changes might be driven by different B cell linages, we were not able to distinguish them with the staining we used due to color limitations on the FACS Aria I machine. The different lineages are namely marginal zone (MZ) B cells, B1 B cells and IgM^+ first round germinal center B cells that contribute to the $CD27^+IgM^+$ B cell pool. The lack of resolution leads to speculation about the origin of the MAG-recognizing IgM antibodies. The first population I would like to discuss are the MZ B cells, which are located in the marginal zone of the spleen. The marginal zone (MZ) in the spleen is an anatomical structure between the red and the white pulp [221]. In humans the MZ B cells ($CD27^+IgM^+IgD^+$) form a double-layer with a T cell layer in-between. In rodents the MZ forms a monolayer [222].

B cells with a MZ B cell surface marker phenotype are found as well in the inner wall of the subcapsular sinus in lymph nodes, in the crypt epithelium of tonsils and under the dome epithelium of Peyer's patches [223-227]. Evidence for distinct MZ B cell maturation sites apart from the spleen are found in patients with congenital asplenia as well as splenectomized patients, which still have MZ B cells but in a lower frequency compared to healthy humans [228]. The frequency of MZ B cells is 15-20% of all B cells and represents the largest IgM^+ fraction in the memory compartment [223] (Figure 32A).

MZ B cell precursors develop during the first years after birth and start to populate the spleen. These precursors separate from the follicular B cell maturation path after passing the T2 [223] or the mature naïve stage [13] and have the capacity to self-renewal [229]. It is not clear if the cells repopulate the spleen in one wave during ontogeny or if the population is slowly renewed [223]. Some evidence was found in bone marrow-transplanted humans, which have a similar repopulation time as newborns [230] and in autoimmune patients with RA treated with an anti human CD20 antibody. In the case of B cell depleted RA patients the MZ B cell recovery rate is less then 1/3 of the initial population after 2 years [231]. These findings might support the concept of a constant renewal of the MZ B cells from blood borne precursors; on the other hand the influx of new cells is not enough to refill the spleen, which indicates that a certain self-sustaining capacity may exist.

In the MZ region mature naïve or T2 B cells develop in a T cell-independent manner (TI) TI-1 and TI-2 to MZ B cells [232]. TI-1 is dependent on BCR activation and stimulation with BAFF and APRIL [98] and TI-2 is based on the repetitive crosslinking of the BCR due to a repeating epitope, which clusters the BCR and starts to signal [99,100]. The MZ B cells are natural effector B cells because they are reacting to blood borne pathogens like Streptococcus pneumoniae in an innate immune response-like manner [85]. MZ B cells are able to produce large amounts of IgM antibodies 3-4 days after TLR stimulation [233]. In contrast to mature naïve B cells MZ B cells express a large set of TLR (2,6,7,8,9,10) similar to class -switched B cells [234-236], which is important to reduce the response time towards blood borne pathogens.

Concerning the level of SHM in the variable region of the BCR, the MZ B cells do have similarities to a GC derived memory B cells in humans (Figure 32B). The immunoglobulin variable regions of these cells are mutated and show features of affinity maturations in humans but not in rodents [224,237,238]. The frequency of mutations is approx. 50% less than for a GC-derived memory B cell [223,239,240] (Figure 32B). How the mutations are introduced in a human MZ B cell is not clear.

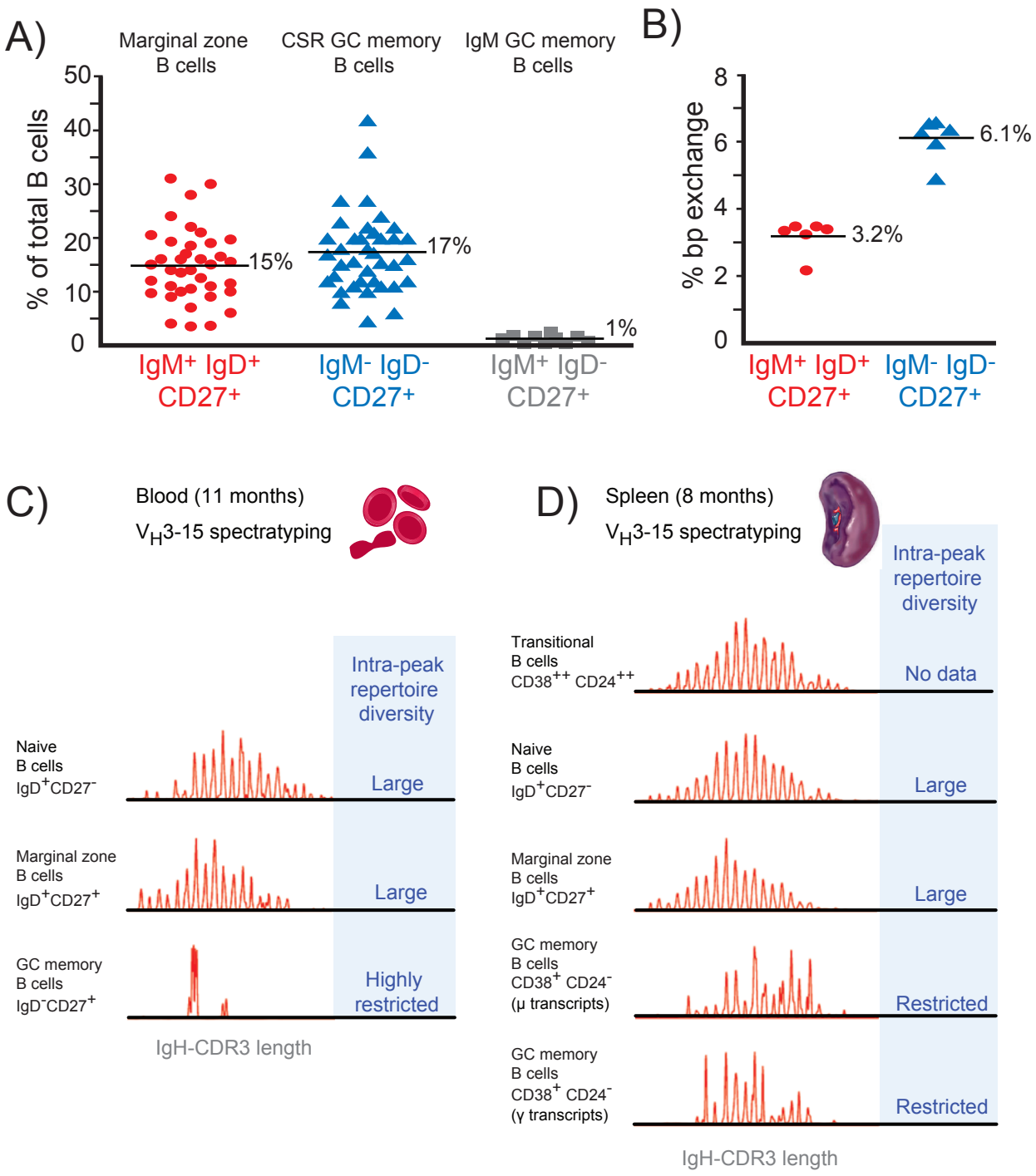

Figure 32: Marginal zone B cells vs. GC B cells

A) Shows the frequency of marginal zone B cells compared to class switch memory B cells. **B)** Illustrates percent base pare exchange in the J_H4 gene segment in blood of marginal zone B cells and class switched memory B cells. **C)** Demonstrates the different length distribution of the CDR3 of V_H3-15 gene segment containing B cells in different B cell linages of the blood in an 11-month old child. **D)** Similar as in **C)** but in the spleen of an 8-month old child. The Figure is adapted from[223,242]

The general process for SHM induction is AID related but in immunohistochemical assays the protein could not be detected [241] and in qRT-PCR only low levels of AID expression were found in children below the age of 2 years [242]. Evidence for an AID involvement was found in AID-deficient patients, which lack mutations in the variable region of immunoglobulins [228].

The overall antibody repertoire of MZ B cells is less restricted than for normal memory B cells. This means that the BCR selection is not as stringent as in the GC reaction, where only a couple of BCR are favored. The restriction of the BCR can be measured by the length distribution of the CDR3 (spectratyping). Analysis of the MZ B cells' CDR3 length by spectratyping showed less restriction than memory B cells. MZ B cells do have a quasi-gaussian distribution, compared to memory B cells with well-defined spikes of the CDR3 length that suggest a strong selection during the GC reaction. The overall length is only slightly shorter than naïve B cells, which indicates less selection in the MZ of the spleen [223,242] (Figure 32 C and D).

One of the remaining questions concerning the MZ B cells is if these cells are in a transitional state and undergo CSR later on or if MZ B cells are the endpoint of their development. Evidence for subsequent CSR was found *in vitro* by treating the MZ B cells with CD40L and measuring IgG levels. In comparison to $CD27^{+}IgM^{+}IgD^{-}$ GC memory B cells MZ B cells have a higher capacity to undergo immunoglobulin class-switching [243]. Puga et al. showed in a recent study that neutrophils in the spleen do express CD40L and are able to induce CSR *in vitro* in a co-culture with MZ B cells [244].

Kruetzmann et al. showed effector B cell function in the $IgM^{+}IgD^{+}CD27^{+}$ B cell compartment due to TLR stimulation 85. It might be possible that the pathogenic B cells are derived from the MZ B cells, which is the largest population in the $CD27^{+}IgM^{+}$ B cell compartment [223] (Figure 15). However there is the new finding from Griffin et al., where they demonstrated the presence of the B1 B cells in humans in 2011. They distinguished two subsets of B1 B cells with similar functions as B1a and B1b cells in the mice [245,246] and a similar phenotype as Kruetzmann defined for the MZ cells [85].

In mice the B1 B cells were described first by Lanier et al. in 1981. He found a B cell tumor with a characteristic expression of CD5 in mice [247]. These cells were then further characterized and subdivided into two populations being B1a (sIgM $CD11b^{+}$ $CD5^{+}$) and B1b B cells (sIgM $CD11b^{+}$ $CD5^{-}$) [248]. Compared to the B2 B cells (all other B cells) the localization of the B1 B cells differs in mice. Few

B1 cells are found in the spleen but the majority of the cells are located in the peritoneal cavity [249-251]. Murine B1 B cells are thought to be the natural effector B cells as they have the capacity to secret IgM in a TI manner, activate T cells and show high levels of phosphorylation of phospholipase C gamma 2 (PLC-γ2) and Syk [245].

Various experiments were performed to find out the progenitors of the B1 B cells. Therefore the mice were irradiated and reconstituted with bone marrow or cells isolated from fetal liver and only mice reconstituted with fetal liver-derived cells were able do reconstitute the B1 cell compartment [252,253]. The bone marrow was only able to reestablish the B2 B cells. Wardemann could show that only mice with a functional spleen reconstituted with a fetal liver cells were able to generated B1a B cells and that these cells were able to respond to a TI vaccine (Pneumovax®23) [254]. Montencine-Rodriguez was able to isolate a B1 progenitor ($Lin^{-}CD93^{+}$ $CD45R^{-or\ lo}$ $CD19^{+}$) from fetal liver with the highest numbers peaking at day 17 of gestation in mice [255]. These cells can differentiate *in vitro* and *in vivo* into B1a and B1b B cells and do not generate other hematopoietic lineages.

Griffin and Rothstein discovered a B1 B cell homologue in humans very recently [245]. The human B1 B cell lineage ($CD27^{+}IgM^{+}IgD^{+}CD43^{+}CD70^{-}CD69^{lo}$) has similar functional properties as the B1 B cells in the mice and their frequency is age dependent. The frequency of the B1 B cells is highest in umbilical cord blood of newborns and declines with aging [245]. Furthermore, they were able to show that human B1 B cells have two subpopulations with or without CD11b expression. Interestingly, the $CD11b^{+}$ cells do express CD86 and are able to activate T cells very efficiently *in vitro* [246]. These $CD27^{+}$ $CD43^{+}CD11b^{+}$ cells occur at frequencies of about 10% of all the B1 B cells in adult peripheral blood and umbilical cord blood. In SLE the level of $CD27^{+}CD43^{+}CD11b^{+}$ cells is elevated in the blood and the CD86 expression is significantly higher. Blocking of CD86 *via* an anti CD86 antibody was able to reduce the T cell activation *in vitro* [246].

The V_H region of the B1 B cells does not differ from the naïve B2 B cells in terms of mutations, N1/N2 additions and CDR3 length but the use of different gene segments during the VDJ recombination distinguishes B1 from B2 B cells. Especially IGHV 3-30 and IGHV1-2 are elevated in the B1 cells [245]. Due to the ability of these cells to secret IgM antibodies anti-MAG neuropathy might be mediated *via* B1 B cells [245,246]. But the overrepresentation of the V_H 3-30 and V_H1-2 element is not present in the expanded sequences of the anti-MAG neuropathy patients. This and the declining frequency of B1 B cells in aging people speaks against the involvement of B1 B cells in anti-MAG neu-

ropathy [245]. The last possible B cell population is the first round germinal center B cells population, which is characterized as $IgM^{+}IgD^{-}CD27^{+}$ B cells. This population has the lowest frequency in the IgM memory compartment [223] (Figure 32A). This low frequency makes it difficult to address the pathological role of the GC IgM memory B cells.

The uncertainty of the pathogenic antibodies origin makes it necessary to use a new staining panel, which includes IgD, CD43, and CD11b as additional markers. These markers would make it possible to dissect the IgM memory compartment in MZ B cells ($CD27^{+}IgM^{+}$ IgD^{+} $CD19^{+}$ $CD43^{?}$ $CD11b^{?}$ $CD70^{?}$), B1 B cells ($CD27^{+}$ IgM^{+} $IgD^{?}$ $CD19^{+}$ $CD43^{+}$ $CD11b^{+/-}$) and the GC derived IgM memory B cells ($CD27^{+}$ IgM^{+} IgD^{-} $CD19^{+}$ $CD43^{-}$ $CD11b^{-}$). Lets assume that the pathological B cells are the MZ B cells. This would implicate that the MZ B cells secrete IgM due to TLR stimulation [85] or the MZ B cells are further maturing to plasma cells, which was proposed by Puga et al [244]. Then the checkpoint in the spleen must be affected. Since the MZ B cells are anyway not that strongly selected the failing of that checkpoint could be much likely. However, B1 B cells are spleen-dependent as well the T1 and T2 B cells have to pass checkpoint in the spleen, which reflects the important role of the spleen and the many layers of selection in this organ [13,87,254].

Evidence for an involvement of a failing checkpoint can be seen in the selection of the CDR3 regions in respect to isoelectric point and length [12,86] (Figure 24). The data suggest that the non-responders have a weaker checkpoint selection before and after Rituximab therapy and that the responders restore the checkpoint after therapy compared to healthy controls. Especially the selection of the isoelectric point is restored in the responders after therapy. The checkpoint failure between the naïve and IgM memory compartment of non-responders could be one of the reasons for the progressive nature of the disease. But since both groups had failed this checkpoint before the therapy particularly between the naïve and IgG memory compartment it might implicate that one of the checkpoints in the GC is failing.

The checkpoint from the naïve to the IgM memory compartment can't be dissected very clearly due to the different B cell lineages in this population. But the absence of the GC checkpoint could give evidence for a failure in the maturation of GC-derived IgM memory B cells. Since the GC-derived IgM memory B cells are only a very small population in the blood compared to MZ B cells, the functional checkpoint of the MZ B cells could mask the pathogenic IgM memory cells.

However, it could be although inverted and the MZ B cells are failing and due to the depletion and the slow recovery rate of MZ B cells the checkpoint of the GC IgM memory B cells turns visible in the assay. Since the non-responders do not have a depletion as complete as the responder's the checkpoint in the IgM memory compartment might be masked in the non responder.

The SHM frequency in the IgG memory compartment is unchanged after Rituximab mediated B cell depletion before and one year after the therapy for anti-MAG neuropathy patients and similar to healthy controls (Figure 30A and 31A). This finding indicates, that the turnover of IgG memory B cells is higher than in the IgM memory B cells compartment. The slow recovery of the IgM memory compartment also observed in Rituximab treated RA patients, where the repopulation of IgM memory B cells was still only 1/3 of the initial population 2 years after Rituximab therapy [231]. On the other hand we could find a lot of clonal expanded IgG memory B cells after Rituximab mediated B cell depletion, which shows the opposite trend as in the IgM memory compartment, where the expansions are reduced in all the Rituximab treated patients. Compared to the IgM^+ $CD27^+$ memory B cells the IgG^+ $CD27^+$ memory B cells are well defined as GC reaction derived B cell population and the clonal expansion could be due to a fast repopulation of the IgG memory compartment through the hyperproliferation in the GC reaction. The Rituximab induced bottleneck situation and the hyperproliferation in the GC leads to an overrepresentation of newly formed clonally expanded GC-derived IgG memory B cells, which can be seen in Figure 21.

In contrast, based on the lack of significant changes in SHM frequencies, we found no evidence for a significant de novo generation of IgM memory B cells in clinical non-responders suggesting that at least a fraction of disease-relevant B cells were not accessible for or susceptible to CD20 immunotherapy. In patients with rheumatoid arthritis, the depleting effect of Rituximab is reported to be more profound in the peripheral blood than in inflamed joints or bone marrow[257-259]. Although the clinical response status was not addressed in the aforementioned studies, the results obtained here suggest that targeting of B cell-depleting antibodies to professional lymphoid tissues and sites of autoimmune inflammation for the sustained elimination of autoreactive B cells might increase the clinical efficacy of CD20 immunotherapy.

Rituximab was evaluated for its clinical efficacy in anti-MAG neuropathy based on its potential to reduce pathogenic IgM antibodies by depleting B cells. Initial uncontrolled phase II studies reported that some patients show clinical improvement following Rituximab therapy [260-262]. Patients who initially responded well to Rituximab in one of the aforementioned clinical trials were prospectively observed without treatment for another 36 months. Despite the reappearance of circulating B cells, a sustained clinical benefit after a single Rituximab course was noted that lasted up to 24 months in 80% and up to 36 months in 60% of patients [263]. Disease recurrence was best correlated with high baseline anti-MAG titers and increasing anti-MAG antibodies at follow-up and the authors suggested that patients with high anti-MAG titers may require additional courses with Rituximab [263].

In a small series of eight patients, administration of a double dose of Rituximab (750 mg/m² every week for 1 month) 17 to 27 months after standard dose treatment (375 mg/m²) improved the clinical outcome. High-dose treatment was also efficient in inducing a first clinical response associated with reduced anti-MAG antibody titers in patients that were refractory to the standard treatment [262].

What we can conclude from the study is that the low level of SHM and the absence of clonal persistence indicated that newly developed B cells repopulated the IgM memory compartment in clinical responders. We found that a high load of oligoclonal B cell expansions before therapy and low efficiency to reduce B cell expansions with Rituximab is associated with a poor clinical response. Our data, suggest that patients who show no clinical improvement after a first round of Rituximab therapy could benefit from additional treatment rounds to deplete or further reduce the frequency of clonally-related autoreactive B cells.

The reason why the non-responder group has a weaker depletion has still to be addressed. One possibility is a FcγR mutation which reduces the efficacy of the ADCC mediated depletion of Rituximab [196-199]. To further address this point the patients from this study should be tested for FcγR polymorphism and compared to the already obtained results. A possible solution to resolve the low B cell depletion efficacy in the non responder is the third generation of anti-CD20 antibodies like GA101, which have a higher binding affinity to the FcγR [200]. This higher binding affinity could compensate for the polymorphism in the non responder group.

Further the IgM memory compartment has to be dissected into B1, MZ and first round GC IgM memory B cells lineages to find the pathogenic B cell population. This could lead to a more precise depletion strategy, which might reduce the side effects of the therapy and keeps the immune system more intact. To achieve this goal the pathogenic B cell linage has to be further characterized to find specific markers that are not present on the other B cell linages and on any other cell population in the body.

The CDR3 results gives some evidence that one of the GC checkpoint might be involved in the disease development and this could indicate that the pathogenic B cell is a GC-derived IgM memory B cell. Since, the knowledge about how the selection mechanisms in B cells checkpoints are working is still very limited, the knowledge of the pathogenic B cell population could give evidences about working mechanism of the checkpoints that are affected in the cause of the disease and could give a more insight view into the pathology of anti-MAG neuropathy.

The deeper understanding of the checkpoints is crucial to understand not only anti-MAG neuropathy, it is as well important for all other autoimmune diseases with an antibody association.

Further the recombinant antibodies, which recognize MAG in a concentration dependent manner, should be used to generate an animal model to understand the pathological character of them. Due to the different V_H element usage in the 5 expanded clones and the different CDRs it is likely that these clones recognize MAG *via* distinctive epitopes or that the avidity of the antibodies is changed (Figure 21). First the antibodies should be tested in a brain slice culture assay together with complement. Since mus musculus and human MAG protein has a high amino acid homology (94.5%) this would give evidences, if the complement system is involved. Extra readout could be the IgM antibody deposits in the myelin sheet (Figure 4B), which are a pathological sign of anti-MAG neuropathy. Additionally the antibodies could be injected into mice to establish an animal model for this rare disease. To achieve this goal the variable region of the antibodies has to be cloned into IgM backbone and expressed. The recombinant IgM antibodies are then intravenous injected and the animals are examined for neurological pathologies over several week.

In conclusion, our data indicate that the therapeutic efficacy of Rituximab in anti-MAG neuropathy depends on efficient depletion of non-circulating B cells and is associated with qualitative imunological changes that indicate reconfiguration of B cell memory. These findings provide a mechanistic basis for the differential clinical response to Rituximab in anti-MAG neuropathy and support the therapeutic concept of ongoing and future clinical trials of B cell-depleting therapies in autoimmune diseases.

Methods

Patients:

We analyzed specimens form patients that were included in a double-blind, placebo-controlled study of Rituximab in patients with anti-MAG demyelinating polyneuropathy which was carried out at the National Institutes of Health in Bethesda, MD, USA (Table 5) [206]. Patients were selected if they had clinical and electrophysiological evidence of a demyelinating neuropathy, a benign IgM monoclonal spike, and anti-MAG antibodies. Patients did not receive any immunosuppressive therapy for at least 6 months before enrollment. At entry, all patients (except one) had impaired function as evidenced by affected balance, coordination, frequent falls, or muscle weakness, reflected in an Inflammatory Neuropathy Course and Treatment (INCAT) disability score of at least 1. The study was conducted at the National Institutes of Health under a Cooperative Research and Development Agreement between National Institute of Neurological Disorders and Stroke and Genetech. The trial was registered at www.ClinicalTrials.gov (ClinicalTrials.gov number NCT00050245), and was conducted under a protocol approved by the National Institute of Neurological Disorders and Stroke institutional review board. After randomization, four weekly intravenous cycles of 375mg/m2 of Rituximab or placebo consisting of a normal saline solution were administered. Patients were premedicated with acetaminophen 650mg and diphenhydramine 25mg before infusions. The primary outcome was a change of at least 1 point in INCAT disability scale score in the lower extremities at month 8. This is a validated scale used before in inflammatory demyelinating neuropathies including the IgM anti-MAG neuropathy. The 4 patients that improved by at least 1 INCAT point after 8 months were classified as Rituximab-responders; the other patients with stable or worsened disease were classifed as non-responders. Individual demographical and clinical profiles of all patients included in this study are given in Table 1.

Flow cytometry and single cell analysis

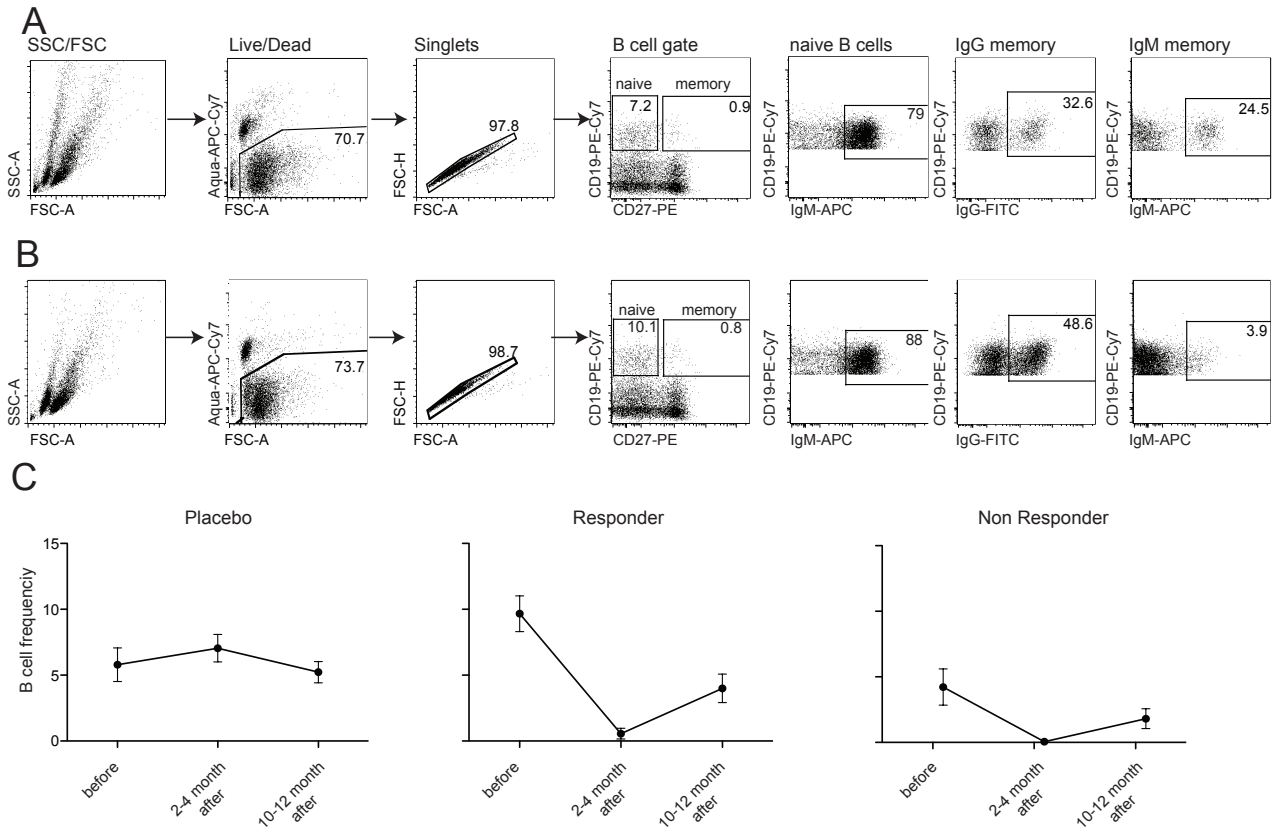

Figure 32: Sorting of single cells and frequency of the B cell in anti-MAG neuropathy patients

Gating strategy to identify naïve, IgM memory and IgG memory B cells before Rituximab therapy **(A)** and 12 months after treatment initiation **(B)**. Panel A and B were generated with data from the same patient. Peripheral blood B cell frequencies from all live cells in the lymphocyte gate are shown in **(C)**.

Frozen PBMCs were thawed in FACS buffer (2mM EDTA, 5% FCS, 20ug/ml DNAse Roche in PBS). After thawing the PBMCs were strained (0.22um cell strainer Becton Dickinson (BD)) and centrifuged for 15min at 150xg and 4°C. The cells were incubated with anti-CD27 PE clone M-T271, anti-CD19 PE-Cy7 clone SJ25C1, anti-IgM APC clone G20-127, anti-IgG Biotin G18-145, streptavidin FITC all from Becton Dickinson and with component H from Invitrogen for dead cell discrimination. Single $CD27^{-}CD19^{+}IgM^{+}$naïve B cells, $CD27^{+}CD19^{+}IgM^{+}$ memory B cells and $CD27^{+}CD19^{+}IgG^{+}$ memory B cells were purified by flow cytometric cell sorting using machine FACS Aria and software Diva from BD. The gating strategy is depicted in Figure 32.

Single Cell PCR:

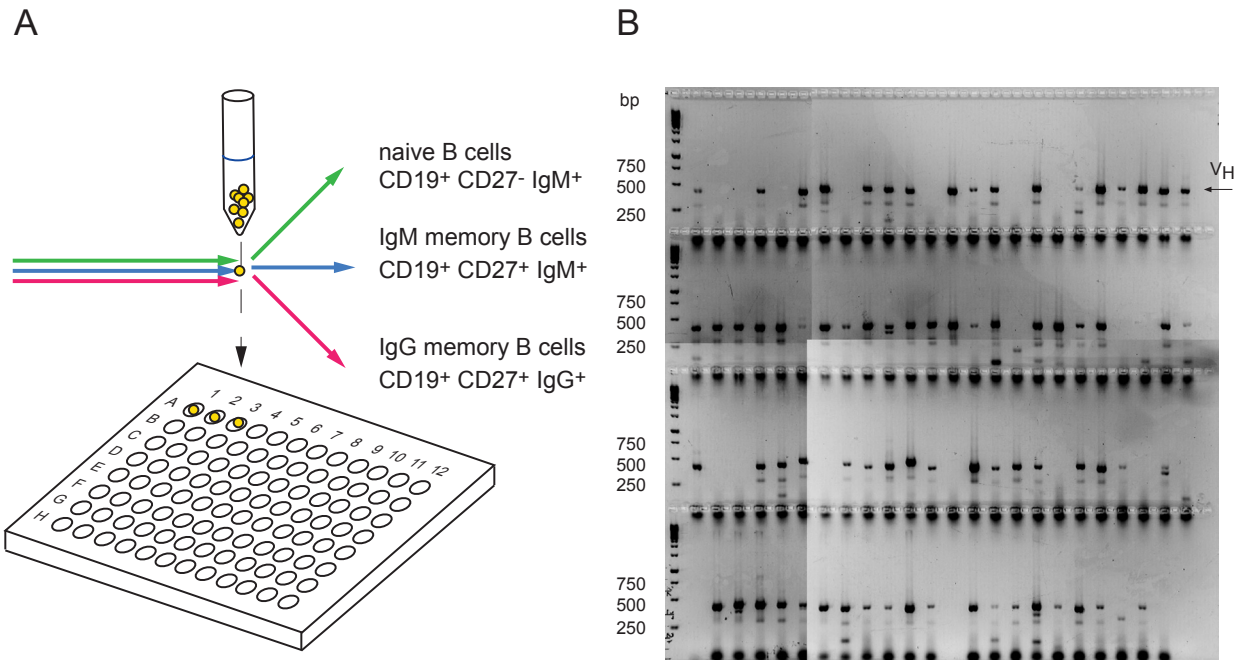

Figure 33: The sorting and amplification of single cell BCRs

A shows the graphic representation of the three B cell compartments, which were single cell sorted into a one step PCR mix containing plate. **B** represents an agarose gel derived from one plate after the PCR amplification. The correct mass of the heavy chain is indicated with an arrow.

Single cell sorting was directly into a 96well plate (thermoquick PCR-Plate Greiner bioOne) with 20 µl of reverse transcription-buffer or Qiagen OneStep RT-PCR reaction mix (Qiagen, Hilden, Germany) supplemented with 0.5 µM each of IgH chain V gene specific forward and IgG/IgM reverse primers per well 208. Directly after sorting, buffer plates were frozen on dry ice and Qiagen OneStep RT-PCR plates were incubated for 60 min at 50 °C for reverse transcription (RT). After the RT step, DNA polymerase was activated with an initial step of 15 min at 95°C. The amplification of the resulting cDNA of the Igh chain was performed at an annealing temperature of 58 °C for 45 seconds, an elongation temperature of 72 °C for 1 minute and a denaturation temperature of 94 °C for 30 seconds for 48 cycles Non-template controls were included to exclude contaminations in the master mix.

To reduce PCR error rates we used the HotStar Taq DNA polymerase from Qiagen with an error rate of 2x10-5 /nucleotide and cycle. PCR amplicons were separated by electrophoresis on a 1.2% agarose gel. To avoid cross contaminations on the gel PCR products were physically separated from each other. Bands with the correct mass (ca 500 bp) were excised using individual sterile scalpels; DNA was ex-

tracted (Qiagen MiniElute Gel Extraction Kit) and sequenced. The sequenced variable region of the amplified IgH chain were corrected with the CLC Main Workbench and analyzed on the international immunogenetic information system[264,265]. The variable region was analyzed for the V_H D_H and J_H usage, somatic hypermutations, CDR3 length, isoelectric point and clonal expansion.

Sequence analysis:

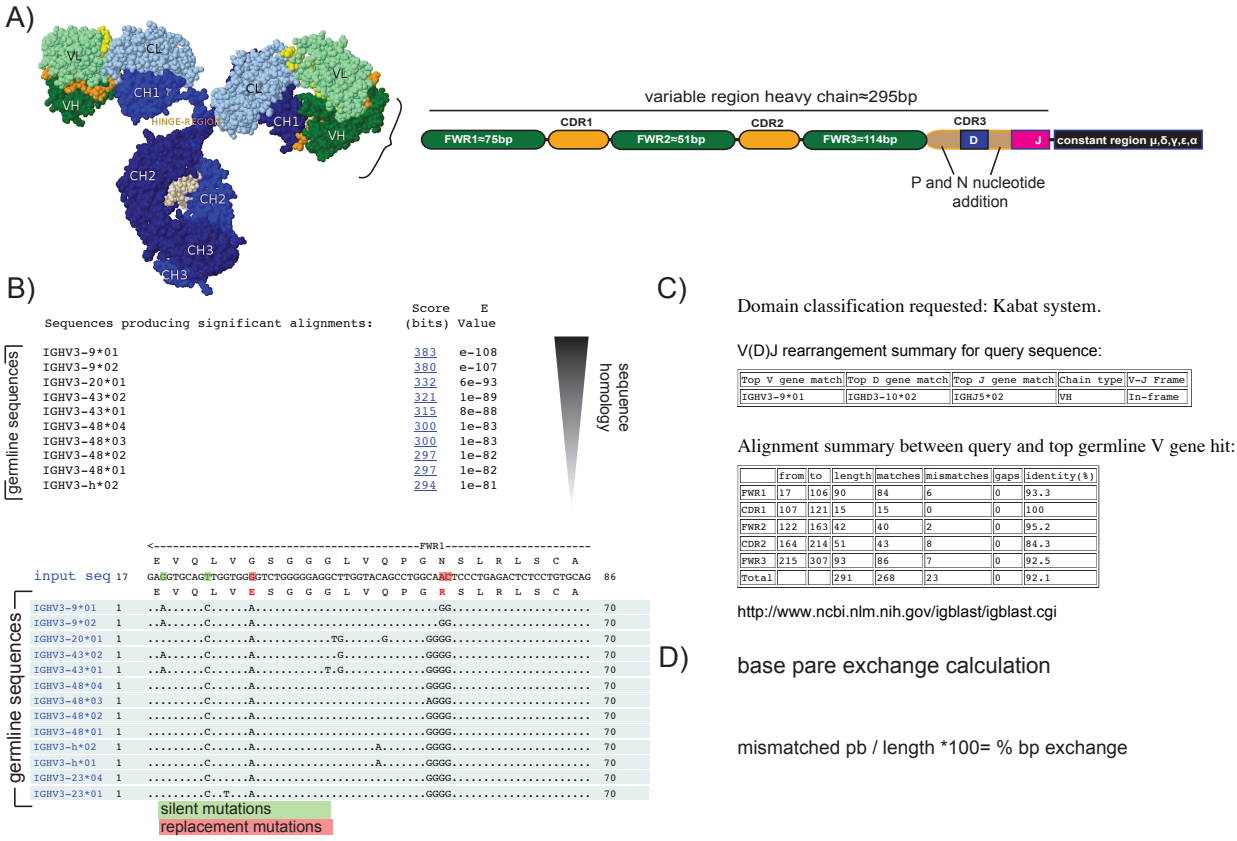

Figure 34: The variable region analysis after

A) dark green indicates the variable region and orange the CDRs of the heavy chain. The IgG molecule is once shown in the native tertiary structure (left site) and in a linear DNA sequence form (right site). **B)** shows the blast result of one representative sequence and the different homology to the germline sequences in the database (upper part). In the lower part the homology of the different germline sequences is represented by the silent and replacement mutations, which can be calculated from the sequence (green are silent and red replacement mutations). **C)** shows the overall blast result with the different V_H, D_H and J_H gene families that are used in this particular recombined sequence (upper part). The lower part is the output summary of the amount of mutations and the length of the V_H, D_H and J_H gene segments. **D)** is the formula used for the calculation of the % bp exchange. Where the length of the gene segment divides by the number of mutation.

After blasting the sequences clonal expansions were determined by similar CDR3 amino acid (aa) sequences and V_H D_H and J_H usage (Figure 34 A and B). The length of the CDR3 is defined as numbers of aa starting form the third position after the cysteine motive of the CDR3 and ending at the tryptophan amino acid. For the isoelectric point (pI) analysis we used the entire aa sequence of the CDR3 and calculated it with the tool on ExPASy proteomics server [266]. The V_H, D_H, and J_H gene usage was weight balanced by the number of sequences derived from each donor to avoid tempering the result by different amount of sequences due to clonal expansion or PCR efficacy. For the SHM analysis, sequences were first blasted against the germline sequences in the database of IMGT. The blast result of unique $CD19^+CD27^+IgM^+$ memory B cells in framework- and CDR-regions was used to calculate the % base pair (bp) exchange by dividing the number of mutations through the length in bp of the individual variable region elements (FWR1, CDR1, FWR2, CDR2 and FWR3) (Figure 34 A, C and D).

Expression vector cloning.

Expanded sequences were reconfirmed *via* an additional PCR from the pre sorted 20ul reverse transcription-buffer plate. The corresponding IgL chain was used to rule out contaminations and the cloning of the antibodies. For this purpose RNA of the single frozen cell was divided into three reverse transcription PCRs one for the Igh and two for the IgL chain gene (lambda and kappa). The recovered heavy chain sequences were then compared to the previous sequences. The corresponding Igh and IgK or IgL chain genes were cloned into expression vectors according to (Figure 35) [208]. The recombinant monoclonal antibodies were expressed in 293T cells after calcium phosphate-mediated transfection with 22.5 µg of each vector DNA (heavy and light chain). After 3 days, antibodies were purified from cell culture supernatants over a protein G column. The elution was performed with 0.1 M glycine pH 2 and dialyzed over night in PBS pH 7.4.

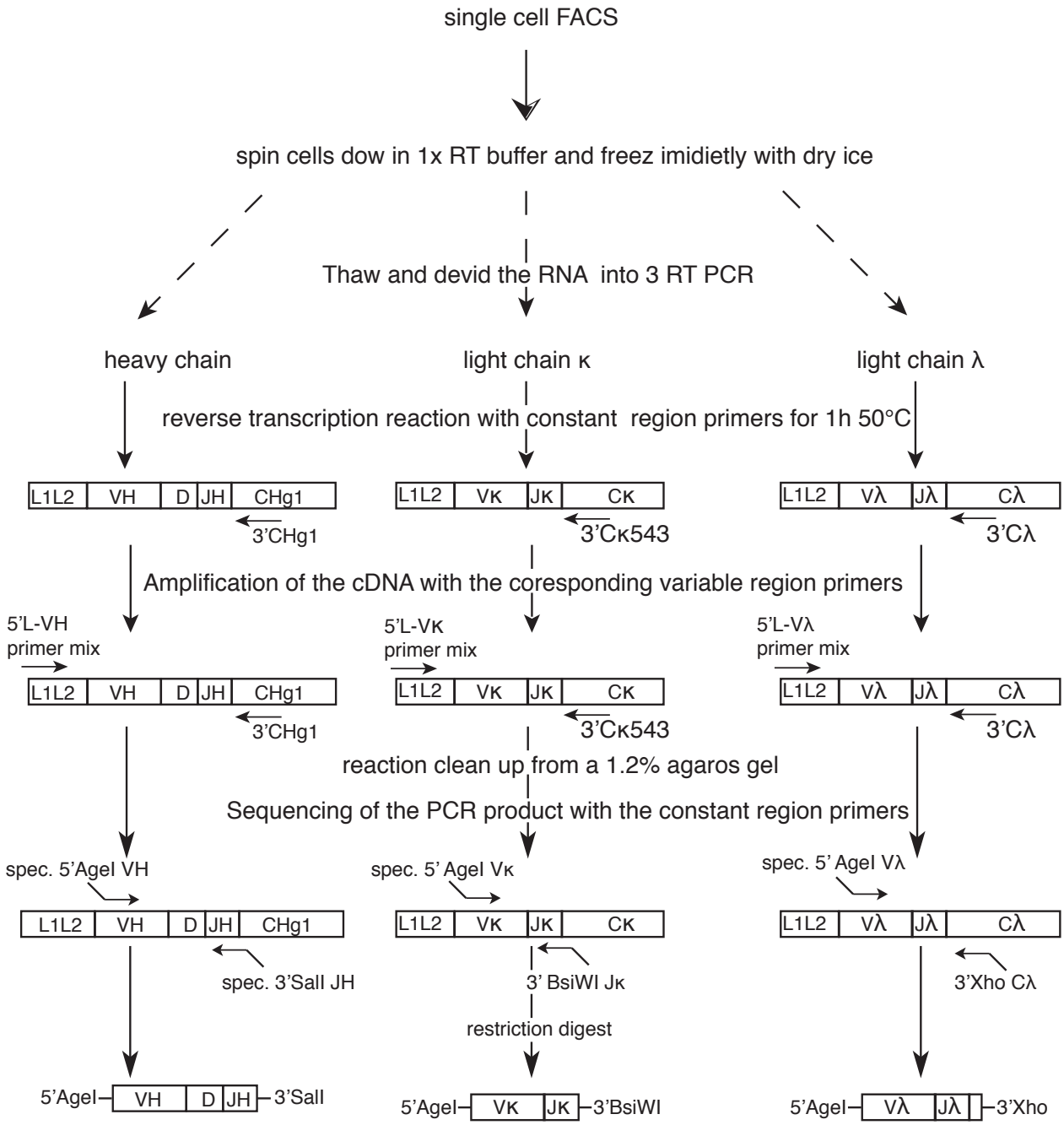

Figure 35: Flowchart for the cloning of single cell derived variable regions into eukaryotic expression vector

The map of the target vector is depicted in Figure 36 The figure is adapted from [208]

ELISA:

Specificities of recombinant antibodies were evaluated at different concentrations 0.001µg/ml, 0.005µg/ml, 0.01µg/ml, 1µg/ml, 10µg/ml and 50µg/ml using three commercially available ELISA kits (anti-SPGP ELISA kit, anti-MAG ELISA kit both from Bühlmann laboratories, Schoenenbuch, Switzerland and an EBNA1 IgG ELISA from Bio-Rad, Dreieich, Germany). The ELISAs were performed according to the manufacturers` recommendations. The OD signal obtained with the negative control provided by the manufacturer was subtracted from the OD signals of experimental samples. To detect the recombinantly expressed IgG molecules, a goat anti-human IgG secondary antibody coupled to HRP was used in the MAG and SGPG ELISA (Sigma-Aldrich, Buchs, Switzerland). The detection was done with TMB substrate that was stopped with 1M H2SO4 and absorbance was measured at 450 nm.

Statistics:

The unpaired student t-test (two-tailed) was used to compare CDR3 length, isoelectric points, length of D_H and N elements, and somatic hypermutation frequencies before and after Rituximab treatment. The two-tailed Fisher`s exact test was used to compare frequencies of V_H gene family usage and the size of clonal expansions. All analyses are based on individual sequences and data in figure parts in which error bars are shown are presented as mean ± SEM throughout the manuscript Since we analyzed pooled sequence data, a repeated observation analysis was not applied. A P value of less than 0.05 was considered significant.

Study approval:

The study was conducted under a protocol approved by the National Institute of Neurological Disorders and Stroke institutional review board. With informed consent from all patients that were included in this study, peripheral blood mononuclear cells were cryo-preserved and used for immunological experiments.

Materials:

Table5: Anti-MAG patients

Pat #	Clinical Subgroup	Age	Gender	Duration of disease (y)	INCAT leg base-line	INCAT leg 8 mo
# 8	Placebo	70	M	18	1	1
# 9	Placebo	56	F	10	1	1
# 11	Placebo	69	F	21	1	1
# 13	Placebo	73	F	8	2	2
# 16	Placebo	68	F	8	3	3
# 21	Placebo	53	M	7	1	1
# 3	Responder	61	M	7	2	1
# 14	Responder	72	F	16	2	1
# 15	Responder	69	M	9	1	0
# 27	Responder	71	M	15	4	1
# 5	Non-Responder	70	F	15	3	3
# 6	Non-Responder	64	M	12	2	4
# 10	Non-Responder	73	M	9	1	1
# 12	Non-Responder	69	M	5	0	0
# 17	Non-Responder	59	M	6	1	1
# 18	Non-Responder	76	M	13	1	1
# 22	Non-Responder	76	M	7	1	1
# 23	Non-Responder	71	M	11	1	1
# 26	Non-Responder	47	M	6	1	1

Table 6 Healthy control

No.	Age	Gender
# 1	57	M
# 2	60	M
# 3	58	M

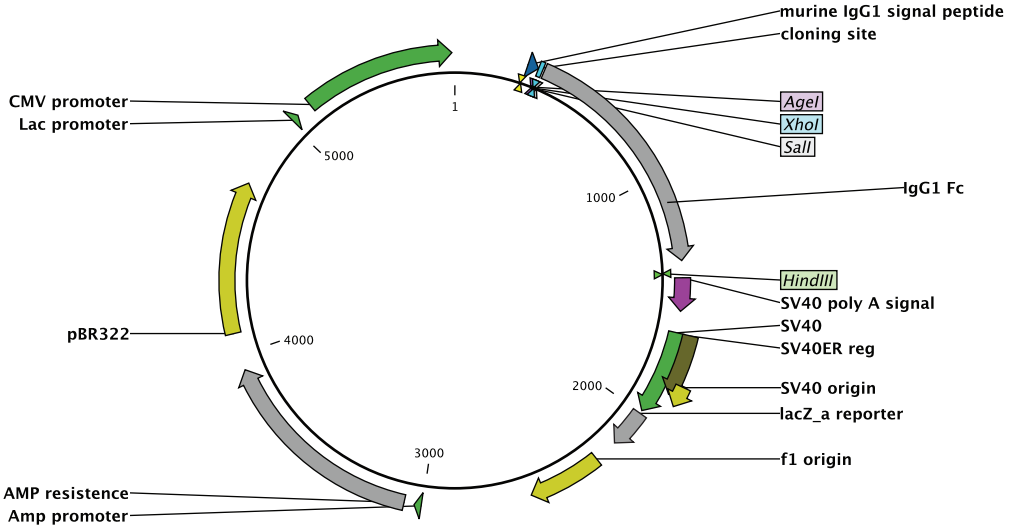

Figure 36: Vector map of the human IgG heavy chain expression vector

The vectore includes the Fc gamma heavy chain, Cytomegalo promoter, SV 40 poly A signal and the AMP resistance cassette.

References

1. Larsson, J. & Karlsson, S. The role of Smad signaling in hematopoiesis. *Oncogene* **24**, 5676–5692 (2005).
2. Janeway, C., Murphy, K. & Travers, P. *Janeway's immuno biology*. (2008).
3. Shimizu, Y. & Demars, R. Demonstration by class I gene transfer that reduced susceptibility of hu man cells to natural killer cell-mediated lysis is inversely correlated with HLA class I antigen expres sion *Eur. J. Immunol.* 1989).
4. Storkus, W. J., Alexander, J., Payne, J. A., Dawson, J. R. & Cresswell, P. Reversal of natural killing susceptibility in target cells expressing transfected class I HLA genes. *Proceedings of the National Academy of Sciences of the United States of America* **86**, 2361–2364 (1989).
5. Lieber, M. R. Site-specific recombination in the immune system. *FASEB J.* 5, 2934–2944 (1991).
6. Bassing, C. H., Swat, W. & Alt, F. W. The mechanism and regulation of chromosomal V(D)J recombination. *Cell* **109 Suppl**, S45–55 (2002).
7. Corbett, S. J., Tomlinson, I. M., Sonnhammer, E. L., Buck, D. & Winter, G. Sequence of the human immunoglobulin diversity (D) segment locus: a systematic analysis provides no evidence for the use of DIR segments, inverted D segments, 'minor' D segments or D-D recombination. *J. Mol. Biol.* **270**, 587–597 (1997).
8. Radic, M. Z. et al. Residues that mediate DNA binding of autoimmune antibodies. *J. Immunol.* **150**, 4966–4977 (1993).
9. Rabbani, H., Pan, Q., Kondo, N., Smith, C. I. & HAMMARSTROM, L. Duplications and deletions of the human IGHC locus: evolutionary implications. *Immunogenetics* **45**, 136–141 (1996).
10. Moura, R., Agua-Doce, A., Weinmann, P., Graça, L. & Fonseca, J. E. B cells from the bench to the clinical practice. *Acta Reumatol Port* **33**, 137–154 (2008).
11. Cerutti, A. & Rescigno, M. The biology of intestinal immunoglobulin A responses. *Immunity* **28**, 740–750 (2008).
12. Yurasov, S., Hammersen, J., Tiller, T., Tsuiji, M. & Wardemann, H. B-cell tolerance checkpoints in healthy humans and patients with systemic lupus erythematosus. *Ann N Y Acad Sci* **1062**, 165–174 (2005).
13. Berkowska, M. A., der Burg, van, M., van Dongen, J. J. M. & van Zelm, M. C. Checkpoints of B cell differentiation: visualizing Ig-centric processes. Ann N Y Acad Sci 1246, 11–25 (2011).
14. Berkowska, M. A. et al. Human memory B cells originate from three distinct germinal center-de pendent and -independent maturation pathways. *Blood* **118**, 2150–2158 (2011).
15. Montecino-Rodriguez, E. & Dorshkind, K. B-1 B cell development in the fetus and adult. *Immunity* **36**, 13–21 (2012).
16. Weigert, M., Gatmaitan, L., Loh, E., Schilling, J. & Hood, L. Rearrangement of genetic information may produce immunoglobulin diversity. *Nature* **276**, 785–790 (1978).
17. Brack, C., Hirama, M., Lenhard-Schuller, R. & Tonegawa, S. A complete immunoglobulin gene is created by somatic recombination. *Cell* **15**, 1–14 (1978).
18. Tonegawa, S. Somatic generation of antibody diversity. *Nature* (1983).
19. Croce, C. M. et al. Chromosomal location of the genes for human immunoglobulin heavy chains. *Proceedings of the National Academy of Sciences of the United States of America* **76**, 3416–3419 (1979).
20. Malcolm, S. et al. Localization of human immunoglobulin kappa light chain variable region genes to the short arm of chromosome 2 by in situ hybridization. *Proceedings of the National Academy of Sciences of the United States of America* **79**, 4957–4961 (1982).
21. McBride, O. W. et al. Chromosomal location of human kappa and lambda immunoglobulin light chain constant region genes. *J Exp Med* **155**, 1480–1490 (1982).
22. Erikson, J., Martinis, J. & Croce, C. M. Assignment of the genes for human λ immunoglobulin chains to chromosome 22. *Nature 294*, 173–175 (1981).
23. Yaoita, Y. et al. The D-J_H complex is an intermediate to the complete immunoglobulin heavy-chain V-region gene. *Nucleic Acids Res* **11**, 7303–7316 (1983).

24. Neuberger, M. S., Caskey, H. M., Pettersson, S., Williams, G. T. & Surani, M. A. Isotype exclusion and transgene down-regulation in immunoglobulin-lambda transgenic mice. *Nature* **338**, 350–352 (1989).
25. Bräuninger, A., Goossens, T., Rajewsky, K. & Küppers, R. Regulation of immunoglobulin light chain gene rearrangements during early B cell development in the human. *Eur. J. Immunol.* **31**, 3631–3637 (2001).
26. Matsuda, F. et al. The complete nucleotide sequence of the human immunoglobulin heavy chain variable region locus. *J Exp Med* **188**, 2151–2162 (1998).
27. Hiom, K. & Gellert, M. Assembly of a 12/23 paired signal complex: a critical control point in V(D)J recombination. **Mol. Cell 1**, 1011–1019 (1998).
28. van Zelm, M. C. et al. Ig gene rearrangement steps are initiated in early human precursor B cell sub sets and correlate with specific transcription factor expression. *J. Immunol.* **175**, 5912–5922 (2005).
29. van Gent, D. C., Hiom, K., Paull, T. T. & Gellert, M. Stimulation of V(D)J cleavage by high mobility group proteins. *The EMBO Journal* **16**, 2665–2670 (1997).
30. Akamatsu, Y. & Oettinger, M. A. Distinct roles of RAG1 and RAG2 in binding the V(D)J recombi nation signal sequences. *Mol. Cell. Biol.* **18**, 4670–4678 (1998).
31. Oettinger, M. A., Schatz, D. G., Gorka, C. & Baltimore, D. RAG-1 and RAG-2, adjacent genes that synergistically activate V(D)J recombination. *Science* **248**, 1517–1523 (1990).
32. Bassing, C. H. & Alt, F. W. The cellular response to general and programmed DNA double strand breaks. *DNA Repair (Amst.)* **3**, 781–796 (2004).
33. McBlane, J. F. et al. Cleavage at a V(D)J recombination signal requires only RAG1 and RAG2 pro teins and occurs in two steps. *Cell* **83**, 387–395 (1995).
34. van Gent, D. C., Mizuuchi, K. & Gellert, M. Similarities between initiation of V(D)J recombination and retroviral integration. *Science* **271**, 1592–1594 (1996).
35. Grawunder, U. & Harfst, E. How to make ends meet in V(D)J recombination. *Curr Opin Immunol* **13**, 186–194 (2001).
36. Xu, Y. DNA damage: a trigger of innate immunity but a requirement for adaptive immune homeosta sis. *Nat Rev Immunol* **6**, 261–270 (2006).
37. Helmink, B. A. et al. MRN complex function in the repair of chromosomal Rag-mediated DNA double-strand breaks. *J Exp Med* **206**, 669–679 (2009).
38. der Burg, van, M. et al. Loss of juxtaposition of RAG-induced immunoglobulin DNA ends is implicated in the precursor B-cell differentiation defect in NBS patients. *Blood* **115**, 4770–4777 (2010).
39. van Gent, D. C. & van der Burg, M. Non-homologous end-joining, a sticky affair. *Oncogene* **26**, 7731–7740 (2007).
40. Moshous, D., Callebaut, I., de Chasseval, R. & Corneo, B. Artemis, a Novel DNA Double-Strand Break Repair/V(D)J Recombination Protein, Is Mutated in Human Severe Combined Immune Deficiency 10.1016/S0092-8674(01)00309-9 : Cell | ScienceDirect.com. *Cell* (2001).
41. Taccioli, G. E. et al. Ku80: product of the XRCC5 gene and its role in DNA repair and V(D)J recombination. *Science* **265**, 1442–1445 (1994).
42. Li, Z. et al. The XRCC4 gene encodes a novel protein involved in DNA double-strand break repair and V(D)J recombination. *Cell* **83**, 1079–1089 (1995).
43. Gu, Y., Jin, S., Gao, Y., Weaver, D. T. & Alt, F. W. Ku70-deficient embryonic stem cells have increased ionizing radiosensitivity, defective DNA end-binding activity, and inability to support V(D)J recombination. *Proceedings of the National Academy of Sciences of the United States of America* **94**, 8076–8081 (1997).
44. Frank, K. M. et al. Late embryonic lethality and impaired V(D)J recombination in mice lacking DNA ligase IV. *Nature 396*, 173–177 (1998).
45. Ahnesorg, P. & Smith, P. XLF Interacts with the XRCC4-DNA Ligase IV Complex to Promote DNA Nonhomologous End-Joining 10.1016/j.cell.2005.12.031 : Cell | ScienceDirect.com. *Cell* (2006).
46. Schlissel, M. S. Structure of nonhairpin coding-end DNA breaks in cells undergoing V(D)J recombination. *Mol. Cell. Biol.* **18**, 2029–2037 (1998).
47. Alt, F. W. & Baltimore, D. Joining of immunoglobulin heavy chain gene segments: implications from a chromosome with evidence of three D-JH fusions. *Proceedings of the National Academy of Sciences of the United States of America* **79**, 4118–4122 (1982).

48. Ramadan, K., Shevelev, I. & Maga, G. De Novo DNA Synthesis by Human DNA Polymerase λ, DNA Polymerase μ and Terminal Deoxyribonucleotidyl Transferase *Journal of molecular Biology* (2004).
49. Gu, J. et al. XRCC4:DNA ligase IV can ligate incompatible DNA ends and can ligate across gaps. *The EMBO Journal* **26**, 1010–1023 (2007).
50. Nussenzweig, M. C. et al. Allelic exclusion in transgenic mice that express the membrane form of immunoglobulin mu. *Science* **236**, 816–819 (1987).
51. Reth, M. & Wienands, J. Initiation and processing of signals from the B cell antigen receptor. *Annu Rev Immunol* **15**, 453–479 (1997).
52. Mårtensson, I. & Keenan, R. The pre-B-cell receptor 10.1016/j.coi.2007.02.006 : £ *Curr Opin Immunol* (2007).
53. Gauthier, L., Rossi, B., Roux, F., Termine, E. & Schiff, C. Galectin-1 is a stromal cell ligand of the pre-B cell receptor (BCR) implicated in synapse formation between pre-B and stromal cells and in pre-BCR triggering. *Proceedings of the National Academy of Sciences of the United States of America* **99**, 13014–13019 (2002).
54. Rossi, B., Espeli, M., Schiff, C. & Gauthier, L. Clustering of pre-B cell integrins induces galectin-1-dependent pre-B cell receptor relocalization and activation. *J. Immunol.* **177**, 796–803 (2006).
55. Espeli, M., Mancini, S. J. C., Breton, C., Poirier, F. & Schiff, C. Impaired B-cell development at the pre-BII-cell stage in galectin-1-deficient mice due to inefficient pre-BII/stromal cell interactions. *Blood* **113**, 5878–5886 (2009).
56. Ghia, P. et al. Ordering of human bone marrow B lymphocyte precursors by single-cell polymerase chain reaction analyses of the rearrangement status of the immunoglobulin H and L chain gene loci. *J Exp Med* **184**, 2217–2229 (1996).
57. Hieter, P. A., Korsmeyer, S. J., Waldmann, T. A. & Leder, P. Human immunoglobulin kappa light-chain genes are deleted or rearranged in lambda-producing B cells. *Nature* **290**, 368–372 (1981).
58. Siminovitch, K. A., Bakhshi, A., Goldman, P. & Korsmeyer, S. J. A uniform deleting element mediates the loss of kappa genes in human B cells. *Nature* **316**, 260–262 (1985).
59. Wardemann, H., Hammersen, J. & Nussenzweig, M. C. Human autoantibody silencing by immunoglobulin light chains. *J Exp Med* **200**, 191–199 (2004).
60. Perez-Andres, M. et al. Human peripheral blood B-cell compartments: a crossroad in B-cell traffic. *Cytometry B Clin Cytom* **78 Suppl 1**, S47–60 (2010).
61. Retter, M. W. & Nemazee, D. Receptor editing occurs frequently during normal B cell development. *J Exp Med* **188**, 1231–1238 (1998).
62. Wardemann, H. et al. Predominant autoantibody production by early human B cell precursors. *Science* **301**, 1374–1377 (2003).
63. Casellas, R. et al. Contribution of receptor editing to the antibody repertoire. *Science* **291**, 1541–1544 (2001).
64. Oberdoerffer, P. & Novobrantseva, T. Expression of a Targeted λ1 Light Chain Gene Is Developmentally Regulated and Independent of Igκ Rearrangements. *J Exp Med* **197** (2003).
65. Meffre, E. & Wardemann, H. B-cell tolerance checkpoints in health and autoimmunity. *Curr Opin Immunol* **20**, 632–638 (2008).
66. Boehmer, von, H. & Melchers, F. Checkpoints in lymphocyte development and autoimmune disease. *Nat Immunol* **11**, 14–20 (2010).
67. Vettermann, C. & Schlissel, M. S. Allelic exclusion of immunoglobulin genes: models and mechanisms. *Immunol Rev* **237**, 22–42 (2010).
68. King, L. B. & Monroe, J. G. Immunobiology of the immature B cell: plasticity in the B-cell antigen receptor-induced response fine tunes negative selection. *Immunol Rev* **176**, 86–104 (2000).
69. Chen, C., Nagy, Z., Luning Prak, E. & Weigert, M. Immunoglobulin heavy chain gene replacement: a mechanism of receptor editing. *Immunity* **3**, 747–755 (1995).
70. Lutz, J., Müller, W. & Jäck, H.-M. VH replacement rescues progenitor B cells with two nonproductive VDJ alleles. *J. Immunol*. **177**, 7007–7014 (2006).
71. Zhang, Z. et al. Contribution of Vh gene replacement to the primary B cell repertoire. *Immunity* **19**, 21–31 (2003).
72. Radic, M. Z. & Zouali, M. Receptor editing, immune diversification, and self-tolerance. *Immunity* **5**, 505–511 (1996).

73. Nussenzweig, M. C. Immune receptor editing: revise and select. *Cell* **95**, 875–878 (1998).
74. Liu, Y., Fan, R., Zhou, S., Yu, Z. & Zhang, Z. Potential contribution of VH gene replacement in immunity and disease. *Ann N Y Acad Sci* **1062**, 175–181 (2005).
75. Wardemann, H. & Nussenzweig, M. B-cell self-tolerance in humans. *Adv Immunol* **vol. 95**, 83–110 (2007).
76. Rolink, A. G. et al. Mutations affecting either generation or survival of cells influence the pool size of mature B cells. *Immunity* **10**, 619–628 (1999).
77. Meffre, E. et al. Circulating human B cells that express surrogate light chains and edited receptors. *Nat Immunol* **1**, 207–213 (2000).
78. Meffre, E. et al. Surrogate light chain expressing human peripheral B cells produce self-reactive antibodies. *J Exp Med* **199**, 145–150 (2004).
79. Allman, D. M., Ferguson, S. E. & Cancro, M. P. Peripheral B cell maturation. I. Immature peripheral B cells in adults are heat-stable antigenhi and exhibit unique signaling characteristics. *J Immunol* **149**, 2533–2540 (1992).
80. Allman, D. M., Ferguson, S. E., Lentz, V. M. & Cancro, M. P. Peripheral B cell maturation. II. Heat-stable antigen(hi) splenic B cells are an immature developmental intermediate in the production of long-lived marrow-derived B cells. *J. Immunol.* **151**, 4431–4444 (1993).
81. Thomas, M. D., Srivastava, B. & Allman, D. Regulation of peripheral B cell maturation. *Cell. Immunol.* **239**, 92–102 (2006).
82. Monroe, J. G. et al. Positive and negative selection during B lymphocyte development. *Immunol. Res*. **27**, 427–442 (2003).
83. Carsetti, R., Rosado, M. M. & Wardmann, H. Peripheral development of B cells in mouse and man. *Immunol Rev* **197**, 179–191 (2004).
84. Loder, F. et al. B cell development in the spleen takes place in discrete steps and is determined by the quality of B cell receptor-derived signals. *J Exp Med* **190**, 75–89 (1999).
85. Kruetzmann, S. et al. Human immunoglobulin M memory B cells controlling Streptococcus pneumoniae infections are generated in the spleen. *J Exp Med* **197**, 939–945 (2003).
86. Tsuiji, M. et al. A checkpoint for autoreactivity in human IgM+ memory B cell development. *J Exp Med* **203**, 393 (2006).
87. Petro, J. B. et al. Transitional type 1 and 2 B lymphocyte subsets are differentially responsive to antigen receptor signaling. *J. Biol. Chem.* **277**, 48009–48019 (2002).
88. Su, T. T. & Rawlings, D. J. Transitional B lymphocyte subsets operate as distinct checkpoints in murine splenic B cell development. *J. Immunol.* **168**, 2101–2110 (2002).
89. Lam, K. P., Kühn, R. & Rajewsky, K. In vivo ablation of surface immunoglobulin on mature B cells by inducible gene targeting results in rapid cell death. *Cell* **90**, 1073–1083 (1997).
90. Kraus, M., Alimzhanov, M. & Rajewsky, N. Survival of Resting Mature B Lymphocytes Depends on BCR Signaling *via* the Igα/β Heterodimer *Cell* (2004).
91. Wang, H. & Clarke, S. H. Evidence for a ligand-mediated positive selection signal in differentiation to a mature B cell. *J. Immunol*. **171**, 6381–6388 (2003).
92. Cyster, J. G., Hartley, S. B. & Goodnow, C. C. Competition for follicular niches excludes self-reactive cells from the recirculating B-cell repertoire. *Nature* **371**, 389–395 (1994).
93. Paul, E., Nelde, A., Verschoor, A. & Carroll, M. C. Follicular exclusion of autoreactive B cells requires FcgammaRIIb. *Int. Immunol.* **19**, 365–373 (2007).
94. Meyer-Bahlburg, A., Andrews, S. F., Yu, K. O. A., Porcelli, S. A. & Rawlings, D. J. Characterization of a late transitional B cell population highly sensitive to BAFF-mediated homeostatic proliferation. *J Exp Med* **205**, 155–168 (2008).
95. Thien, M. et al. Excess BAFF rescues self-reactive B cells from peripheral deletion and allows them to enter forbidden follicular and marginal zone niches. *Immunity* **20**, 785–798 (2004).
96. Mackay, F. et al. Mice transgenic for BAFF develop lymphocytic disorders along with autoimmune manifestations. *J Exp Med* **190**, 1697–1710 (1999).
97. Batten, M., Groom, J. & Cachero, T. Baff Mediates Survival of Peripheral Immature B Lymphocytes. *J Exp Med*. (2000).
98. Litinskiy, M. B. et al. DCs induce CD40-independent immunoglobulin class switching through BLyS and APRIL. *Nat Immunol **3***, 822–829 (2002).

99. Mond, J. J., Vos, Q., Lees, A. & Snapper, C. M. T cell independent antigens. *Curr Opin Immunol* **7**, 349–354 (1995).
100. Mond, J. & Lees, A. T cell-independent antigens type 2. *Annu Rev Immunol* (1995).
101. Han, J. H. et al. Class switch recombination and somatic hypermutation in early mouse B cells are mediated by B cell and Toll-like receptors. *Immunity* **27**, 64–75 (2007).
102. Ueda, Y., Liao, D., Yang, K., Patel, A. & Kelsoe, G. T-independent activation-induced cytidine deaminase expression, class-switch recombination, and antibody production by immature/transitional 1 B cells. *J. Immunol*. **178**, 3593–3601 (2007).
103. Shlomchik, M. J. Sites and stages of autoreactive B cell activation and regulation. *Immunity* **28**, 18–28 (2008).
104. Stavnezer, J., Guikema, J. E. J. & Schrader, C. E. Mechanism and regulation of class switch recombination. *Annu Rev Immunol* **26**, 261–292 (2008).
105. Poltoratsky, V., Goodman, M. F. & Scharff, M. D. Error-prone candidates vie for somatic mutation. *J Exp Med* **192**, F27–30 (2000).
106. MacLennan, I. C. Germinal centers. *Annu Rev Immunol* **12**, 117–139 (1994).
107. Pape, K. A. et al. Visualization of the genesis and fate of isotype-switched B cells during a primary immune response. *J Exp Med* **197**, 1677–1687 (2003).
108. Küppers, R. Mechanisms of B-cell lymphoma pathogenesis. *Nat Rev Cancer* **5**, 251–262 (2005).
109. Ramiro, A. R. et al. AID Is Required for c-myc/IgH Chromosome Translocations In Vivo. *Cell* **118**, 431–438 (2004).
110. Robbiani, D. F. et al. AID Is Required for the Chromosomal Breaks in c-myc that Lead to c-myc/IgH Translocations. *Cell* **135**, 1028–1038 (2008).
111. KATAOKA, T., Miyata, T. & Honjo, T. Repetitive Sequences in Class-Switch Recombination Regions of Immunoglobulin Heavy-Chain Genes. *Cell* **23**, 357–368 (1981).
112. Dunnick, W., Hertz, G. Z., Scappino, L. & Gritzmacher, C. DNA sequences at immunoglobulin switch region recombination sites. *Nucleic Acids Res* **21**, 365–372 (1993).
113. Min, I., Rothlein, L. & Schrader, C. Shifts in targeting of class switch recombination sites in mice that lack μ switch region tandem repeats or Msh2. *J Exp Med* 201 (2005).
114. Tran, T. H. et al. B cell–specific and stimulation-responsive enhancers derepress Aicda by overcoming the effects of silencers. *Nature Publishing Group* **11**, 148–154 (2009).
115. Park, S.-R. et al. HoxC4 binds to the promoter of the cytidine deaminase AID gene to induce AID expression, class-switch DNA recombination and somatic hypermutation. *Nature Publishing Group* **10**, 540–550 (2009).
116. Klein, U. et al. Transcription factor IRF4 controls plasma cell differentiation and class-switch recombination. *Nat Immunol* **7**, 773–782 (2006).
117. Dengler, H. S. et al. Distinct functions for the transcription factor Foxo1 at various stages of B cell differentiation. *Nature Publishing Group* **9**, 1388–1398 (2008).
118. Muramatsu, M. et al. Class switch recombination and hypermutation require activation-induced cytidine deaminase (AID), a potential RNA editing enzyme. *Cell* **102**, 553–563 (2000).
119. Revy, P. et al. Activation-induced cytidine deaminase (AID) deficiency causes the autosomal recessive form of the Hyper-IgM syndrome (HIGM2). *Cell* **102**, 565–575 (2000).
120. Petersen-Mahrt, S., Harris, R. & Neuberger, M. AID mutates E-coli suggesting a DNA deamination mechanism for antibody diversification. *Nature* **418**, 99–103 (2002).
121. Chaudhuri, J. et al. Transcription-targeted DNA deamination by the AID antibody diversification enzyme. *Nature* **422**, 726–730 (2003).
122. Dickerson, S., Market, E. & Besmer, E. AID Mediates Hypermutation by Deaminating Single Stranded DNA. *J Exp Med* **197** (2003).
123. Pham, P., Bransteitter, R., Petruska, J. & Goodman, M. F. Processive AID-catalysed cytosine deamination on single-stranded DNA simulates somatic hypermutation. *Nature* **424**, 103–107 (2003).
124. Xu, Z. et al. 14-3-3 adaptor proteins recruit AID to 5‘-AGCT-3’-rich switch regions for class switch recombination. *Nature Publishing Group* **17**, 1124–1135 (2010).
125. Rada, C. et al. Immunoglobulin isotype switching is inhibited and somatic hypermutation perturbed in UNG-deficient mice. *Curr. Biol*. **12**, 1748–1755 (2002).
126. Schrader, C. E., Linehan, E. K., Mochegova, S. N., Woodland, R. T. & Stavnezer, J. Inducible DNA breaks in Ig S regions are dependent on AID and UNG. *J Exp Med* **202**, 561–568 (2005).

127. Guikema, J. E. J. et al. APE1- and APE2-dependent DNA breaks in immunoglobulin class switch recombination. *J Exp Med* **204**, 3017–3026 (2007).
128. Casellas, R. et al. Ku80 is required for immunoglobulin isotype switching. *The EMBO Journal* **17**, 2404–2411 (1998).
129. Manis, J. P. et al. Ku70 is required for late B cell development and immunoglobulin heavy chain class switching. *J Exp Med* **187**, 2081–2089 (1998).
130. Pan-Hammarström, Q. et al. Impact of DNA ligase IV on nonhomologous end joining pathways during class switch recombination in human cells. *J Exp Med* **201**, 189–194 (2005).
131. Morita, R. et al. Human blood CXCR5(+)CD4(+) T cells are counterparts of T follicular cells and contain specific subsets that differentially support antibody secretion. *Immunity* **34**, 108–121 (2011).
132. Smith, K. G., Light, A., Nossal, G. J. & Tarlinton, D. M. The extent of affinity maturation differs between the memory and antibody-forming cell compartments in the primary immune response. *The EMBO Journal* **16**, 2996–3006 (1997).
133. Takahashi, Y., Dutta, P. & Cerasoli, D. In Situ Studies of the Primary Immune Response to (4-Hydroxy-3-Nitrophenyl)Acetyl. V. Affinity Maturation Develops in Two Stages of Clonal Selection. *J Exp Med* **187** (1998).
134. Gonzalez, S. F. et al. Trafficking of B cell antigen in lymph nodes. *Annu Rev Immunol* **29**, 215–233 (2011).
135. Phan, T. G., Green, J. A., Gray, E. E., Xu, Y. & Cyster, J. G. Immune complex relay by subcapsular sinus macrophages and noncognate B cells drives antibody affinity maturation. *Nat Immunol* **10**, 786–793 (2009).
136. Delemarre, F. G., Kors, N., Kraal, G. & van Rooijen, N. Repopulation of macrophages in popliteal lymph nodes of mice after liposome-mediated depletion. *J. Leukoc. Biol*. **47**, 251–257 (1990).
137. Hume, D. A., Robinson, A. P., MacPherson, G. G. & Gordon, S. The mononuclear phagocyte system of the mouse defined by immunohistochemical localization of antigen F4/80. Relationship between macrophages, Langerhans cells, reticular cells, and dendritic cells in lymphoid and hematopoietic organs. *J Exp Med* **158**, 1522–1536 (1983).
138. Szakal, A. K., Holmes, K. L. & Tew, J. G. Transport of immune complexes from the subcapsular sinus to lymph node follicles on the surface of nonphagocytic cells, including cells with dendritic morphology. *J. Immunol.* **131**, 1714–1727 (1983).
139. Junt, T. et al. Subcapsular sinus macrophages in lymph nodes clear lymph-borne viruses and present them to antiviral B cells. *Nature* **450**, 110–114 (2007).
140. Iannacone, M. et al. Subcapsular sinus macrophages prevent CNS invasion on peripheral infection with a neurotropic virus. *Nature* **465**, 1079–1083 (2010).
141. Sixt, M., Kanazawa, N., Selg, M., Samson, T. & Roos, G. The Conduit System Transports Soluble Antigens from the Afferent Lymph to Resident Dendritic Cells in the T Cell Area of the Lymph Node. *Immunity* (2005).
142. Roozendaal, R. et al. Conduits Mediate Transport of Low-Molecular-Weight Antigen to Lymph Node Follicles. *Immunity* **30**, 264–276 (2009).
143. Cyster, J. G. B cell follicles and antigen encounters of the third kind. *Nat Immunol* **11**, 989–996 (2010).
144. Yang, B.-G. et al. Binding of lymphoid chemokines to collagen IV that accumulates in the basal lamina of high endothelial venules: its implications in lymphocyte trafficking. *J. Immunol.* **179**, 4376–4382 (2007).
145. Ansel, K. M. et al. A chemokine-driven positive feedback loop organizes lymphoid follicles. *Nature* **406**, 309–314 (2000).
146. Cyster, J. G. et al. Follicular stromal cells and lymphocyte homing to follicles. *Immunol Rev* **176**, 181–193 (2000).
147. Cyster, J. G. et al. A B-cell-homing chemokine made in lymphoid follicles activates Burkitt's lymphoma receptor-1. *Nature* **391**, 799–803 (1998).
148. Bajénoff, M., Egen, J., Koo, L., Laugier, J. & Brau, F. Stromal Cell Networks Regulate Lymphocyte Entry, Migration, and Territoriality in Lymph Nodes. *Immunity* (2006).
149. Mempel, T. R., Junt, T. & Andrian, von, U. H. Rulers over randomness: stroma cells guide lymphocyte migration in lymph nodes. *Immunity* **25**, 867–869 (2006).

150. Fazilleau, N., McHeyzer-Williams, L. J., Rosen, H. & McHeyzer-Williams, M. G. The function of follicular helper T cells is regulated by the strength of T cell antigen receptor binding. *Nat Immunol* **10**, 375–384 (2009).
151. Fazilleau, N., Mark, L., McHeyzer-Williams, L. J. & McHeyzer-Williams, M. G. Follicular helper T cells: lineage and location. *Immunity* **30**, 324–335 (2009).
152. Paul, E., Lutz, J., Erikson, J. & Carroll, M. C. Germinal center checkpoints in B cell tolerance in 3H9 transgenic mice. *Int. Immunol*. **16**, 377–384 (2004).
153. Mandik-Nayak, L., Bui, A. & Noorchashm, H. Regulation of Anti–double-stranded DNA B Cells in Nonautoimmune Mice: Localization to the T–B Interface of the Splenic Follicle. *J Exp Med* (1997).
154. Noorchashm, H. et al. Characterization of anergic anti-DNA B cells: B cell anergy is a T cell-independent and potentially reversible process. *Int. Immunol*. **11**, 765–776 (1999).
155. Kerfoot, S. M. et al. Germinal center B cell and T follicular helper cell development initiates in the interfollicular zone. *Immunity* **34**, 947–960 (2011).
156. Coffey, F., Alabyev, B. & Manser, T. Initial clonal expansion of germinal center B cells takes place at the perimeter of follicles. *Immunity* **30**, 599–609 (2009).
157. McHeyzer-Williams, M., Okitsu, S., Wang, N. & McHeyzer-Williams, L. Molecular programming of B cell memory. *Nat Rev Immunol* **12**, 24–34 (2011).
158. Lederman, S. et al. Molecular interactions mediating T-B lymphocyte collaboration in human lymphoid follicles. Roles of T cell-B-cell-activating molecule (5c8 antigen) and CD40 in contact-dependent help. *J. Immunol.* **149**, 3817–3826 (1992).
159. Foy, T. M. et al. In vivo CD40-gp39 interactions are essential for thymus-dependent humoral immunity. II. Prolonged suppression of the humoral immune response by an antibody to the ligand for CD40, gp39. *J Exp Med* **178**, 1567–1575 (1993).
160. Walker, L. S. K. et al. Established T cell-driven germinal center B cell proliferation is independent of CD28 signaling but is tightly regulated through CTLA-4. *J Immunology* **170**, 91 (2003).
161. Stüber, E. & Strober, W. The T cell-B cell interaction *via* OX40-OX40L is necessary for the T cell-dependent humoral immune response. *J Exp Med* **183**, 979–989 (1996).
162. Choi, Y. S. et al. ICOS receptor instructs T follicular helper cell versus effector cell differentiation *via* induction of the transcriptional repressor Bcl6. *Immunity* **34**, 932–946 (2011).
163. Nurieva, R. I. et al. Generation of T follicular helper cells is mediated by interleukin-21 but independent of T helper 1, 2, or 17 cell lineages. *Immunity* **29**, 138–149 (2008).
164. Leonard, W. J. & Spolski, R. Interleukin-21: a modulator of lymphoid proliferation, apoptosis and differentiation. *Nat Rev Immunol* **5**, 688–698 (2005).
165. Vogelzang, A. et al. A fundamental role for interleukin-21 in the generation of T follicular helper cells. *Immunity* **29**, 127–137 (2008).
166. Linterman, M. A. et al. IL-21 acts directly on B cells to regulate Bcl-6 expression and germinal center responses. *J Exp Med* **207**, 353–363 (2010).
167. Toellner, K. M. et al. T helper 1 (Th1) and Th2 characteristics start to develop during T cell priming and are associated with an immediate ability to induce immunoglobulin class switching. *J Exp Med* **187**, 1193–1204 (1998).
168. Zotos, D. et al. IL-21 regulates germinal center B cell differentiation and proliferation through a B cell-intrinsic mechanism. *J Exp Med* **207**, 365–378 (2010).
169. Kroese, F. G., Wubbena, A. S., Seijen, H. G. & Nieuwenhuis, P. Germinal centers develop oligoclonally. *Eur. J. Immunol.* **17**, 1069–1072 (1987).
170. Allen, C. D. C., Okada, T. & Cyster, J. G. Germinal-center organization and cellular dynamics. *Immunity* **27**, 190–202 (2007).
171. MacLennan, I. & Toellner, K. Extrafollicular antibody responses *Immunological Reviews* (2003).
172. Sciammas, R. et al. Graded expression of interferon regulatory factor-4 coordinates isotype switching with plasma cell differentiation. *Immunity* **25**, 225–236 (2006).
173. Kallies, A. et al. Plasma cell ontogeny defined by quantitative changes in blimp-1 expression. *J Exp Med* **200**, 967–977 (2004).
174. Nutt, S. L., Fairfax, K. A. & Kallies, A. BLIMP1 guides the fate of effector B and T cells. *Nat Rev Immunol* **7**, 923–927 (2007).

175. Xin, A., Nutt, S. L., Belz, G. T. & Kallies, A. Blimp1: driving terminal differentiation to a T. Adv. *Exp. Med. Biol*. **780**, 85–100 (2011).
176. Reimold, A., Iwakoshi, N. & Manis, J. Plasma cell differentiation requires the transcription factor XBP-1. *Nature* (2001).
177. Braun, P. E., Frail, D. E. & Latov, N. Myelin-associated glycoprotein is the antigen for a monoclonal IgM in polyneuropathy. *J. Neurochem.* **39**, 1261–1265 (1982).
178. Steck, A. J., Murray, N., Meier, C., Page, N. & Perruisseau, G. Demyelinating neuropathy and monoclonal IgM antibody to myelin-associated glycoprotein. *Neurology* **33**, 19–23 (1983).
179. Nobile-Orazio, E. et al. Frequency and clinical correlates of anti-neural IgM antibodies in neuropathy associated with IgM monoclonal gammopathy. *Ann. Neurol.* **36**, 416–424 (1994).
180. Rajabally, Y. A. Neuropathy and paraproteins: review of a complex association. *Eur J Neurol* (2011).doi:10.1111/j.1468-1331.2011.03380.x
181. Kyle, R. A. & Rajkumar, S. V. Monoclonal gammopathies of undetermined significance: a review. *Immunol Rev* **194**, 112–139 (2003).
182. Saleun, J. P., Vicariot, M., Deroff, P. & Morin, J. F. Monoclonal gammopathies in the adult population of Finistère, France. *J. Clin. Pathol.* **35**, 63–68 (1982).
183. Crawford, J., Eye, M. K. & Cohen, H. J. Evaluation of monoclonal gammopathies in the 'well' elderly. *Am. J. Med*. **82**, 39–45 (1987).
184. Kelly, J. J., Adelman, L. S., Berkman, E. & Bhan, I. Polyneuropathies associated with IgM monoclonal gammopathies. *Arch Neurol* **45**, 1355–1359 (1988).
185. Steck, A. J., Stalder, A. K. & Renaud, S. Anti-myelin-associated glycoprotein neuropathy. *Curr Opin Neurol* **19**, 458–463 (2006).
186. D F, K. Guidelines for Clinical and Laboratory Evaluation of Patients With Monoclonal Gammopathies. *Arch pathol Lab Med* **106–107** (1999).
187. Lunn, M. Immunotherapy for IgM anti-myelin-associated glycoprotein paraprotein-associated peripheral neuropathies. *Cochrane Database Syst Rev* (2006).
188. Leget, G. A. & Czuczman, M. S. Use of Rituximab, the new FDA-approved antibody. *Curr Opin Oncol* **10**, 548–551 (1998).
189. Edwards, J. B-cell targeting in rheumatoid arthritis and other autoimmune diseases : *Nat Rev Immunol* (2006).
190. World Health Organization International nonproprietary names (INN) for biological and biotechnological substances. *World Health Organization* (2006).
191. Dalakas, M. B cells as therapeutic targets in autoimmune neurological disorders. *Nature Clinical Practice Neurology* **4**, 557–567 (2008).
192. Reff, M. E. et al. Depletion of B cells in vivo by a chimeric mouse human monoclonal antibody to CD20. *Blood* **83**, 435–445 (1994).
193. Deans, J. P., Robbins, S. M., Polyak, M. J. & Savage, J. A. Rapid redistribution of CD20 to a low density detergent-insoluble membrane compartment. *J. Biol. Chem.* **273**, 344–348 (1998).
194. Cragg, M. S. et al. Complement-mediated lysis by anti-CD20 mAb correlates with segregation into lipid rafts. *Blood* **101**, 1045–1052 (2003).
195. Cragg, M. S. & Glennie, M. J. Antibody specificity controls in vivo effector mechanisms of anti-CD20 reagents. *Blood* **103**, 2738–2743 (2004).
196. Cartron, G. et al. Therapeutic activity of humanized anti-CD20 monoclonal antibody and polymorphism in IgG Fc receptor FcγRIIIa gene. *Blood* **99** (2002).
197. Treon, S. P. et al. Polymorphisms in FcgammaRIIIA (CD16) receptor expression are associated with clinical response to Rituximab in Waldenström's macroglobulinemia. *J Clin Oncol* **23**, 474–481 (2005).
198. Treon, S., Yang, G. & Hanzis, C. Attainment of complete/very good partial response following Rituximab-based therapy is an important determinant to progression-free survival, and is impacted by polymorphisms in FCGR3A in Waldenstrom macroglobulinaemia *British Journal of Haematology* (2011).
199. Weng, W.-K. & Levy, R. Two immunoglobulin G fragment C receptor polymorphisms independently predict response to Rituximab in patients with follicular lymphoma. *J Clin Oncol* **21**, 3940–3947 (2003).

200. Lim, S. H. et al. Fc gamma receptor IIb on target B cells promotes Rituximab internalization and reduces clinical efficacy. *Blood* **118**, 2530–2540 (2011).
201. Dörner, T., Radbruch, A. & Burmester, G. R. B-cell-directed therapies for autoimmune disease. *Nat Rev Rheumatol* **5**, 433–441 (2009).
202. Willison, H., Trapp, B. & Bacher, J. Demyelination induced by intraneural injection of human antimyelin-associated glycoprotein antibodies *Muscle & Nerve* **11** (1988).
203. Tatum, A. Experimental paraprotein neuropathy, demyelination by passive transfer of human IgM anti-myelin-associated glycoprotein. *Ann. Neurol.* (1993).
204. Ilyas, A. A., Gu, Y., Dalakas, M. C., Quarles, R. H. & Bhatt, S. Induction of experimental ataxic sensory neuronopathy in cats by immunization with purified SGPG. *J Neuroimmunol* **193**, 87–93 (2008).
205. Latov, N. Pathogenesis and therapy of neuropathies associated with monoclonal gammopathies. *Ann. Neurol.* **37** Suppl 1, S32–42 (1995).
206. Dalakas, M., Rakocevic, G. & Salajegheh, M. Placebo-controlled trial of Rituximab in IgM anti–myelin-associated glycoprotein antibody demyelinating neuropathy. *Ann. Neurol.* (2009).
207. Wei, C., Anolik, J., Cappione, A. & Zheng, B. A New Population of Cells Lacking Expression of CD27 Represents a Notable Component of the B Cell Memory Compartment in Systemic Lupus Erythematosus. *J Immunol* **178** (2007).
208. Tiller, T. et al. Efficient generation of monoclonal antibodies from single human B cells by single cell RT-PCR and expression vector cloning. *Journal of Immunological Methods* **329**, 112–124 (2008).
209. Ilyas, A. A. et al. IgM in a human neuropathy related to paraproteinemia binds to a carbohydrate de terminant in the myelin-associated glycoprotein and to a ganglioside. *Proceedings of the National Academy of Sciences of the United States of America* **81**, 1225–1229 (1984).
210. Mendell, J. R. et al. Polyneuropathy and IgM monoclonal gammopathy: studies on the pathogenetic role of anti-myelin-associated glycoprotein antibody. *Ann. Neurol.* **17**, 243–254 (1985).
211. Dalakas, M. Pathogenesis and Treatment of Anti-MAG Neuropathy. *Current treatment options in neurology* (2010).
212. Maurer, M. A. et al. Rituximab induces sustained reduction of pathogenic B cells in patients with peripheral nervous system autoimmunity. *J. Clin. Invest.* (2012).doi:10.1172/JCI58743
213. Kriangkum, J. et al. Clonotypic IgM V/D/J sequence analysis in Waldenstrom macroglobulinemia suggests an unusual B-cell origin and an expansion of polyclonal B cells in peripheral blood. *Blood* **104**, 2134–2142 (2004).
214. Chng, W. J. et al. Gene-expression profiling of Waldenstrom macroglobulinemia reveals a phenotype more similar to chronic lymphocytic leukemia than multiple myeloma. *Blood* **108**, 2755–2763 (2006).
215. Mamani-Matsuda, M. et al. The human spleen is a major reservoir for long-lived vaccinia virus-specific memory B cells. *Blood* **111**, 4653–4659 (2008).
216. Pinna, D., Corti, D., Jarrossay, D., Sallusto, F. & Lanzavecchia, A. Clonal dissection of the human memory B-cell repertoire following infection and vaccination. *Eur. J. Immunol.* **39**, 1260–1270 (2009).
217. Rosado, M. M. et al. Switched memory B cells maintain specific memory independently of serum antibodies: the hepatitis B example. *Eur. J. Immunol.* **41**, 1800–1808 (2011).
218. Bielekova, B. et al. Encephalitogenic potential of the myelin basic protein peptide (amino acids 83-99) in multiple sclerosis: results of a phase II clinical trial with an altered peptide ligand. *Nat Med* **6**, 1167–1175 (2000).
219. Kent, S. C. et al. Expanded T cells from pancreatic lymph nodes of type 1 diabetic subjects recognize an insulin epitope. *Nature* **435**, 224–228 (2005).
220. Skulina, C. et al. Multiple sclerosis: brain-infiltrating CD8+ T cells persist as clonal expansions in the cerebrospinal fluid and blood. *Proceedings of the National Academy of Sciences of the United States of America* **101**, 2428–2433 (2004).
221. Steiniger, B. & Timphus, E. Histochemistry and Cell Biology, Volume 126, Number 6 *Histochemistry and cell biology* (2006).
222. Mebius, R. E. & Kraal, G. Structure and function of the spleen. *Nat Rev Immunol* **5**, 606–616 (2005).

223. Weill, J.-C., Weller, S. & Reynaud, C.-A. Human marginal zone B cells. *Annu Rev Immunol* **27**, 267–285 (2009).
224. Spencer, J., Perry, M. E. & Dunn-Walters, D. K. Human marginal-zone B cells. *Immunol. Today* **19**, 421–426 (1998).
225. Stein, H., Bonk, A., Tolksdorf, G. & Lennert, K. Immunohistologic analysis of the organization of normal lymphoid tissue and non-Hodgkin's lymphomas. *The Journal of Histochemistry and Cytochemistry* (1980).
226. Spencer, J., Finn, T., Pulford, K. A., Mason, D. Y. & Isaacson, P. G. The human gut contains a novel population of B lymphocytes which resemble marginal zone cells. *Clin. Exp. Immunol.* **62**, 607–612 (1985).
227. Dono, M. et al. Heterogeneity of tonsillar subepithelial B lymphocytes, the splenic marginal zone equivalents. *J. Immunol.* **164**, 5596–5604 (2000).
228. Weller, S. et al. Human blood IgM 'memory' B cells are circulating splenic marginal zone B cells harboring a prediversified immunoglobulin repertoire. *Blood* **104**, 3647–3654 (2004).
229. Hao, Z. & Rajewsky, K. Homeostasis of peripheral B cells in the absence of B cell influx from the bone marrow. *J Exp Med* **194**, 1151–1164 (2001).
230. Avanzini, M., Locatelli, F. & Santos, C. B lymphocyte reconstitution after hematopoietic stem cell transplantation: functional immaturity and slow recovery of memory CD27+ B cells *Experimental Hematology* (2005).
231. Roll, P., Palanichamy, A., Kneitz, C., Dörner, T. & Tony, H.-P. Regeneration of B cell subsets after transient B cell depletion using anti-CD20 antibodies in rheumatoid arthritis. *Arthritis Rheum.* 54, 2377–2386 (2006).
232. Weller, S. et al. CD40-CD40L independent Ig gene hypermutation suggests a second B cell diversification pathway in humans. *Proceedings of the National Academy of Sciences of the United States of America* **98**, 1166–1170 (2001).
233. Martin, F., Oliver, A. M. & Kearney, J. F. Marginal zone and B1 B cells unite in the early response against T-independent blood-borne particulate antigens. *Immunity* **14**, 617–629 (2001).
234. Bernasconi, N. L., Onai, N. & Lanzavecchia, A. A role for Toll-like receptors in acquired immunity: up-regulation of TLR9 by BCR triggering in naïve B cells and constitutive expression in memory B cells. *Blood* **101**, 4500–4504 (2003).
235. Bourke, E. The toll-like receptor repertoire of human B lymphocytes: inducible and selective expression of TLR9 and TLR10 in normal and transformed cells. *Blood* **102**, 956–963 (2003).
236. Lanzavecchia, A. & Sallusto, F. Toll-like receptors and innate immunity in B-cell activation and antibody responses. *Curr Opin Immunol* **19**, 268–274 (2007).
237. Tierens, A., Delabie, J., Michiels, L., Vandenberghe, P. & De Wolf-Peeters, C. Marginal-zone B cells in the human lymph node and spleen show somatic hypermutations and display clonal expansion. *Blood* **93**, 226–234 (1999).
238. Dammers, P. M., Visser, A., Popa, E. R., Nieuwenhuis, P. & Kroese, F. G. Most marginal zone B cells in rat express germline encoded Ig VH genes and are ligand selected. *J. Immunol*. **165**, 6156–6169 (2000).
239. Toellner, K.-M. et al. Low-level hypermutation in T cell-independent germinal centers compared with high mutation rates associated with T cell-dependent germinal centers. *J Exp Med* **195**, 383–389 (2002).
240. Tian, C. et al. Evidence for preferential Ig gene usage and differential TdT and exonuclease activities in human naïve and memory B cells. *Mol Immunol* **44**, 2173–2183 (2007).
241. Willenbrock, K., Jungnickel, B., Hansmann, M.-L. & Küppers, R. Human splenic marginal zone B cells lack expression of activation-induced cytidine deaminase. *Eur. J. Immunol*. **35**, 3002–3007 (2005).
242. Weller, S. et al. Somatic diversification in the absence of antigen-driven responses is the hallmark of the IgM+ IgD+ CD27+ B cell repertoire in infants. *J Exp Med* **205**, 1331–1342 (2008).
243. Werner Favre, C. et al. IgG subclass switch capacity is low in switched and in IgM-only, but high in IgD^+ IgM^+, post-germinal center (CD27+) human B cells. *Eur. J. Immunol.* **31**, 243–249 (2001).
244. Puga, I. et al. B cell-helper neutrophils stimulate the diversification and production of immunoglobulin in the marginal zone of the spleen. *Nat Immunol* **13**, 170–180 (2012).

245. Griffin, D. O., Holodick, N. E. & Rothstein, T. L. Human B1 cells in umbilical cord and adult peripheral blood express the novel phenotype $CD20^+$ $CD27^+$ $CD43^+$ $CD70^-$. *J Exp Med* **208**, 67–80 (2011).
246. Griffin, D. O. & Rothstein, T. L. A small CD11b+ human B1 cell subpopulation stimulates T cells and is expanded in lupus. *J Exp Med* **208**, 2591–2598 (2011).
247. Lanier, L. L., Warner, N. L., Ledbetter, J. A. & Herzenberg, L. A. Expression of Lyt-1 antigen on certain murine B cell lymphomas. *J Exp Med* **153**, 998–1003 (1981).
248. Kantor, A. Origin of Murine B Cell Lineages - Annual Review of Immunology, 11(1):501. *Annu Rev Immunol* (1993).
249. Hardy, R., Hayakawa, K. & Parks, D. Murine B cell differentiation lineages. *J Exp Med* **159** (1984).
250. Hayakawa, K., Hardy, R. R., Parks, D. R. & Herzenberg, L. A. The 'Ly-1 B' cell subpopulation in normal immunodefective, and autoimmune mice. *J Exp Med* **157**, 202–218 (1983).
251. Hayakawa, K., Hardy, R. R., Herzenberg, L. A. & Herzenberg, L. A. Progenitors for Ly-1 B cells are distinct from progenitors for other B cells. *J Exp Med* **161**, 1554–1568 (1985).
252. Kantor, A. B., Stall, A. M., Adams, S., Herzenberg, L. A. & Herzenberg, L. A. Differential development of progenitor activity for three B-cell lineages. *Proceedings of the National Academy of Sciences of the United States of America* **89**, 3320–3324 (1992).
253. Kantor, A. B., Stall, A. M., Adams, S., Watanabe, K. & Herzenberg, L. A. De novo development and self-replenishment of B cells. *Int. Immunol.* **7**, 55–68 (1995).
254. Wardemann, H., Boehm, T., Dear, N. & Carsetti, R. B-1a B cells that link the innate and adaptive immune responses are lacking in the absence of the spleen. *J Exp Med* **195**, 771–780 (2002).
255. Montecino-Rodriguez, E., Leathers, H. & Dorshkind, K. Bipotential B-macrophage progenitors are present in adult bone marrow. *Nat Immunol* **2**, 83–88 (2001).
256. Montecino-Rodriguez, E. & Dorshkind, K. Stromal cell-dependent growth of B-1 B cell progenitors in the absence of direct contact. *Nat Protoc* **1**, 1140–1144 (2006).
257. Leandro, M. J., Cooper, N., Cambridge, G., Ehrenstein, M. R. & Edwards, J. C. W. Bone marrow B-lineage cells in patients with rheumatoid arthritis following Rituximab therapy. *Rheumatology (Oxford)* **46**, 29–36 (2007).
258. Teng, Y. K. O. et al. Immunohistochemical analysis as a means to predict responsiveness to Rituxi mab treatment. *Arthritis Rheum*. **56**, 3909–3918 (2007).
259. Thurlings, R. M. et al. Synovial tissue response to Rituximab: mechanism of action and identification of biomarkers of response. *Ann. Rheum. Dis*. **67**, 917–925 (2008).
260. Levine, T. D. & Pestronk, A. IgM antibody-related polyneuropathies: B-cell depletion chemotherapy using Rituximab. *Neurology* **52**, 1701–1704 (1999).
261. Benedetti, L. et al. Predictors of response to Rituximab in patients with neuropathy and anti-myelin associated glycoprotein immunoglobulin *M. J. Peripher. Nerv. Syst*. **12**, 102–107 (2007).
262. Renaud, S. et al. High-dose Rituximab and anti-MAG-associated polyneuropathy. *Neurology* **66**, 742–744 (2006).
263. Benedetti, L. et al. Long-term effect of Rituximab in anti-mag polyneuropathy. *Neurology* **71**, 1742–1744 (2008).
264. Brochet, X. & Lefranc, M. IMGT/V-QUEST: the highly customized and integrated system for IG and TR standardized V-J and V-D-J sequence analysis. *Nucleic Acids Res* (2008).
265. Giudicelli, V., Brochet, X. & Lefranc, M.-P. IMGT/V-QUEST: IMGT standardized analysis of the immunoglobulin (IG) and T cell receptor (TR) nucleotide sequences. *Cold Spring Harb Protoc* **2011**, 695–715 (2011).
266. Gasteiger, E. et al. ExPASy: The proteomics server for in-depth protein knowledge and analysis. *Nucleic Acids Res* **31**, 3784–3788 (2003).

Abbreviations

ADCC	antibody dependent cell-mediated cytotoxicity
AID	activation induced cytidine deaminase
BAFF	B cell activating factor of the tumor necrosis factor family
BCR	B cell receptor
C	cytidine
CDC	complement dependent cytotoxicity
CDR	complementarity determining region
CH1, 2, 3	constant region 1, 2 ,3
CL	constant region light chain
CNS	central nervous system
CSR	class switch recombination
DC	dendritic cell 
D_H	diversity region heavy chain element
DNA	deoxyribonucleic acid
DSB	double strand breaks
DSB	double strand breaks
EBI-2	G-protein coupled receptor 183
ELISA	enzyme linked immunosorbent assay
FACS	fluorescence activated cell sorting
Fc R	fragment crystallizable region receptor
FDC	follicular dendritic cell 
FOXO1	fork head box O1
FRC	fibroblastic reticular cell 
G	guanine
GC	germinal center
HEV	high endothelial venules

HMGB	high mobility group protein
HOXC4	homeobox C4
HSC	hematopoietic stem cells
IC	immune complex
IFN	interferon
Ig	immunoglobulin
IgH	immunoglobulin heavy chain
IGHD	diversity region heavy chain segment
IGHJ	joining region heavy chain segment
IGHV	variable region heavy chain segment
IgK	immunoglobulin kappa light chain
IgL	immunoglobulin lambda light chain
IgL	immunoglobulin light chain
Il	interleukin
IRF	interferon regulatory factor
IVIG	Intravenous immunoglobulin
J_H	joining region heavy chain element
KDE	kappa deletion element
mAb	monoclonal antibody
MAG	myelin-associated glycoprotein
MGUS	monoclonal gammopathy of undetermined significance
MHC	major histocompatibility complex
MM	medullary macrophage 
MRC	marginal reticular cells
MS	multiple sclerosis
MZ	marginal zone
N-elements	non-template-encoding-nucleotides
NHEJ	non-homologous end joining
NK	natural killer cell 
NMO	neuromyelitis optice
PAMP	pathogen-associated molecular patterns
PAX5	paired box protein 5

PCR	polymerase chain reaction
PI	isoelectric point
PNS	peripheral nervous system
RAG	recombination activating genes
RSS	recombination signal sequence
RT	reverse transcription
SEM	standard error mean
SCS	subcapsular sinus macrophage 
SHM	somatic hyper mutation
SLE	systemic lupus erythematosus
SSM	subcapsular sinus macrophage
T cell	thymus derived immune cell 
TCR	T cell receptor
T_{FH}	follicular helper T cell 
TGF	transforming growth factor
TLR	toll like receptor
UNG	uracil DNA glycosylases
VDJ	recombination variable diversity joining DNA rearrangement
V_H	variable region heavy chain element
Xpb-1	X-box binding protein-1

Curriculum Vitae

Name:	Michael Andreas Maurer
Date of birth:	17.04.1976
Place of Origin:	Vechigen BE
Address:	Leutholdstrasse 22 8037 Zürich Switzerland
Phone:	+41 78 776 01 60
Email:	Michael.Maurer@neuroimm.uzh.ch

Education

2007-2012	PhD thesis Institute of Experimental Immunology University of Zürich Department of Neuroinflammation Head of lab: Jan Lünemann Department of Neuroimmunology University Hospital of Zurich Department of Neuroinflammation Head of lab: Norbert Goebels
2007	Internship Department of Gynecology University Hospital Zurich Topic: Cancer research (cancer cell specific induction of apoptosis)
2006	Master of science (MSc) in biochemistry and molecular biology ETH Zurich Final exam in: biochemistry, gene- and enzyme technology, bioorganic chemistry, cell biology, molecular biology and biophysics
2004-2005	Diploma thesis: In vitro and in vivo studies of TMX3 - a novel thioredoxin-related transmembrane protein Institute of Biochemistry ETH Zürich Head of lab: Lars Ellgaard former junior group leader in the lab of Ari Helenius
1997- 2000	Matura type C at Feusi BE
1997	Technical college Burgdorf BE
1996	Military service
1993-1996	Apprenticeship as chemical laboratory technician Department for neurological diseases Hoffmann-La Roche Basel Chemical laboratory technician
1988-1993	Secondary school in Meiringen

Publications

1. **Michael A Maurer**, Goran Rakocevic, Carol S Leung, Isaak Quast, Martin Lukačišin, Norbert Goebels, Christian Münz, Hedda Wardemann, Marinos Dalakas, and Jan D Lünemann.
Rituximab induces sustained reduction of pathogenic B cells in patients with peripheral nervous system autoimmunity,
J. Clin. Invest. (2012).

2. Kristina Kakalacheva, **Michael A Maurer**, Björn Tackenberg, Christian Münz, Nick Willcox, and Jan D Lünemann
Intrathymic epstein-barr virus infection is not a prominent feature of myasthenia gravis,
Ann. Neurol. (2011).

3. Johannes Haugstetter, **Michael A Maurer**, Thomas Blicher, Martin Pagac, Gerhard Wider, and Lars Ellgaard
Structure-function analysis of the endoplasmic reticulum oxidoreductase TMX3 reveals inter domain stabilization of the N-terminal redox-active domain,
Journal of Biological Chemistry (2007).

4. Carol S. Leung, **Michael A. Maurer**, Sonja Meixlsperger, Anne Lippmann, Cheolho Cheong, Jianmin Zuo, Tracey A. Haigh, Graham S. Taylor and Christian Münz,
Robust T cell stimulation by Epstein-Barr virus-transformed B cells after antigen targeting to DEC-205, *Blood* (2013).

In preparation

5. **Michael. A. Maurer** Marcus Dorner, David Nadal, Christian Münz, Jan D. Lünemann & and Norbert Goebels
LMP2 is required for class switch recombination and somatic hypermutation induced in naïve B cells by infection with the Epstein Barr virus. revision *JV*

6. **Michael A. Maurer,** Jan D. Lünemann
Rituximab does not change SHM in the IgG memory compartment

7. **Michael A. Maurer**, Christian W Keller, Thomas Tuschel, Olivier Devuyst and Jan D. Lünemann
miRNA down regulate CLCN5 expression in MS lesions

8. **Michael A Maurer**, Fischer K., Goebels N
The comparison of EBV infected B cells in blood and CSF

Acknowlegement

First of all, I would like to thank Jan Lünemann, for the opportunity to finish my PhD studies in the field of neuroimmunology in his lab. I appreciated the freedom of action in the different projects I was working on and independency during my PhD thesis. I thank my supervisors Christian Münz, Burkhard Becher, Norbert Goebels and Adriano Fontana for supporting my work with helpful discussions.
I specially thank Norbert Goebels who gave me the opportunity to learn the single cell PCR technique. And as well Monica Gulati and Sandra Küenzli, which invested a lot of time to show me the important parts of this technique.
I would like to thank Hedda Wardemann for the important discussion concerning my single cell antibody analysis as well Cornelius Fischer for the amazing support at the FACS sorter, Eliane Escher for the sequencing of my antibody sequences and Goran Rakocevic for the samples I could use.
Thank to all the current and former lab members of the institute of Experimental Immunology specially Johannes vom Berg, Isaak Quast, Carol Leung and Rosa Barreira Da Silva for their scientific and mental support during my PhD. Deeqa Osman and Patrick Weber for the precise work and support of the projects. Kristina Kakalacheva, Christina Sina and Christian Keller for the great atmosphere in our Lab and the scientific input for my projects.

I also thank all the members of the Münz-, Lünemann-, Becher-, Fontana- and Wong-Groups for their discussions and help not only during the progress reports.

Special thanks go to Franziska Morger, thank you for your patience and continuous support during the hard phases of my PhD and last but not least to my family, who always supported my studies and encouraged me to go on and to give my best.

Declaration

Herewith I declare that I have written this thesis myself and only used the stated references. Further, I declare that myself have performed all the experiments with assistance from Deeqa Osman, Martin Lukačišin and Cornelius Fischer for the sequencing part and Isaak Quast contributed to the FACS analysis.

Zürich, 2.3.2013 

Michael Andreas Maurer, Zürich, Switzerland